The effect of phytosubstances and plant-derived synthetic analogs on acute myeloid leukemia cells

The thesis is submitted in partial fulfillment of the requirements for the

degree of Master of Pharmacy

By

Luwam Ghebrihiwet Weldeab

Centre for Pharmacy and Department of Clinical Science

University of Bergen, Norway

May 2021

Acknowledgment

First of all, I would like to give thanks to my supervisors Prof. Lars Herfindal and Prof. Torgils Fossen for their guidance, their support by answering my questions and sharing your knowledge throughout this semester. I would also like to thank Dr. Reidun Æsøy for her kindness, patience, and guidance in writing this thesis and the different laboratory techniques. My master' thesis would not have been so interesting without all of them.

Further, I would like to thank all the staff from Herfindal Lab group for having me there and guiding me through different challenges in laboratory.

I would also to thank my fellow students, especially Noah Erchinger and Anne Oldeide Hay for their encouragement and support. I want also to thank Catherine Nguyen, Vilde S. S. Bulling and Malgorzata D. Szymczak for letting to study their isolated natural compounds in this thesis.

At last, I am greatly thankful to my family and friends for their support, being there for me and not letting me to give up. I especially want to thank my brother Noh Weldeab and my friend Meron Yohannes for their encouragement and support on writing this thesis.

Thank you, I could not have done this without you.

Luwam Ghebrihiwet Weldeab

Table of Contents

Abbreviations

AML = Acute myeloid leukemia

ALL = acute lymphoblastic leukemia

WHO = World Health Organization

WW-II = Second World War

DNR = daunorubicin

AraC = cytarabine

HSCT = hematopoietic stem cell transplantation

alloHSCT = allogeneic hematopoietic stem cell transplantation

autoHSCT = autologous hematopoietic stem cell transplantation

CR = complete remission

OS = overall survival

CNS = central nervous system

GVHD = graft-versus-host disease

TRM = therapy-related mortality

LDAC = low dose cytarabine

HDAC= High dose cytarabine

HU = hydroxyurea

CRi= complete remission with incomplete hematologic recovery

HSC = hematopoietic stem cells

GIT = gastrointestinal tract

t-AML = therapy-related AML

VA = vinca alkaloids

TKI = tyrosine kinase inhibitors

ATCC = American Type Culture Collection

FBS = fetal bovine serum

PBS = phosphate buffered saline

WST = Water soluble tetrazolium salt

CBB = Coomassie brilliant blue G-250

BSA = Bovine serum albumin

MDS = myelodysplastic syndromes

SDS = sodium dodecyl sulfate

IDH = Isocitrate dehydrogenase

GO = Gemtuzumab ozogamicin

Thr = threonine

Tyr = tyrosine

Abstract

Background: Acute myeloid leukemia (AML) is a heterogeneous disease that is associated with a low survival rate. The current induction treatment of AML has remained without significant change over the past 30-40 years, and it has severe side effects. Therefore, more individualized treatments and less toxic drugs are needed to be developed. In this present study, 30 natural product and synthetic analogs were explored to identify potential antileukemic drugs or lead compounds for the treatment of AML.

Methods: A screening assay of 30 natural compounds were performed on AML cell line MOLM-13 and the normal kidney cell line NRK cells to evaluate the cytotoxicity effect of the compounds. The cell viability was determined using WST-1 before the cells were fixated. Based on the result from the screen, ten compounds were selected for further tests on two AML cells, OCI-AML3 and MV4-11, and a cardiomyocyte cell line, H9C2 cells. These ten compounds were also tested in combination with other chemotherapeutic drugs to reveal possible synergistic activity. Finally, western blot analysis was done to investigate the mechanism of apoptosis on MOLM-13 cells.

Results: Nine of 30 compounds showed high selectivity toward MOLM-13 cells, and compounds **4**, **15** and **19** showed selective cytotoxic activity towards OCI-AML3 and MV4-11 cell lines over the two normal cell lines. Even though compounds **1** and **28** did to some extent induce apoptosis in the normal cell lines, they had good effect towards AML cells with large EC50 value ratio between cancerous and non-cancerous cell lines. Compound **12** also had high potency towards leukemic cells, however, it was toxic towards the two normal cell lines. Further, compounds **1** and **11** showed synergistic effect in combination with DNR, compound **15** in combination with venetoclax, and compound **6** in combination with both DNR and venetoclax.

Conclusion: Compounds **1** and **15** could be possible drugs or lead compounds for AML, based on their synergistic effect with DNR and venetoclax and the high potency of these compounds. Compound **6** had good cytotoxicity, however it exhibited intermediate potency on H9C2 cells, therefore, it needs to be examined further in different toxicity test prior to verifying as potential cancer lead compound.

1. Introduction

1.1 Leukemia

Leukemia can be defined as a group of malignant disorder which is characterized by a high degree proliferation, survival and immature hematopoietic stem cells in the blood and bone marrow (1, 2). Concerning registration, leukemia is the 15th most common diagnosed cancer and the 11th most common cause of cancer death worldwide (3).

Hematopoiesis is a production of differentiated blood cells in the organisms (4). This process is carried out by hematopoietic stem cells which are founded in bone marrow (4). These stem cells, via self-renewal mechanism, differentiate both to hematopoietic progenitor cells and hematopoietic stem cells: the hematopoietic stem cells repeat the prosses of differentiating, while hematopoietic progenitor cells divide into two different progenitors which are myeloid- and lymphoid progenitor. Furthermore, these cells develop continually to all types of blood cells as Figure 1 shows (5, 6). If deviation happens during the prosses of differentiation, it can lead to uncontrolled growth, and eventually leukemia.
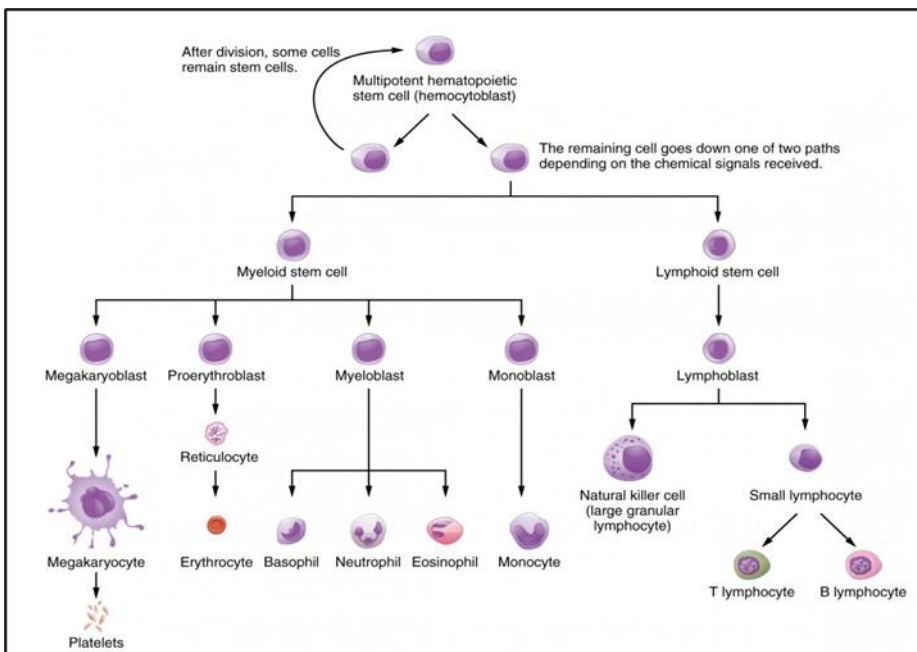

Figure 1. Schematic diagram of hematopoiesis and the differentiation of hematopoietic stem cells (7).

Leukemia can further be classified as acute or chronic, based on their clinical course, biological and morphological characteristics (8). Chronic leukemia develops gradually and slowly, and the symptoms appear over years (3, 8). Chronic leukemia cells can be characterized as mainly

mature and functional cells, and it can be classified both to chronic myeloid and chronic lymphoid leukemia, as shown in Figure 1 (8).

In contrast, acute leukemia develops much quicker, within days or months. It can be defined as a malignant disorder which is characterized by immature and less differentiated hematopoietic cells (3). Acute leukemia can be classified as either acute myeloid or lymphoid leukemia, based on its morphological, cytochemical or immunological characteristics (9, 10). Acute lymphoblastic leukemia (ALL) is one type of acute leukemia which occurs in lymphoid lineage of hematopoietic progenitor cells (Figure 1) (8). Mostly, ALL affects children, and it makes up 80% of pediatric leukemia (1, 11). It can also be seen in adults where it accounts for 20% of all leukemias (1, 11). Acute myeloid leukemia is the other type of acute leukemia, and this thesis will focus on this cancerous disease.

1.1.2 Acute myeloid leukemia

Acute myeloid leukemia (AML) is a heterogeneous disease characterized by poorly differentiated myeloid lineage cells and uncontrolled proliferation of immature myeloid progenitors (12, 13). AML is the most common leukemia with adults (1), and it accounts for approximately 80% of cases in this group (14). The incidence of AML varies from three to five cases per 100 000 population in the US, and it rises with age. In 2015, almost 20 830 patients were diagnosed with AML and 10 000 were deceased due to this disease in US (14). In Norway, the number of diagnosed patients is almost 150 each year (15). AML occurs more frequently with men than with women (15), and the median age is 70 (15, 16).

1.1.3 Diagnosis and disease progression of AML

In most cases, the cause of AML is unknown, but some risk factors have been identified to increase the risk of AML, and the following are the risk factors: previous exposure to radiation and chemotherapy, benzene and benzene-containing compounds. These can affect the bone marrow and can lead to AML (1, 14). People who were exposed to and survived the atomic bomb during WW-II in 1945, had more frequently instability in chromosomes 5 and 7, that are associated with AML disease. Moreover, people who work in the nuclear industry also have an increased risk of getting AML (16). However, in most of the AML cases, it is *de novo* malignancy (14).

When AML blasts fail to differentiate and respond to hormonal signals and cellular interactions, they accumulate within the bone marrow and lead to suppression of the growth and differentiation of normal blood cells (9, 17). This particularly affects the development of red blood cells, granulocytes and platelets as shown in Figure 1 (14). Consequently, it leads to different severe conditions, like anemia, infection, and hemorrhage (17, 18). Besides, AML blasts can also metastasize to other organ systems, like spleen, lymph nodes, liver, central nervous system (CNS), and skin after they have entered the peripheral blood (9).

Acute leukemia is diagnosed when the number of blasts in the blood or in the bone marrow is 20% or more (14). Further testing of the blasts is performed to find it the leukemia is of myeloid or lymphoid origin. For AML, positive tests are for instance myeloperoxidase activity, immunophenotyping or by identification of Auer rods in the cells (14). The diagnosis of AML can also be made even if the number of blasts is less than 20% and if leukemia-related cytogenetics or molecular genetics are present in the patient (19).

AML can be categorized into two systems: FAB and WHO-classification. For the past of 30 years, in the classification of AML, French- American-British (FAB) was utilized, and defined AML in eight subtypes (M0-M7) (1). In this system, the categorization of AML is based on cytomorphology and cytochemistry, and the diagnosis of AML began when blast count in the bone marrow was 30% (16). The WHO system is the most widely accepted classification system today and has replaced the FAB system (1). Unlike the FAB system, the WHO classification system has lowered the amount of blast to a minimum of 20% (16). Now, on the basis of WHO classification system, AML is classified as it is listed in Table 1 (1).

Table 1. WHO classification system of AML

AML with recurrent genetic abnormalities
AML with myelodysplastic (MDS)-related changes
Therapy-related myeloid neoplasms
Myeloid sarcoma
Myeloid proliferation related to Down's syndrome
AML not otherwise specified
Blastic plasmacytoid dendritic cell neoplasm

1.1.4 Current treatment of AML

The AML therapy consists of two phases: standard induction and postremisson or consolidation treatment (16). For nearly 30-40 years, the induction treatment in AML has remained without any significant changes (16).

The AML treatment should be started as soon as possible, within 5 days as the diagnosis of AML is made (15). The standard induction therapy consists of "7+3" regimens, where the patients receive a combination of 100-200 mg/m^2 cytarabine (AraC) continuous infusion for 7 days and an intravenous infusion of daunorubicin each day for the first three days (1). The first goal with induction treatment is a complete remission (CR) (20), and it is the sign of how effective the treatment was (16, 20). The CR is expected to be between 55-80 % in patients under the age of 60 (1). The CR can be defined as having less than 5% blasts in the bone marrow, the neutrophils count greater than 1000, platelets over 100 000 (1, 16) and no extramedullary disease (1) .

In case the patients of AML have reached CR, they receive consolidation treatment. This treatment consists of either high dose cytarabine (HiDAC) or hematopoietic stem cell transplantation (HSCT) (1, 21). The majority of the AML patients can risk relapsing the disease within four to eight months after induction treatment if they do not receive postremission treatment (1).

HiDAC is suitable for patients owing favorable cytogenetic AML disease, since HSCT is not recommended due to high risk of therapy-related mortality (TRM) (12). The most usual dose is 3 g/m^2 for every 12 hours over 3 days (Days 1, 3, and 5) for 3-4 cycles (1).

HSCT can be classified as autologous or allogenic HSCT and is another option in postremission treatment (21). In allogeneic HSCT (alloHSCT), the hematopoietic stem cells are donated from a healthy donor, often from family member (22), while in autoHSCT, the patients use their own stem cells (22) which were harvested and frozen before the patients receive intensive chemotherapy (23). AlloHSCT therapy is often recommended for patient with intermediate and poor risk disease (1, 24), and the treatment can reduce relapse of AML compared to chemotherapy alone, especially for patients with adverse cytogenetics (1, 25). However, alloHSCT is associated with increased risk of TRM due to graft-versus-host disease (GVHD) (26). Furthermore, intermediate cytogenetics AML patients can also receive autoHSCT

treatment (1). The advantage of this therapy is that the patient has a greater chance of receiving chemotherapy at the same time without an increased risk of GVHD (1). Besides, autoHSCT reduces TRM, but it is a higher risk of relapse and relapse-related mortality (24).

"Although advances in the treatment of AML have led to significant improvements in outcomes for younger patients, prognosis in the elderly who account for the majority of new cases remains poor" (14). About 50 percent of the patients diagnosed with AML are older than 70 years (12), and the incidence continues to increase with age (27). Elderly patients with AML often have unfavorable cytogenic and molecular risk factors, and this increases the risk of resistance to chemotherapy and relapse (27).

Patients diagnosed with AML in older age, often have multidrug resistance, other comorbidity, and poor performance status, in addition to unfavorable risk cytogenetics (1, 12). These factors make it difficult to treat elderly patients (28) because of high incidence of comorbidity and reduced performance make them less tolerant for intensive chemotherapy (20, 29), and in these patients, the cytostatic drugs increase the risk of toxicity and causality (1, 20). Another alternative is to treat them by low dose cytarabine (LDAC), hypomethylating agents (HMAs), supportive care, including hydroxyurea (HU) and clinical investigational drugs (29, 30). The advantage with these treatments is that they are associated with less treatment-related mortality compared to induction regimes, but the results in elderly patients are still poor (12).

However, some elderly patients may be considered as good candidates and have benefit from "7+3" induction regimens with chemotherapy, especially if the patients have favorable cytogenetic AML and good performance status (20). CR can be achieved in 40-60% of elderly patients, but the outcomes are still poor (28), and 15-20 % of those who receive intensive care die due to treatment-related complications (30).

Chemotherapeutic agents can have both short-term and long-term side effects, and this can limit in increasing the dose of the drugs. In addition to cancer cells, chemotherapy also affects normal cells that grow rapidly, for example hair follicle cells, hematopoietic stem cells (HSC) and cells in the gastrointestinal tract (GIT). This then increases the risk of side effects such as bone marrow toxicity and infection, inflammation in GIT and hair loss (alopecia) (31).

DNR and cytarabine can cause severe bone marrow suppression and are cardiotoxic and neurotoxic, respectively (32, 33). Chemotherapies can also lead to therapy-related AML (t-AML) which is a late complication (34). Patients with t-AML often have poor prognosis and adverse cytogenetics compared to *de novo* AML (34), and it is resistant to conventional chemotherapy for AML. Currently, there are no effective treatments (35).

1.1.5 New therapies for AML

As described above, elderly patients do not tolerate the AML treatment because of decreased performance status and comorbidities. Besides, multidrug resistance and unfavorable-risk cytogenetic AML is seen often, and this makes them respond poorly to the treatment. Therefore, the OS in adult is very low, and approximately 70% of elderly patients > 65 years die from the disease within one year (14). The current AML treatment is not satisfactory (29), and a further improvement and more individualized treatments for AML patients is needed. There are approved some specific AML drug candidates in recent years, and more candidates are in clinical trials. These drug candidates are classified as a cytotoxic drug, targeted small-molecule inhibitors, and monoclonal antibodies (36). Some of the currently approved drugs are listed below:

Midostaurin is a type 1 FLT3 inhibitor which is certified as induction, consolidation, and maintenance therapy for patients with relapsed/refractory AML in Europe (37). FLT3 is a transmembrane ligand-activated receptor tyrosine kinase (RTK) which is important in early stages of both myeloid and lymphoid lineage development (38). FLT3 mutations occurs on 30-35% new diagnosed AML patients (38), and this drug has an overall survival benefit in combination with induction chemotherapy, consolidation and as maintenance therapy (37, 38).

Venetoclax is an inhibitor of the antiapoptotic protein BCL-2, and it is an effective and well-tolerated drug for elderly AML patients, in combination with hypomethylating agents such as azacitidine or decitabine. This combination has also enhanced overall survival (OS) and has high complete remission (CR) and complete remission with incomplete hematologic recovery (CRi) (37).

Isocitrate dehydrogenase (IDH) enzymes catalyze the conversion of isocitrate to α-ketoglutarate in the oxidative decarboxylation cycle (37). Mutation in IDH proteins occur in 20 % of AML patients (37), and there are two types IDH mutations: IDH1 and IDH2. These mutant enzymes convert the isocitrate to 2-hydroxyglutarate which leads to pro-leukemic epigenetic changes

(37). IDH1 and IDH2 are substrates for targeted therapy of IDH inhibitors, Ivosidenib and Enasidenib, respectively (38). IDH inhibitors are a treatment for patients with relapsed AML, and CR and OS on these patients shows to be ameliorated (37). The inhibition of IDH enzymes leads to maturation and differentiation of leukemic cells (38). The problem with IDH inhibitors is the release of inflammatory cytokines from leukemic promyelocytes, which can be fatal unless the medication is discontinued (38).

Glasdegib is a smoothened (SMO) inhibitor which inhibits the Hedgehog signaling pathway (37). This drug was approved in November 2018 and is used in combination with low dose cytarabine to treat newly diagnosed AML patients who are more than 75 years old and patients with comorbidities (38). Compared with low dose cytarabine alone, low dose cytarabine has demonstrated an improved OS and CR in combination with Glasdegib (37).

Gemtuzumab ozogamicin (GO) is anti-CD33 monoclonal antibody conjugated to antibiotic drug calicheamicin, which is toxic to leukemic cells. GO was approved in 2001 to treat patients with relapsed AML. An improved event-free survival (EFS), relapse-free survival and OS have been shown in studies with GO in combination with chemotherapy on patients with favorable cytogenetic AML (37). However, the drug had severe side effects such as hepatic and hematologic toxicity and increased the risk of veno-occlusive disease after allogenic HSCT, and this led to withdrawal of the drug from the market in 2010 (37).

The new therapies have improved the treatment of AML in some way, but many of them still have severe side effects, and most of them work on the specific mutations. Besides, none have been able to replace the standard induction therapy of DNR and cytarabine. Therefore, there is still a need to develop drugs for improved treatment of AML.

1.2 Plant-derived anticancer drugs

Phytosubstances are already used in treatment of cancer, and it is also believed that many natural products with anticancer activity have not been yet discovered. The word "phyto" is derived from Elinika, the official language of Greece, which means plant. Generally, phytosubstance is interpreted as substances from plants. Across many cultures, natural medication is an important source in the treatment of various diseases (39), and natural products have been playing and still play a significant role in the discovery and development of

medicines (40, 41). Many drugs originate from natural sources such as plants, microorganisms, fungus, and marine organisms (41).

Plants contain many natural products that can have a growth inhibitory effect on other plants or prevent that they become attractive to herbivores. These compounds also comprise the molecular defense system of the plants against pathogenic organisms such as bacteria, viruses, and fungi. Examples of such natural products found in plants are tannins. When the herbivores start eating these plants, the plant secretes ethylene into the air which stimulates the production of tannins on neighboring plants. Tannins make the plants unpalatable or poisonous to the animals (40). In this way, the plants manage to survive (40), but at the same time tannins and other substances can be medically important in the treatment of diseases (42).

Furthermore, plants contain many compounds that can contribute to the prevention and treatment of cancer (39), and at least 35 000 high plant species have been screened for potentially anticancer activity (43). Of these, 3 000 plants were shown to contain cytotoxic activity (43). Nature is the source of more than 60% of chemotherapeutic drugs available on the market (40, 44), and many of the antineoplastic drugs are plant-derived agents (39). Some of the plant-derived anticancer drugs are further modified through synthesis, where parts of the molecule are modified to improve the drug's specificity, potency, selectivity, and bioavailability. These drugs are called semisynthetic drugs (45). Plants are still important in the discovery of new cancer drugs (43).

Today, there are 4 classes of chemotherapeutic agents that originate from plants and are used clinically in the treatment of cancer (40, 43). They are vinca alkaloids, epipodophyllotoxins, taxanes and camptothecin derivatives (43).

Vinca alkaloid (VA) compounds were first isolated from *Caratharathus roseus* (*C.roseus*) (Apocynaceae) (31, 40) found in the rainforest of Madagascar (40). These drugs have hypoglycemia and anticancer activity (46). Among the VA which are used to treat cancer are vincristine, vinblastine, vindesine and vinorelbine, all are used in the treatment of Hodgkin's disease, breast, liver, leukemia, testes, and lung cancer (31, 40). Vinorelbine, vindesine, vinfositline and vinovelbine are semisynthetic VA drugs, and they are used either alone or in combination with other chemotherapeutics drugs (31). The mechanism of action is binding to

tubulin, which inhibits polymerization of microtubules (46). This cause arrest of cell cycle at metaphase and eventually cell death (31).

Etoposide is a semisynthetic epipodophyllotoxin derivative (47) which is obtained from the mandrake plant *Podophyllum peltatum* and the wild chervil *Podophyllum emodi* (40). Etoposide works on late S- and G2-phase of the cell cycle, by inhibiting type II DNA topoisomerase and inhibiting the DNA synthesis, which leads to DNA strand breaks and apoptotic cell death (40, 47). Etoposide is amongst other, utilized in treatment of testicular cancer in combination with bleomycin and cisplatin, and against small cell lung cancers (40).

Taxanes, paclitaxel and docetaxel are derived from *Taxus baccata* trees. Paclitaxel was isolated from bark of *T. baccata*, *T.canadensis* and recently from the unrelated hazel tree, *Corus avellana*, while docetaxel is semi-synthetic esterified product of 10-deacetyl baccatin III, which is extracted from the renewable and readily available leaves of the European yew tree (48). Taxanes acts by stabilizing microtubules depolymerization and preventing chromosome separation which lead to mitotic arrest at M-phase (40, 49). Paclitaxel is used to treat ovarian, breast and lung cancers, while docetaxel has been effective in curing breast, pancreas, prostate, and lung cancer (31). In addition, paclitaxel is also used off-label in the treatment of gastroesophageal, endometrial, cervical, prostate, leukemia, sarcoma, lymphoma, and head and neck cancers (49).

Camptothecin was extracted from a Chinese ornamental tree, *Camptotheca acuminata Decne* (Nyssaceae). It is a potent topoisomerase I inhibitor (31), however it could not be used clinically due to its toxic effect to the urine bladder (50). After several research on camptothecin, two camptothecin derivatives have been developed, namely irinotecan and topotecan (31, 50). Camptothecin derivatives function as inhibitors of type I DNA topoisomerase enzymes (40). Irinotecan is used to treat colorectal cancers, while topotecan is used in the treatment of ovarian and small cell lung cancer (31, 50).

There are many anticancer drugs isolated from plants and natural products which are under investigation. Discovering new chemotherapeutics drugs has given researchers more interest in exploring natural source for other potential anticancer compounds (51, 52). Some of the antineoplastic drugs which are under development are flavopiridol and homoharringtonine.

Flavopiridol is a semi-synthetic flavone (31). The synthesis of flavopiridol is based on the chromone alkaloid, rohitukine, which was derived from four different plants *Amoora rohituka*, *Dysoxylum binectariferum, Schumanniophyton magnificum* and *Schumanniophyton problematicum* (51). Flavopiridol is on the phase II clinical trials (40, 51) and has shown cytotoxic activity, both used alone or in combination with cytostatic drugs (51). Flavopiridol inhibits the activation of cyclin-dependent kinase (Cdk) and block the cell cycle progression at the growth phase G1 or G2 (40).

Cephalotaxus alkaloids, harringtonine and homoharringtonine, are protein synthesis inhibitors which have good anticancer activity in combination with DNR and cytarabine against AML (53). They are isolated from the Chinese tree *Cephalotaxus harringtonia* (Cephalotaxacea) (40). Homoharringtonine in combination with harringtonine have been used to treat both acute and chronic myeloid leukemia in China (31).

Emetine is used to treat amoebiasis infection, and it is extracted from roots of *Cephaelis ipecacuanha* A, but it is also found in Alangiaceae, Icacinaceae, and Rubiaceae tree families. Emetine was entered phase I and II clinical studies in 1970s, but it exhibited severe side effects such as cardiotoxicity and this led to discontinuation of the clinical trials on emetine (54). However, an emetine derivate is under development (54). The mechanism of action of emetine is inhibition of protein and DNA synthesis and increase pro-apoptotic factors (54, 55).

1.3 Different stage of anticancer drug discovery

The discovery of a drug is complicated and expensive. Furthermore, it takes several years for a newly discovered drug to be accessible on the market (56). Before a drug candidate can be tested on human beings, it must goes through many different studies (56). Drug screening starts with *in vitro* studies which are carried out on different cell lines or biochemical assays (56). This way of testing is cheaper and easier to perform (57). Natural products and other potential anticancer drugs are for instance tested to assess whether the compounds have the ability to inhibit the growth of cancer cells (56). In this thesis, *in vitro* testing was utilized where several natural products were screened for a potential anticancer activity on leukemia cell lines.

A drawback of *invitro* studies is that the complexity of the cancer is not reflected in cell lines and a drug that exhibits a positive potential of cytotoxic activity in *in vitro* may fail later due to for instance poor pharmacokinetic properties (56).

When a drug is found to have a promising anticancer activity, it proceeds to be tested on animals (*in vivo* studies) (56). This method further helps to analyze the toxicity of the drug, its bioavailability and therapeutic effect before it proceeds into clinical studies (58).

1.4 Aims

This study aimed to explore natural compounds with anticancer effect on acute myeloid leukemia. The work was divided into four parts:

1. Screen natural compounds for cytotoxicity towards one AML cell line (MOLM-13) and one normal cell line (NRK) in order to identify compounds which selectively kills leukemia cells.

2. Based on the result from part 1, select compounds with desired cytotoxic activity and further examine their antileukemic potential by testing on two other leukemic cell lines and one more normal cell line (H9C2).

3. Test the selected compound for cytotoxic activity on MOLM-13 cells in combination with chemotherapeutic drugs. This, to find if the compounds can be used in combination therapy.

4. Examine the molecular mechanisms behind the cytotoxic activity of 1-3 compounds on MOLM-13 cell by western blot analysis of key death and survival proteins.

2. Experimental theory

2.1 Cell lines

In this thesis, three different leukemic cell lines (MOLM-13, MV4-11 and OCI-AML3) and two normal cell lines (NRK and H9C2) were used.

MOLM-13 (ACC-554, DSMZ) is the most used AML cell line in this study (59). It was initially collected from the peripheral blood of a 20-year-old man with relapsed AML in 1995 after initial myelodysplastic syndromes (MDS). MOLM-13 is classified as M5a AML by FAB classification system (59).

MV4-11 (ATCC, CRL-9591) was established from blast cells of a 10-year-old male with biphenotypic B myelomonocytic leukemia (60), while OCI-AML3 (ACC-582, DSMZ) is a FAB M4 leukemia cell line which was developed from peripheral blood of a 57-year-old male patient with AML in 1987 (61).

NRK (ATCC, CRL-6509) is a normal epithelial rat kidney cell line which was derived from adult Osborne-Mendel rat (62), while H9C2 (ATCC, CRL-1446) is a cardio myoblast cell line derived from embryonic rat heart tissue (63).

2.2 Cell viability assay

In this study, two viability assays, measurement of metabolic activity, and nuclear staining assay, were used to determine the cytotoxicity effect of the natural products on the different cell lines.

2.2.1 Metabolic activity-based WST 1 assay

Cell viability assay is utilized to determine the amount of living cells after they are treated with drug compounds during drug screening (64). In this study, WST-1 was used to measure the cell viability based on the metabolic activity of the examined cells. WST-1 added to the cell culture medium, diffuses into the cells where it is converted into a water-soluble formazan dye by mitochondrial dehydrogenase enzymes of metabolic active cells as shown in Figure 2 (64, 65). This can usually be detected after 0,5 - 4 hours of incubation. The formazan product has a distinct color that can be detected by a spectrophotometer, measuring absorbance at 450 nm, with a reference read at 620 nm. A well with high proportion of viable cells has high enzyme activity and will produce a higher signal compared to a well with less viable cells. Thus, it can

be concluded that the amount of formed formazan dyes is proportional to the number of living cells (65). The percentage of viable cells were estimated by dividing to untreated viable control cells.
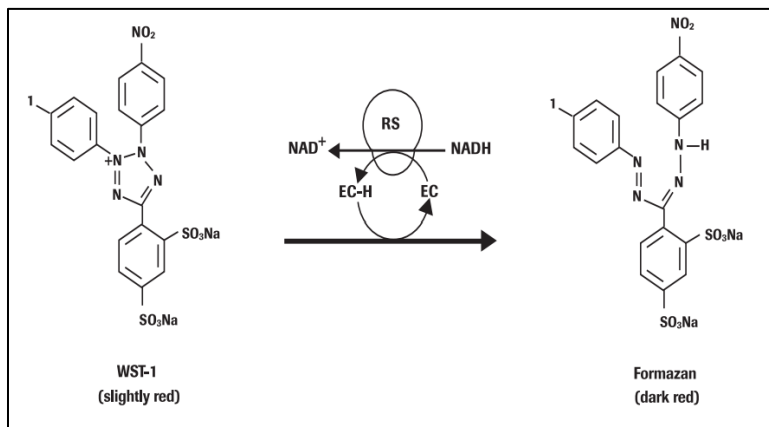

Figure 2: Conversion of WST-1 to formazan by mitochondrial enzyme activity on viable cells. (EC = electron coupling reagents, NAD = nicotinamide adenine dinucleotide, H = hydrogen) (65)

2.2.2 Nuclear staining assay for determination of cell viability

Another method to determine cell viability is to stain the cell nucleus by adding the DNA dye Hoechst 33342 to cells that are fixed with formaldehyde. It binds at adenine-thymine (A-T) base pairs in the minor groove of the double helix (66, 67).

The morphology of the treated cells is examined under the UV-microscopy (66). Apoptotic cells stained with Hoechst often have hypercondensed or fragmented nuclei, while normal cells have less condensed DNA, and the nuclei appear less bright (68).

In this study, the examined cells were fixated in a 2 % buffered formaldehyde solution containing the Hoechst 33342 dye after the WST-1 absorbance were determined.

2.3 Bradford assay and western blot analysis

Bradford assay, also known as Coomassie brilliant blue protein assay, is a colorimetric assay that is used to measure protein concentration in a sample before performing western blot analysis (69, 70). Bradford assay is based on the use of Coomassie Brilliant Blue G-250 (CBB), which is one of the two Coomassie dyes. Coomassie R-250 is utilized only to stain protein gels, not in protein assays (71).

CBB dye reacts with proteins by forming ionic and hydrophobic bond with amino acids in acidic condition (70, 72). These interactions produce a dye-protein complex, and an absorbance shift from 465 to 595 nm, which is used to quantify the concentration of protein samples (72).

In Bradford assay, the procedure is performed with blank, a series of standards with known concentration of Bovine serum albumin (BSA) and protein samples with unknown concentration (69). Standards are used to make calibration curve, and the estimates of the unknown protein concentrations should be within the standard curve since the concentration is calculated based on the equation from calibration curve (69).

Western blot is a technique often used to separate and detect a specific protein in a protein sample, after the concentration of protein is determined by Bradford assay. The protein concentration is then used to calculate the volume of protein which will be loaded in electrophoresis gel. Furthermore, the protein lysates are mixed with a loading buffer, which gives the proteins a negative charge, and a dye which helps to visualize the protein during running in polyacrylamide gel. The protein samples are also denatured by heat to primary structure (73).

Then, the proteins are subjected to gel electrophoresis, where they are separated based on their molecular weight. The negative charge of the proteins enables them to move towards positive side in the electric field (73).

The polyacrylamide gel electrophoresis in a western blot consists of two different gels: stacking gel and separating gel. The stacking gel is the upper layer which is slightly acidic (pH 6.8) and has a low concentration of acrylamide. This layer does not affect the separation of proteins, but it makes them form thin and defined bands. The secondary layer is a basic separating gel with pH around 8.8 and has a high concentration of acrylamide which tightens the pores of the gel. This allows the proteins with smaller weight to migrate more easily and faster, while the largest proteins move slower (73).

After the proteins are separated, they are transferred to a nitrocellulose or polyvinylidene fluoride (PVDF) membrane using electric field. It is important that the membrane is placed on the correct side, that is on the positively charged side, and the gel on the negatively charged side, so that the negatively charged proteins move toward the positive field and bind to the

membrane. After that, the membrane is blocked to prevent unspecific binding of the antibodies and incubated with a primary antibody which has a specific binding site to a specific protein. Unbound primary antibody then is removed by washed steps before, the membrane is incubated with a secondary antibody. The secondary antibody is coupled to a fluorescent or chemiluminescent probe which allows the specific protein of interest to be detected (73).

3. Materials and Methods

3.1 Natural compounds

All compounds were supplied by Professor Torgils Fossen, Department of Chemistry, University of Bergen, and details and structures are listed in Appendix I. Four compounds were synthetic, and others were prepared by pharmacy students during their masters' thesis from 2019, 2020 and 2021. The structure of all the natural products had been determined by NMR. In total, 30 natural products were received. 23 of these compounds were dissolved in DMSO by Pr. Torgils, while the remaining seven were provided as a powder and were dissolved in DMSO (Sigma-Aldrich, Darmstadt, Germany) to obtain a concentration of 100 mg/ml. However, two of them could not be dissolved at this concentration and was dissolved in lower concentration by adding more DMSO and treating by heat at 37^0C. All compounds were stored at -80^0C and were brought to room temperature during the experiments. Further dilutions of the compounds were in cell culture medium.

Compounds 3-6 are isolated from *Plantago major* (Plantaginaceae). Compounds 3 and 5 are flavones, while compounds 4 and 6 belongs to a class of compound known as phenylpropanoid glycoside.

Compounds 2, 7, 10 and 11 were isolated from *Peucedanum ostruthium*. Compounds 2, 7 and 10 belongs to a class called flavonoids and the last compound is a polyphenol. Compounds 8, 9, 12 and 13 are isolated from Norway maple (*Acer platanoides*), and compounds 8, 9 and 13 are flavonoids, while compound 12 is gallotannin.

Compounds 18 and 19 belong to a class of compound known as phenylpropanoid glycoside and they were extracted from the world's oldest tree, Japanese umbrella-pine (*Sciadopitys verticillata*). Natural products 27-30 were isolated from Nuphar lutea by pharmacy student Vilde S. S. Bulling. The two first compounds are tannins, while the two later are flavones.

Compounds 20-25 were obtained from *Pteridium aquilinum* by pharmacy student Malgorzata D. Szymczak. Compounds 20, 21 and 25 are members of the polyphenolic class, while compounds 23 and 24 are flavonoids. Moreover, compounds 23 and 24 turned out to be identical with compounds 8 and 9, respectively (Appendix I). Compound 26 was isolated from *Matricaria chamomilla* (known as chamomile) by pharmacy student Catherine Nguyen.

The synthetic products in this study are compound 1, and 14 - 16, which are chalcone and belongs to flavonoid family, NSAID, phytosteroid sapogenin and polyphenol, respectively. Compound 17 is a human metabolite which was obtained from Dr. Rune Slimestad.

3.2 Cell culture conditioning

3.2.1 Cell culturing

All cells were incubated in humidified atmosphere at 37^0C and 5% CO_2, and all cell handling were conducted in a Scanlaf Laminar Air Flow (LAF) Mars safety bench from Labogene (Allerød, Denmark) under sterile condition. The culture mediums were supplemented with 10% fetal bovine serum (FBS), 100 IU/ml penicillin and 100 mg/ml streptomycin. The culture media were stored at 2-8ºC. All culture medium and supplements were from Sigma-Aldrich (Germany).

Culturing of suspension cell lines

MOLM-13, MV4-11 and OCI-AML3 cell lines are suspension cells, and they are cultured in three different culture media. MOLM-13 were cultured in Roswell Park Memorial Institute (RPMI)-1640, MV4-11 in Iscove's Modified Dulbecco's Medium (IMDM) and OCI-AML3 in Dulbecco's Modified Eagle's Medium (DMEM). RPMI and DMEM were supplemented with 2mM L-glutamine (Sigma-Aldrich), while IMDM were supplemented with 4mM L-glutamine. Otherwise, all the media contained the supplements which are mentioned above in addition to L-glutamine. These cells were maintained at a density $10\text{-}70*10^4$ cells/ml and were diluted by adding fresh medium every 2-3 days in a new suspension culture flask (25 or 75 cm^2). The cell concentration was determined by counting the cells using a hemocytometer and a light microscope.

Culturing of adherent cell lines

The normal kidney epithelial cell line (NRK) and cardiomyocyte H9C2 cell line are adherent cells, and they were cultured in DMEM with the same supplement as in OCI-AML3 cell line. These cells were cultured until they reached 70-90% of confluence. Then, they were split by removing the medium, washing them with autoclaved phosphate buffered saline (PBS, Sigma-Aldrich) and adding trypsin (Sigma-Aldrich) so that the cells detach from the tissue flask. The cells were incubated with trypsin for 2-3 minutes to ensure sufficient detachment, before 5mL DMEM was added, which inactivates the trypsin. The cell suspensions were transferred to

centrifuge tubes and centrifuged at 200 X relative centrifugal force (RCF) for 5 minutes. Then, the supernatant was removed, while the cell pellet was resuspended in fresh DMEM and the cells cultured in new tissue flask (25 or 75 cm^2) at 20-35% confluence. Adherent cells were not utilized after 12-14 passages.

3.3 Cell screening assay

3.3.2 Determination of cell viability based on metabolic activity and nuclear morphology

To estimate the amounts of viable cells after 24 or 72 hours of treatment, 10 μL of the WST-1 reagent diluted 1:1 with sterile PBS (Roche Diagnostics GmbH. Cell Proliferation Reagent WST-1. Sigma-Aldrich, Merck) was added to each well. Afterward, it was incubated for 2 hours to allow viable cells to convert the WST-1 reagent to reporter dye, before measuring the absorbance of formazan by using a 2103 Envision Multilabel plate reader (Perkinelmer) at 450 nm wavelength and a reference wavelength at 620nm. Finally, the cells were added 100 μl 4% buffered formaldehyde solution containing 0.1% Hoechst 33342 DNA stain (Sigma-Aldrich). Then, the plate was stored at + 4°C in a dark place.

Most of the natural compounds were colored which interfered the measurement of absorbance from formazan. This problem was solved by measuring the absorbance of compounds mixed with culture medium without cells at the same concentration which was used on the screening assay. They were incubated both for 24 and 72 hours before the absorbance was quantified on microplate reader. These absorbances were subtracted from the values of cell screening to minimize the effect of the color. The absorbance of formazan was estimated using the equation below:

$$\frac{\text{Average A of treated cells} - \text{average A of the background control}}{\text{Average A of untreated cells} - \text{A of the background control}} \qquad \text{Eq (1)}$$

where A = absorbance

The fixed cells were studied using Nikon Diaphot 300 inverted microscope fitted with a Nikon DS-Fi3 camera. The cells were counted using the software ImageJ 1,53e (Wayne Rasband and contributors, National institute of Health, USA), and the living and dead cells were counted based on their nucleus morphology as it is shown on Figure 3. The dead cells were strong fluorescent and they had either fragmented or hyper-condensed DNA.

The data from counted viable cells were used to confirm the result from WST-1 by finding the ratio between the viable cells and the total counted cells to find the percentage viable cells. To estimate the percentage of viable cells in relation to untreated cells, it was divided by untreated control viable cells.
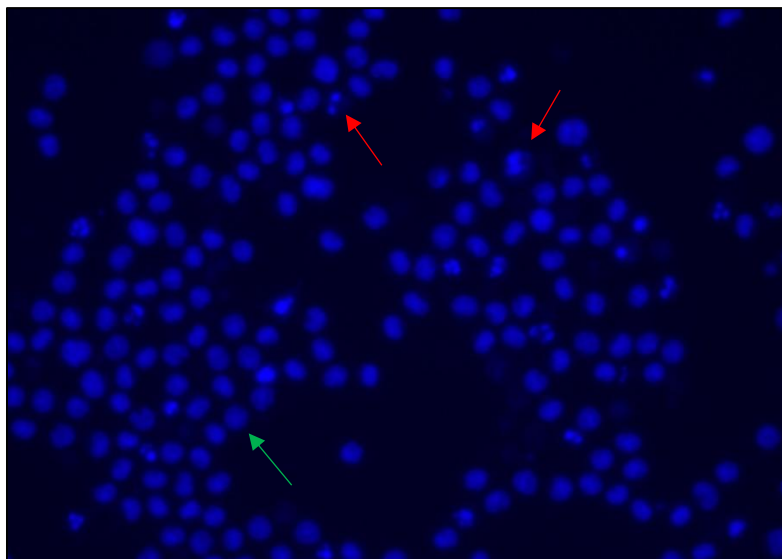

Figure 3: A picture of fixed MOLM-13 cells in 2% buffered formaldehyde solution containing fluorescent Hoechst DNA dye. The red arrows show the apoptosis, and the living cells are shown by green arrow.

3.3.1 Cytotoxicity assay

MOLM-13, NRK, OCI-AML3, MV4-11 and H9C2 were cultured in 96 well plate with a total volume of 100 μl/well. The suspension cells (MOLM-13, OCI-AML3 and MV4-11) were seeded with a concentration of 15 000 cells/well when incubated for 24 hours, and 7000 cells/well for 72 hours incubation. The suspension cells were treated the same day as they were seeded. The cell concentration of the adherent cell lines (NRK and H9C2) was 2500 and 1000 cells/well for 24 and 72-hours incubation, respectively, and they were seeded the day before testing to ensure they attached to the 96 well flat bottom plate.

All compounds were first screened on MOLM-13 and NRK cell lines with three parallels for each compound. The tests were done with high start concentration of the compounds in serial dilution to explore the cytotoxic potential on these cells. For instance, compounds 1, 2 and 6 were first tested with high start concentration, which resulted in too high apoptosis, particularly on MOLM-13. Therefore, these compounds were tested again with lower starting concentration on MOLM-13.

Many of the natural compounds showed cytotoxic activity on both cell lines. However, only 10 test compounds were selected based on their potency and efficiency, to be tested further on OCI-AML3, MV4-11 and H9C2 cell lines. Test on these cells were performed similarly to MOLM-13 and NRK cell lines, and the start concentration of the 10 chosen compounds were determined based on the results from MOLM-13 and NRK cells.

3.3.3 Calculation of the EC_{50} value of cytotoxic compounds

Half maximal effective concentration (EC_{50}) is a concentration of a drug that gives 50% of maximum effect, which in this study is 50% cell death after a certain exposure time. After the data from WST-1 assay were collected, EC_{50} value of each compound which had cytotoxic effect was estimated by four parameter non-linear regression using software SigmaPlot 2004, version 9.01. The equation for four parameters non-linear regression is expressed on Equation **Feil! Fant ikke referansekilden.** .

$$y = \min + \frac{(\max - \min)}{1 + \left(\frac{EC50}{x}\right)^h} \qquad \text{Eq (2)}$$

y is the response or the apoptosis, x is the dose of the compounds, max and min is maximal and minimum cell death which is limited between 0 and 1.

3.3.4 Test of synergy between natural compounds and anticancer drugs, and calculation of coefficient of drug interaction (CDI)

From the compounds with cytotoxic activity, compounds 1, 2, 4, 6, 11, 12, 15, 19, 27 and 28 were tested in combination with cytostatic drugs to reveal potential synergistic effects. The chemotherapeutic drugs which were utilized in the assay were daunorubicin (Sanofi Aventis, Lysaker, Norway), emetine (Sigma-Aldrich), venetoclax (Cayman Chemical, Ann Arbor, Michigan, USA), cytarabine (Fresenius Kabi, Bad Homburg vor der Höhe, Germany), cisplatin (Accord healthcare, Durham, North Carolina, USA) and bortezomib (Accord healthcare). All compounds and drugs were tested in three different concentrations in two parallels on MOLM-13 cell lines. The concentration of both the compounds and cytostatic drugs were first determined by testing them alone. This experiment lasted for 24 hours. The cell viability was analyzed by WST-1, and the results were utilized to determine the coefficient of drug

interaction (CDI), which is defined as the ratio between the results from combination drugs and the product of the compound and anticancer drug alone. CDI is expressed in the equationEq (3) (74):

$$CDI = \frac{R_{Combination}}{R_{Drug\ 1}\ \times\ R_{Drug\ 2}} \qquad \text{Eq (3)}$$

A CDI below 0.7 shows that the combination drugs have synergistic effect, and the antagonistic effect is defined when the value is above one. A CDI between 0.7-1 indicates additive effect.

Moreover, one-sample t-test for CDI results of the ten compounds was done to examine whether the average CDI value for each combination was statistically different from one, using software SigmaPlot 2004, version 14. If the data did not show normal distribution, the software analyzed the data using a one sample signed rank t-test instead. This applies to compound 1 in combination with emetine and bortezomib, and combination of compound 11 and cytarabine. The values were considered as statistically significant when $p < 0.05$, and the p-values are treated as following: * indicate p-value < 0.05, ** p value < 0.01 and *** p-value < 0.005.

3.3.5 Time kinetic experiment

MOLM-13 cells were seeded in 12-well plates at a density of 500 000 cells/well and incubated with compounds 1, 6 and 11. The plate was placed in the incubator, and at 0.5, 1, 3, 6, 9, 12 and 24 hours 50 μl of the cell culture was transferred to 96 well plate containing 50 μl 4% fixative solution in each well. The day after the experiment, the cells were analyzed under the microscopy and two pictures of each well were taken. The cells were counted as described on section 3.3.2 Determination of cell viability based on metabolic activity and nuclear morphology, and the percentage cell death was calculated using equation Eq (4).

$$\% \text{ apoptosis in sample} - \left(\% \text{ apoptosis in ctrl} \times \frac{100 - \% \text{ apoptosis in sample}}{100 - \% \text{ apoptosis in ctrl}} \right) \qquad \text{Eq (4)}$$

, where ctrl = untreated control cells and sample = cells treated with natural compounds

3.3.6 Cell lysis preparation of protein extracts

MOLM-13 cells were treated and incubated with two different concentrations of compounds 1, 6 and 11, in addition to DMSO for 2 hours. Then, 50 µl from cell solutions were transferred to 50 µl 4% buffered formaldehyde containing fluorescent DNA dye Hoechst. Afterward, the remaining cell solutions were transferred to microtubes and were washed with 4^0C 0.9% NaCl solution and centrifuged 200X RCF at 4^0C for 5 minutes twice. Then, the supernatant was removed before the cell pellets were resuspended by adding 50 µl lysis SHIEH buffer, which containing 10mM Tris-HCl (pH 7.5), 1mM EDTA, 400mM NaCl, 10% glycerol, 0.5% NP-40, 5mM NaF, 0.5mM Na-orthovanadate, 1mM dithiolthreitol (DTT) supplemented with Complete Mini Protease Inhibitor Cocktail (Sigma-Aldrich).

Next, the cell lysates were left on ice for 30 minutes before being centrifuged at 13 000 RPM for 30 minutes using Allerga X-22R Refrigerated benchtop Centrifuge (Beckman Coulter). The protein lysates were next transferred to a new microtube and were stored at -80ºC.

3.3.7 Bradford assay and western blotting

Braford assay was utilized to determine the amounts of proteins in the lysates. Five microtubes for standard curve, one for blank and ten for each lysate were prepared. All solutions and the protein lysate were brought to room temperature. The blank was filled with 1000 µl Quick Start Bradford 1x Dye Reagent (#5000205, Bio-Rad, Hercules, California, USA). Bovine serum albumin (BSA, 2 mg/ml) was transferred to standard curve samples with increasing volume (1, 2, 3, 4, 5 µl), and each microtube was filled with Bradford dye reagent up to 1 ml. The concentration of BSA in the five microtubes were 2, 4, 6, 8 and 10 µg/ml, respectively. For protein samples, 999 ml of Bradford dye reagent was added to all ten new microtubes before 2 µl of each protein lysate was added.

When the solution changed its color, 200 µl of the samples were transferred to a 96 well plate in triplicate. Finally, the absorbance was measured using 2103 Envision Multilabel plate reader at wavelength of 595 nm. The calibration curve was then determined using the results from the blank and standard curve samples, and the concentration of protein lysate was estimated by linear regression from the calibration curve.

The desired amount of the protein lysates was mixed with 5x and 1x loading buffer containing 20% sodium dodecyl sulfate (SDS) solution, 1M Tris-HCl, bromophenol Blue, dithiothreitol

(DTT), glycerol and Milli-Q water (Milli-Q Direct, Merck Life Science AS, Darmstadt, Germany). Afterward, the samples were heated at 100°C for 5 minutes, and then they were placed on ice for 5 minutes.

Then, 30 µl sample was loaded on two 10 % Mini-PROTEAN TGX Precast Protein Gels (Bio-Rad, Hercules, California, USA), and the chambers were filled with a 1X running buffer, containing 900 ml Milli-Q water and 100 ml 10x Tris-glycine-SDS (TGS, Bio-rad). Precision Plus Protein (#161-0373, Bio-rad) was used as protein ladder on both gels, and the gels ran at 100 V for 90 minutes.

Further, the proteins were transferred to two PVDF membranes using electric field in blotting buffer which was made of 800 ml Milli-Q water, 100 ml 10x TGS and 100 ml methanol (Sigma-Aldrich) at 100 V for 70 minutes. Then, the membranes were stained by a Ponceau S solution (#P7170, Sigma-Aldrich) for 5 minutes to visualize the protein bands and washed with water, NaOH and TBS-T which contained 10X TBS, 900 ml Milli-Q water and 1 ml Tween. The membranes were further blocked by 5% nonfat milk blocking buffer (containing 5g Skim Milk Powder (Sigma-Aldrich) diluted in 100ml TBS-T). The membranes were then washed with TBS-T before they incubated with primary antibody at 4°C overnight.

The primary antibody solution were removed, and the membranes were washed with TBS-T, and then incubated with secondary antibody for 1 hour. The primary and secondary antibodies used in this analysis are listed in **Feil! Fant ikke referansekilden.**. Anti β-actin was utilized as loading control.

The instrument ImageQuant LAS 4000 camera system (Cytiva) was used to detect the specific protein. The membranes were incubated in SuperSignal West Pico Chemiluminescent Substrate (#34080, ThermoScientific) for 3 minutes before detection. If no protein bands were detected, the membranes were further incubated with SuperSignal West Femto Maximum Sensitivity Substrate (#34096, ThermoScientific) for 1 minute, and the process was repeated.

Before using the next primary antibody, the membranes were stripped by Restore Plus Western Blot Stripping buffer (#46430, ThermoScientific, Waltham, Massachusetts, USA) and washed by TBS-T and blocked by blocking buffer as described previously.

All densitometric was quantified from western blotting pictures using ImageJ 1,53e (Wayne Rasband and contributors, National institute of Health, USA).

Table 2. Antibodies used for western blot analysis

Antibody (*=secondary antibody)	Molecular Weight (kDa)	Diluted in blocking buffer (*=diluted in TBS-T)	Source of antibody	Manufacturer
PAPR (#9542)	89 and 116	1:1000	Rabbit	Cell Signaling Technology, Inc (Danvers, US)
caspase 7 (#12827)	20 and 35	1:1000	Rabbit	Cell Signaling Technology, Inc (Danvers, US)
stat 5 (#9363)	90	1:1000	Rabbit	Cell Signaling Technology, Inc (Danvers, US)
p stat 5 (#9359)	90	1:1000	Rabbit	Cell Signaling Technology, Inc (Danvers, US)
caspase 9 (#9508)	49/39/37	1:1000	Mouse	Cell Signaling Technology, Inc (Danvers, US)
gamma-H2Ax (#NB100-384)	15	1:10 000	Rabbit	Novus Biologicals, USA
p 4E BP1 (#2855)	15-20	1:1000	Rabbit	Cell Signaling Technology, Inc (Danvers, US)
4E BP1 (#2845)	15-20	1:1000	Rabbit	Cell Signaling Technology, Inc (Danvers, US)
Peroxidase-conjugated AffiniPure Donkey Anti-Rabbit IgG (H+L)*	-	1:10 000	Rabbit	Jackson ImmunoResearch Europe Ltd, (Cambridgeshire, UK)
Peroxidase-conjugated AffiniPure Donkey Anti-Mouse IgG (H+L)*	-	1:10 000	Mouse	Jackson ImmunoResearch Europe Ltd, (Cambridgeshire, UK)

| Anti β-actin (#A5441) | 42 | 1:5000 | Mouse | Sigma-Aldrich, Inc (Darmstadt, Germany) |

4. Results

4.1 Cytotoxic potential of natural compounds

4.1.1 Screening for cytotoxic activity towards MOLM-13 and NRK cells

The purpose of this screening assay was to find out which compounds had cytotoxic activity on MOLM-13 and NRK cell line. In addition to that, to select compounds showing low EC_{50} value on MOLM-13 cells and less toxicity towards NRK cells for further experiment, since this would indicate that the compounds may selectively act toward AML cells. Therefore, the screening was first conducted by testing the 30 natural compounds on MOLM-13 and NRK cells.

All the 30 natural compounds were diluted with DMSO as described in section 3.1 Natural compounds and were first screened on MOLM-13 and NRK cell lines in triplicate. All screening tests were performed for 24 and 72 hours, and the cell viability was determined by WST-1 assay before the cells were fixated. Graphic illustration of the results is given in Figure 4 and for some selected compounds the dose-response results are also shown in Figure 5. The EC_{50} values were estimated using four parameter non-linear regression and the specific values are given in Appendix II. The EC_{50} values of each compound was graded according to its effect on both MOLM-13 and NRK cell lines simultaneously. The EC_{50} values was defined as low if the value was < 100 µM, high if > 500 µM, and intermediate when the value was between 100 – 500 µM (Figure 4). Figure 6 illustrate an example of UV-microscopic image for treated MOLM-13 and NRK cells with compound 6 for 24 hours.

As illustrated in Figure 4 and Appendix II, after 24 hours treatment of MOLM-13 cells, nine of 30 natural compounds exhibited low EC_{50} values, twelve compounds displayed intermediate EC_{50} value between 100-500 µM, and four compounds demonstrated low potency with EC_{50} value > 500 µM. The remaining five compounds had poor activity, and the EC_{50} value of these compounds were not estimated (see Figure 4 and Appendix II). When MOLM-13 cells were treated for 72 hours, sixteen compounds demonstrated high potency, four compounds showed intermediate EC_{50} value, and six compounds had low potency. Four compounds had no cytotoxic activity towards MOLM-13 cells (for more details see Figure 4 and Appendix II).

When NRK cells were screened with these 30 test compounds for 24 hours, one compound (**12**) had low EC_{50} value, three compounds exhibited intermediate potency, and eleven compounds had high EC_{50} value. The other fifteen compounds had no cytotoxic effect towards NRK cells. While upon 72-hour treatment of NRK cells, three compounds showed high potency, eight compounds had intermediate EC_{50} value, and seven compounds demonstrated low potency with EC_{50} value greater than 500 µM. Twelve compounds had poor cytotoxic effect, where the EC_{50} value could not be calculated (see Figure 4 and Appendix II).

As illustrated in Figure 4, compounds **4** (at 24 hours), **9**, **10**, 11 (at 24 hours), **15**, **17**, **19** and **26** did not shown cytotoxicity on NRK cells. However, only compounds 15 and 19 were chosen for further screening based on their selectivity and potency. Even though, the EC_{50} value of compounds 4 and 11 after 24 hours treatment towards MOLM-13 was calculated, the data had huge variations. Therefore, it is not certain that the compounds were cytotoxic.

First, the compounds were tested using a dilution series with max dose equal to 1% DMSO, which is the highest tolerable dose of DMSO for the cells. The compounds that were very potent, were additionally tested at lower starting concentrations. Compound **1** was screened with three different start concentrations (62.5, 250 and 1000µM) on MOLM-13, and all three concentrations showed antileukemic effect on MOLM-13 cells both for 24 and 72 hours (Figure 4, Figure 5 and Appendix II). The EC_{50} values for these three concentrations was identical both after 24 and 72 hours treatment, (11.3, 12.6 and 11.1 µM vs 7.2, 5.6, 5.3 µM, respectively) (Figure 5, Appendix II). However, NRK cells were only screened with 250 and 1000 µM start concentration of compound **1**. The EC_{50} value was slightly reduced after treatment with 250 µM of compound **1** (from 126 to 108.4 µM) (Figure 5, Appendix II). However, the NRK cells demonstrated some increasing on EC_{50} value after 72 hours treatment, but the EC_{50} values at 24 and 72 hours was also assumed to be similar, since the differences between the values were not large (see Figure 5, Appendix II). These data from MOLM-13 and NRK cells revealed that the experiment was nearly accurate, and the reproducibility was good.

MOLM-13 cells were treated with two different start concentrations of compounds **2** and **6**: 3.6 and 29.2 mM of compound **2**, and 1 and 7.8mM of compound **6**. The low and high start concentrations of compound **2** were cytotoxic for MOLM-13 cells, however, the EC_{50} values were unexpectedly highest for the lowest high concentrations after both 24 and 72 hours screening (479.3 vs 1056.2 µM) (Figure 5, Appendix II). Besides, the potency of both

concentrations of compound **2** decreased with time (Appendix II). However, the EC_{50} values of two start concentrations of compound **6** was similar both after 24- and 72-hours treatment (Appendix II).

As mentioned above, both MOLM-13 and NRK cell lines were tested with natural compounds for 24 and 72 hours. As expected, most of the EC_{50} values of the compounds were lower after 72 hours treatment (Figure 4, Appendix II). This applies for both MOLM-13 and NRK cell lines (Appendix II). However, in some cases the potency was the similar (same EC_{50} results) for the two incubation times. For instance, compounds **12** examined on MOLM-13 cells and compound **1** on NRK cell line had the similar EC_{50} results after the cells were treated for 24 and 72 hours (Appendix II).

Furthermore, compound **8** and **23**, as well as **9** and **24** are identical compounds from different plants, but with different stock concentrations. Compounds **23** and **24** had higher stock concentration than compounds **8** and **9**, and they demonstrated to have antileukemic effect in MOLM-13 cells after both 24- and 72-hours incubation (Figure 4). In contrast, the cytotoxicity of compounds **8** and **9** were shown only after 72 hours screening. In addition, the potency of these compounds on MOLM-13 cells are different. Compound **8** had low potency than compound **23**, while compound **24** showed somewhat higher EC50 values than compound **9** (Appendix II). When NRK cells were treated with these compounds, compounds **23** and **24** had cytotoxic activity on NRK cells for 24- and 72-hours incubation, but it was only compound **8** that showed cytotoxic effect after 72 hours treatment. However, the ratio of the EC50 value for these three compounds between MOLM-13 and NRK cells was over 4 (for more details see Appendix II).

Compounds **1**, **2**, **4**, **6**, **11**, **12**, **15**, **19**, **27** and **28** were selected to be further tested on OCI-AML3, MV4-11 and H9C2 cell lines based on their ability to distinguish between MOLM-13 and NRK cells. The ratio of the EC_{50} values between the two cell lines was over 4, except for compound 12 upon 72 hours treatment.
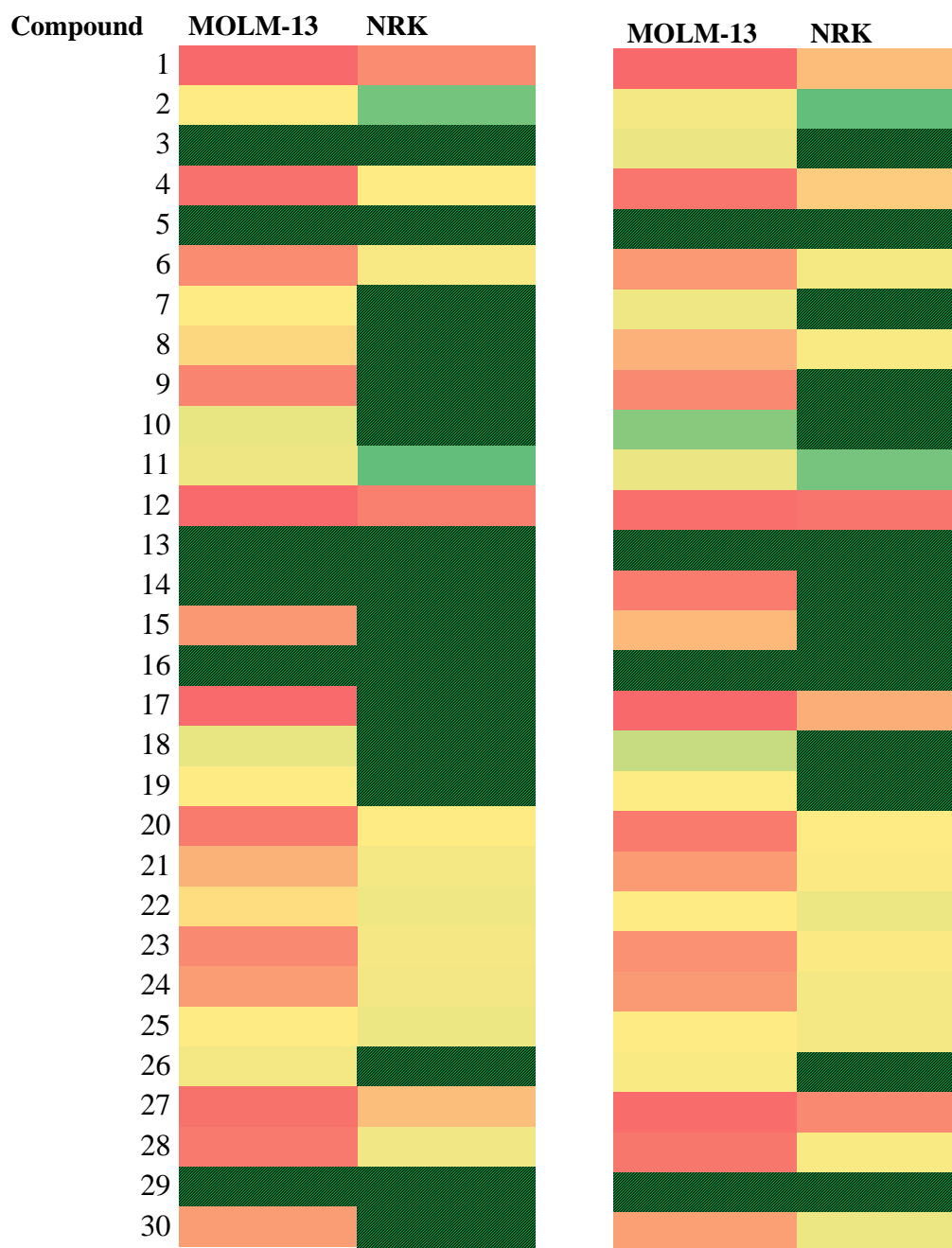
Figure 4: Screening test of 30 natural compounds on MOLM-13 and NRK cell lines for 24 and 72 hours. The EC50 values were estimated using equation Eq (2), and the values are given in Appendix II. The colors red, yellow, and green demonstrate the EC50 values from low to high. It was defined as low and high when the value was <100

and > 500µM, respectively, while intermediate when the value is between 100-500 µM. The compounds which are presented in black-green diagonal stripes, did not have cytotoxic activity on either MOLM-13 or NRK cell lines. Therefore, the EC50 value of these compounds were not calculated.
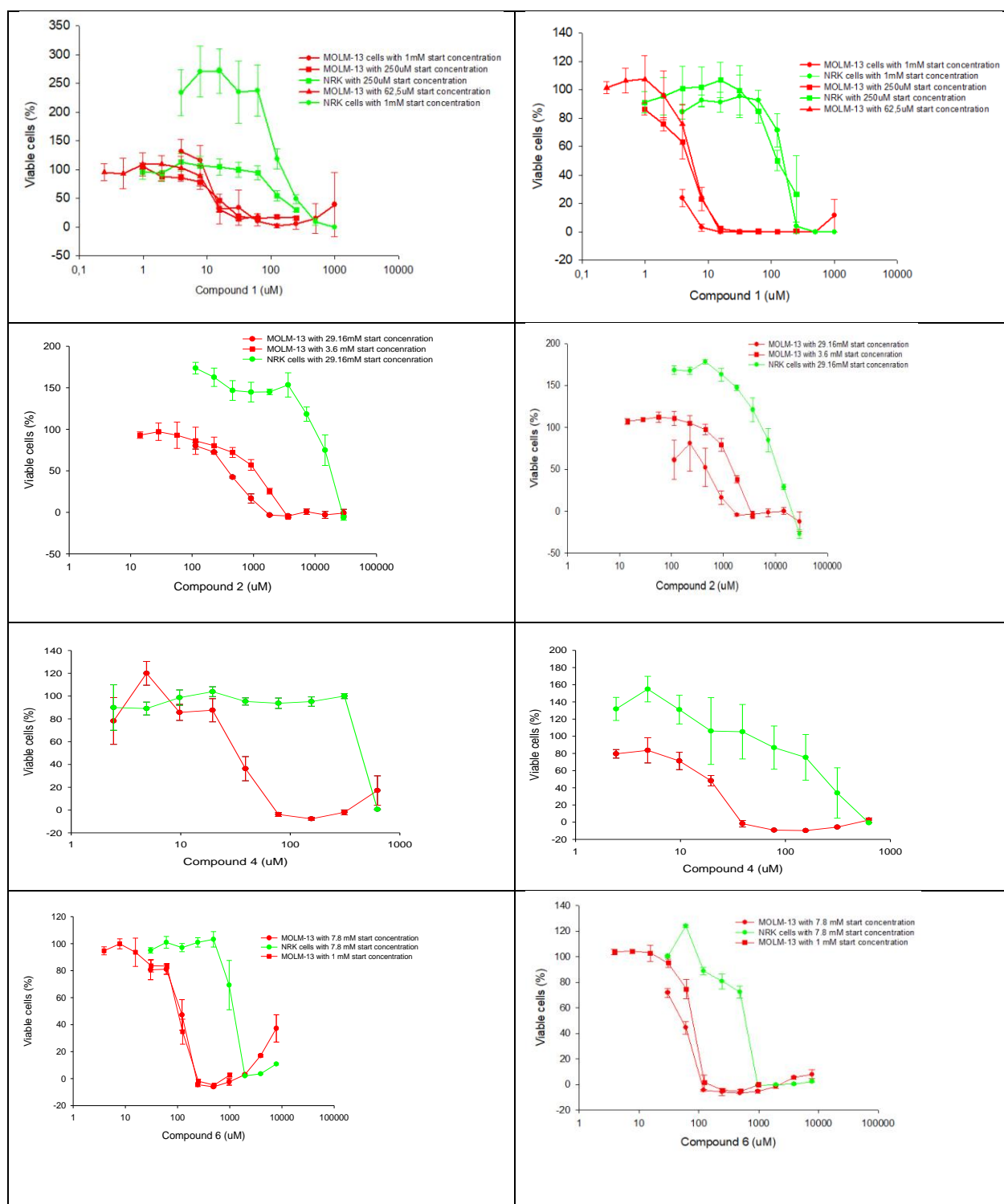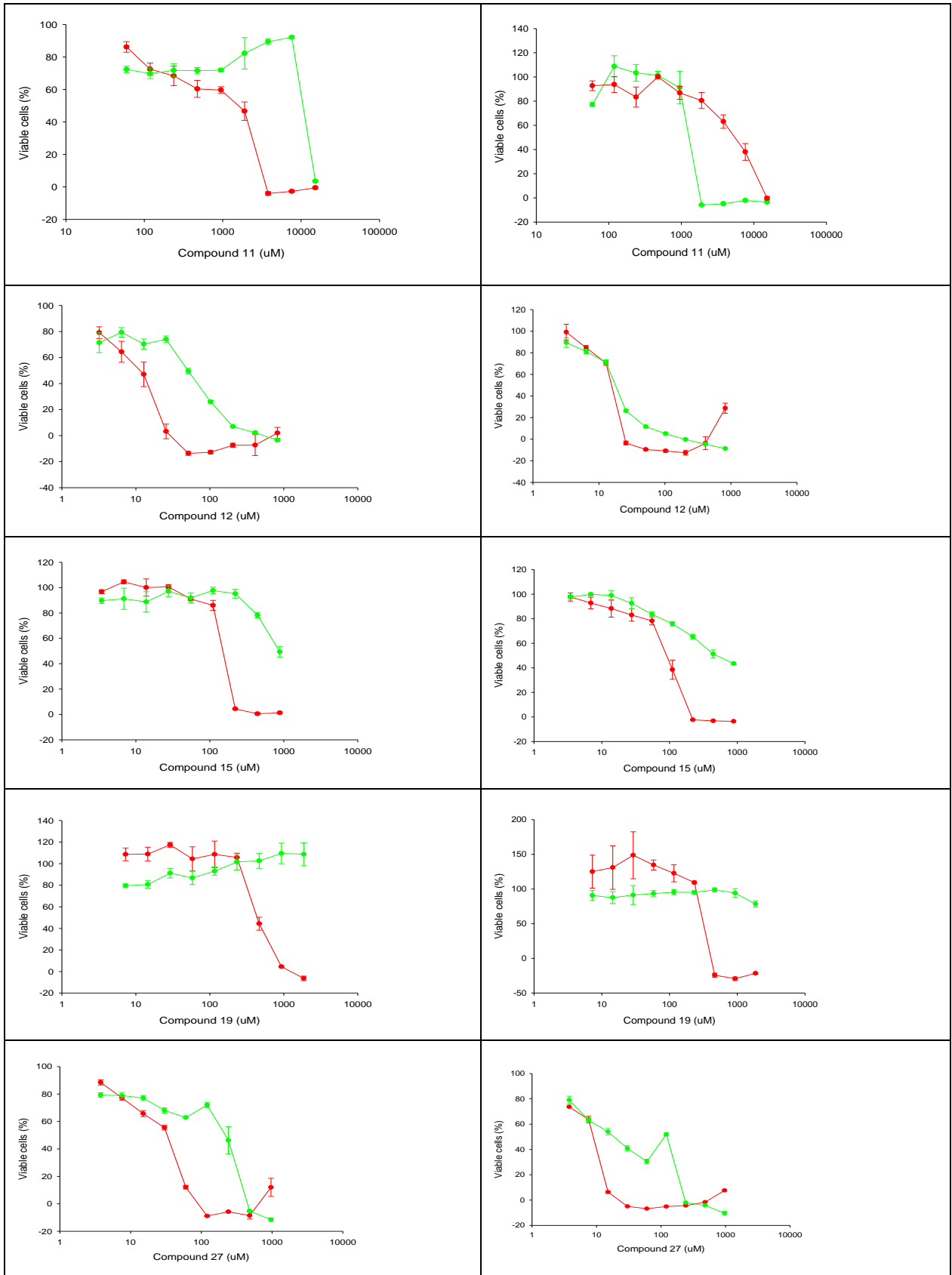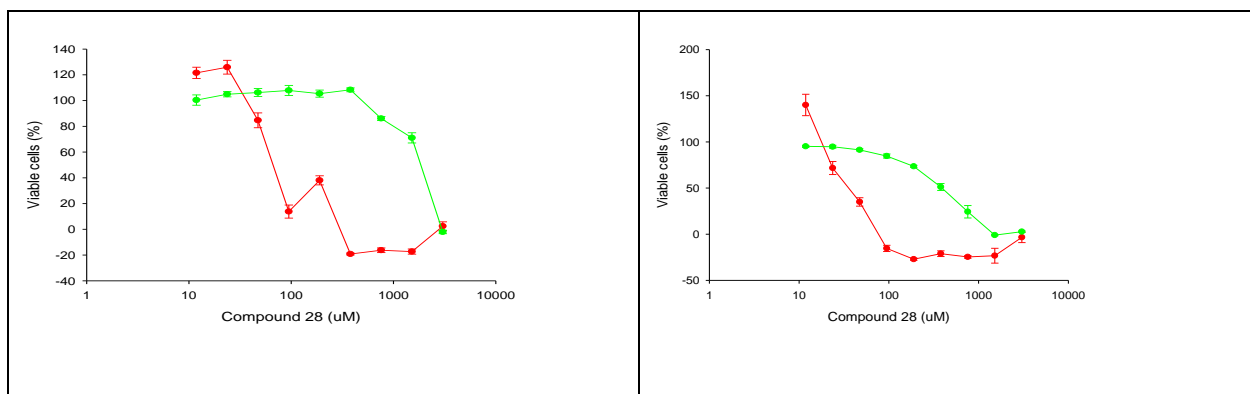
Figure 5: Dose-response curves from compounds **1**, **2**, **4**, **6**, **11**, **12**, **15**, **19**, **27** and **28** on MOLM-13 (red) and NRK (green) cells. The diagrams on the left are results from 24 hours screening, while those on the right are from 72 hours. Except for compounds **4** and **11** (for 24 hours), **15** and **19**, all other compounds were cytotoxic for NRK cells.
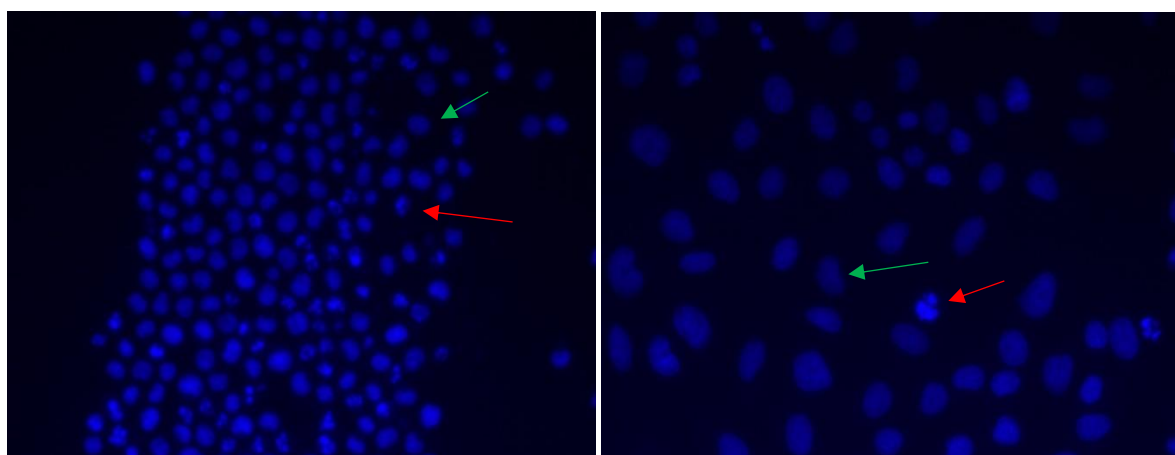
Figure 6: Fluorescence-microscope image of MOLM-13 (left) and NRK (right) cells. After WST-1 analyses, the cells were fixed in 2% buffered formaldehyde with the DNA-specific dye Hoechst 33342 in order to visualize the nuclear morphology. The red arrows demonstrate apoptotic nuclei, whereas the green arrows show the normal nuclei after 24 hours of treatment with compound **6**.

4.1.2 Drug sensitivity screening on OCI-AML3, MV4-11 and H9C2 cells

As described previously, ten selected compounds were further tested on OCI-AML3, MV4-11 and H9C2 cell lines to obtain a better impression of their anti-AML potential. The results are presented in Figure 7 and

Figure 8. Figure 9 shows an image of apoptotic and normal OCI-AML3, MV4-11 and H9C2 cells after the cells were treated with compound **2** for 24 hours and fixated and stained with Hoechst 33342.

All three cell lines were tested with compounds **1**, **2**, **4**, **6**, **11**, **12**, **15**, **19**, **27** and **28** for both 24 and 72 hours before the cell viability were quantified by WST-1 and fixated. However, some of the WST-1 results were not satisfactory, even though the experiments were repeated several times. This applies to OCI-AML3 and H9C2 cells treated with compound **12**, and H9C2 cell line examined with compounds **2**, **4** and **6**. The viability of these cells were therefore determined by counting the normal and apoptotic/necrotic nuclei (Figure 9). In order to calculate the EC_{50} values, four-parameters non-linear regression was used, and the values are listed in **Feil! Fant ikke referansekilden.**. The EC_{50} values were defined as mentioned earlier; low if the value was $< 100\,\mu M$, high if $> 500\,\mu M$, and intermediate when the value was between $100 - 500\,\mu M$ (Figure 7).

To investigate the cytotoxicity of these compounds, the EC_{50} values of the selected compounds were evaluated on all three cell lines. The EC_{50} values for each compound was graded based on their effects on each cell line. Seven of the compounds had low to intermediate EC_{50} values towards leukemic cells, while the potency of compound **2** and **11** was very low (Appendix III and Figure 7). Compound **28** had no cytotoxicity on OCI-AML3, while it was very potent on MV4-11 cells, and compound **19** had high EC_{50} value on OCI-AML3 cells than MV4-11 cells (Figure 7,

Figure 8 and Appendix III). As demonstrated in Figure 7 and Appendix III, expect compound **15** and **19** (for 24 hours), eight of ten compounds also showed cytotoxicity towards H9C2 cells in different potency. However, even though EC_{50} values for compound **4** and **19** (at 72 hours) towards H9C2 cells was determined, the data had huge variations, and thus it is not certain that these compounds were cytotoxic activity towards H9C2 cells. As these compounds also showed strong to intermediate cytotoxicity towards OCI-AML3 and MV4-11 cells, they could be promising drug candidates. In addition, compound **12** was among the compounds which demonstrated high potency with low EC_{50} values, however this compound also was toxic toward H9C2 cells (Figure 7 and Appendix III).

When comparing EC_{50} value for the ten selected compounds in the leukemic cell lines, OCI-AML3 cell line had high EC_{50} results in many compounds, for instance compounds **11**, **15**, **19** and **28**, particularly at 72 hours screening (Appendix II and **Feil! Fant ikke referansekilden.**). Often, EC_{50} values on MOLM-13 cells were low compared to the other two leukemic cells, and the ratio between MOLM-13 and MV4-11 on some compounds like

15, **19** was not huge. Moreover, compound 28 had no cytotoxic activity towards OCI-AML3 at 24 hours analysis, even though it was active towards MOLM-13 and MV4-11 cell lines. However, at 72 hours incubation, the compound was cytotoxic towards OCI-AML3 with high EC_{50} value (Figure 4, Figure 7 and Appendix II,**Feil! Fant ikke referansekilden.**).
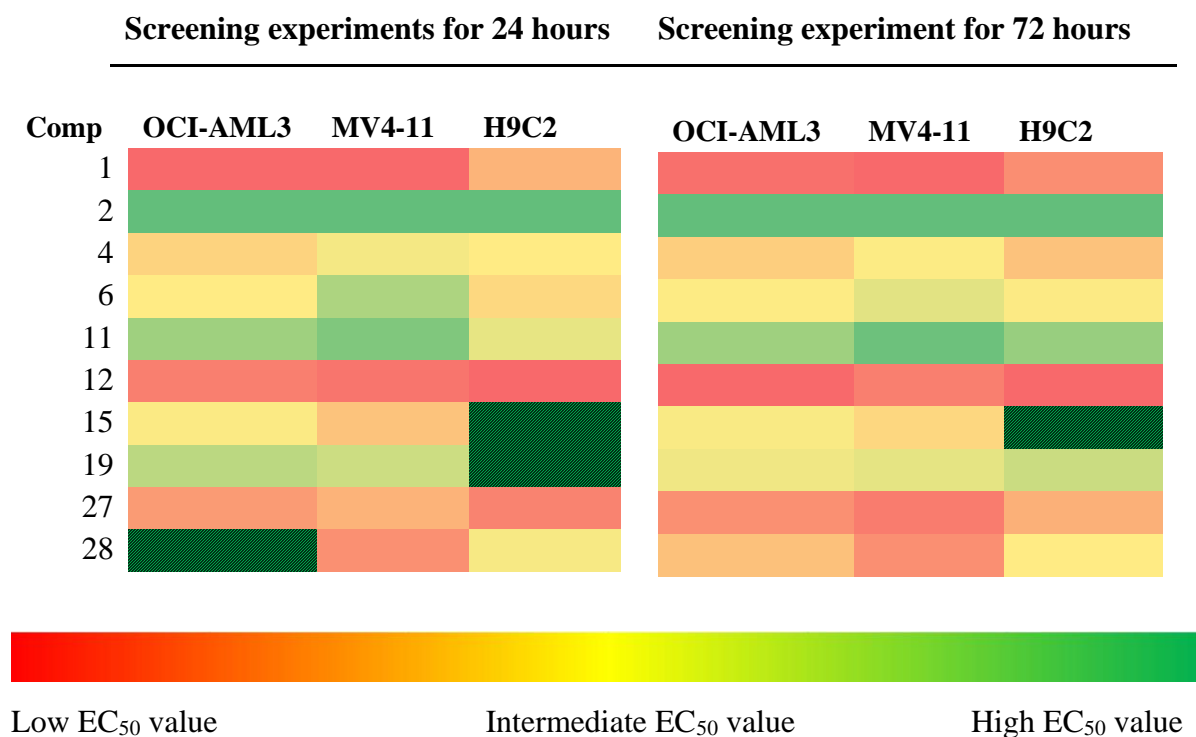

Figure 7: Screening results from ten selected compounds towards OCI-AML3, MV4-11 and H9C2 cells. The viability of the examined cells was determined using WST-1. However, some of WST-1 results were not satisfactory, and the cell viability was instead determined by microscopic evaluation of their nuclear morphology. This applies to OCI-AML3 and H9C2 cells treated with compound 12, and H9C2 cell line treated with compounds 2, 4 and 6 for 72 hours. The specific EC_{50} values are given in **Feil! Fant ikke referansekilden.**. The colors red, yellow, and green demonstrate the EC_{50} values from low to high. The EC_{50} values was defined as low and high when the value was < 100 and > 500 µM, respectively, while intermediate when the value was between 100 - 500 µM. The compounds which are presented in black-green diagonal stripes, did not had cytotoxic activity on either OCI-AML3 or H9C2 cell lines.

Graphs from 24 hours screening
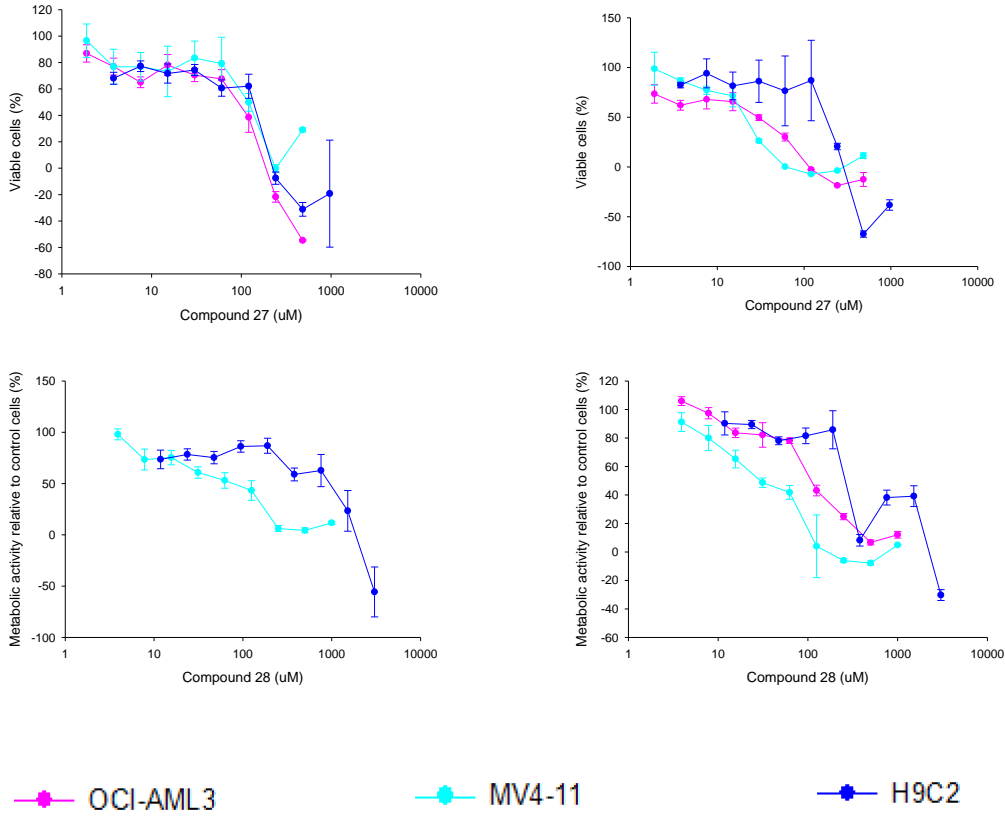
Graphs from 72 hours screening
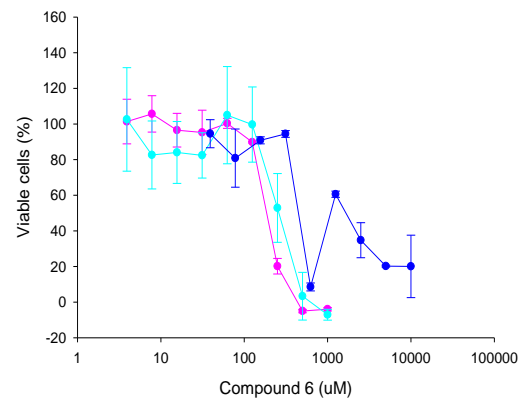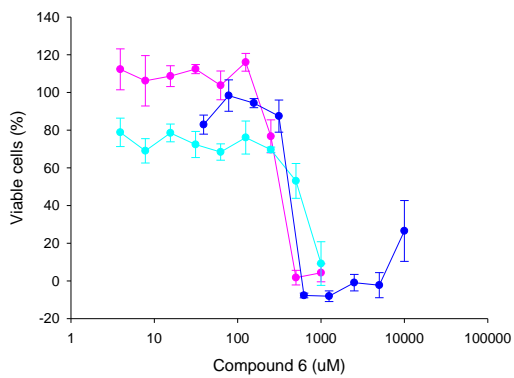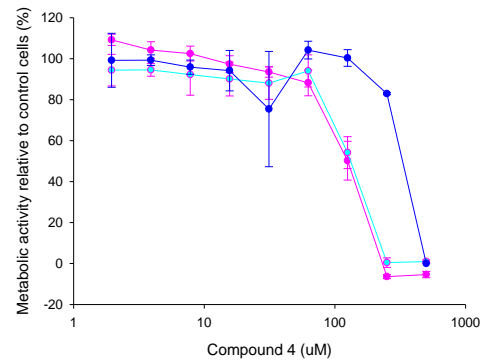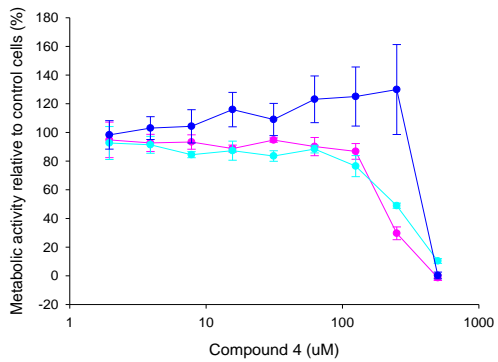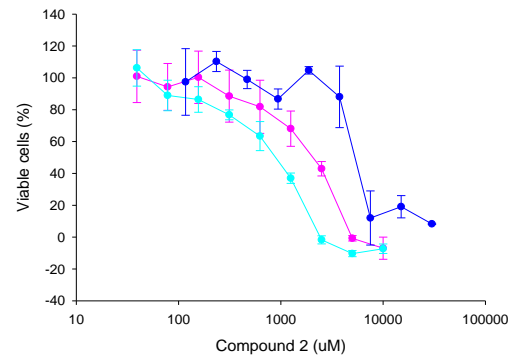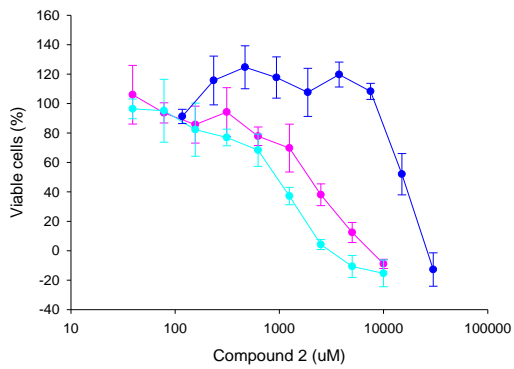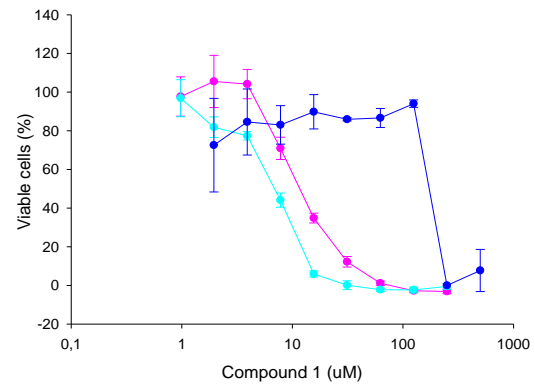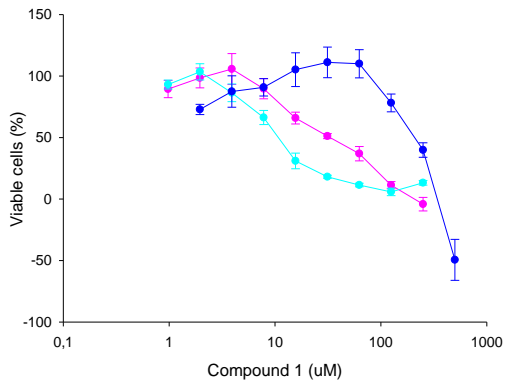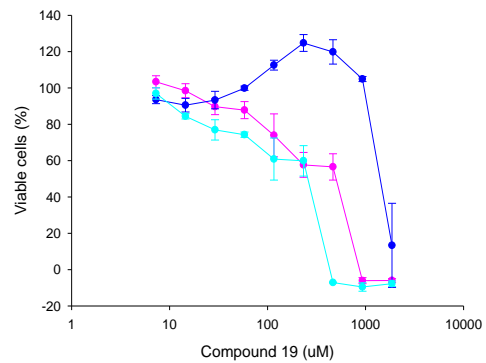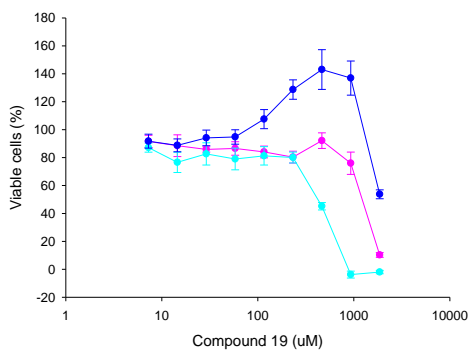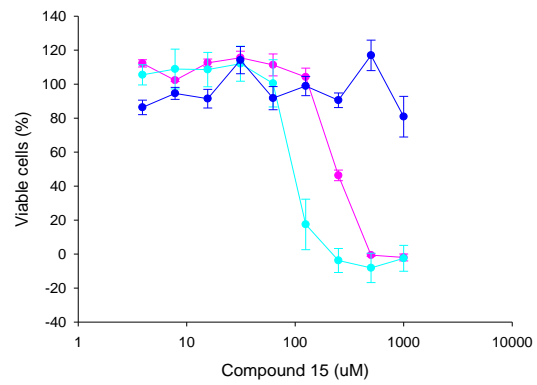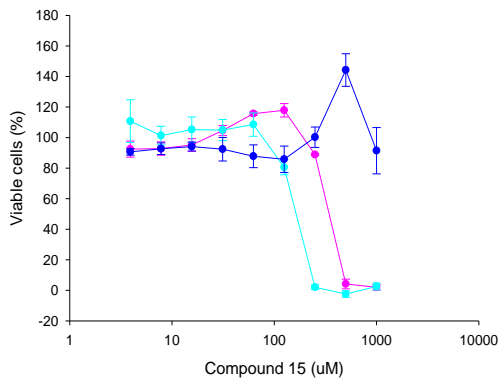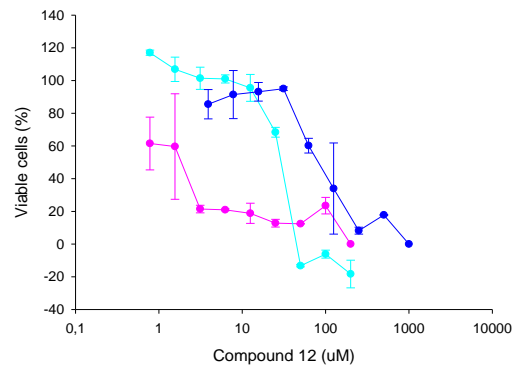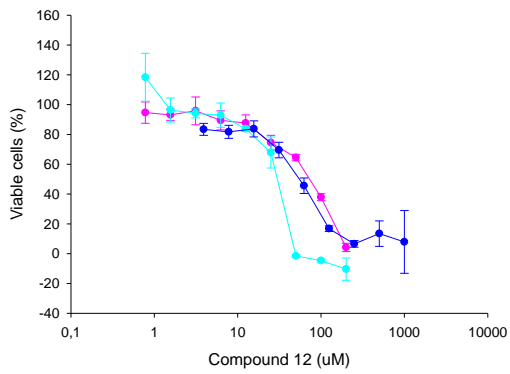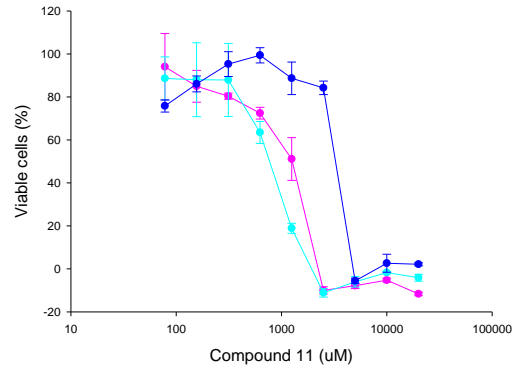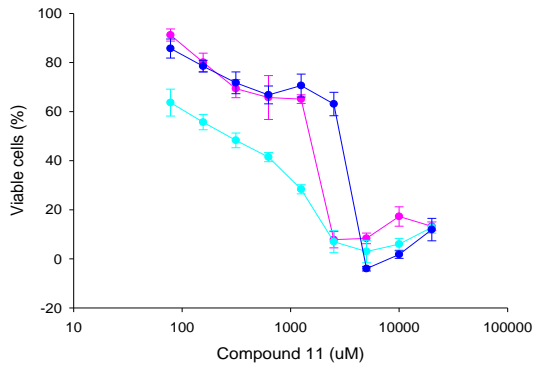
Figure 8: Dose-response curve from the screening of compounds **1**, **2**, **4**, **6**, **11**, **12**, **15**, **19**, **27** and **28** on OCI-AML3, MV4-11 and H9C2 cells. The graphs on the left are results from 24 hours experiment, while those on the right are from 72 hours. Even though the EC_{50} values for compounds **4** and **19** is calculated, they are not cytotoxic for H9C2 cell line, otherwise the remaining compounds were cytotoxic toward H9C2 cells. The EC_{50} (μM) values were estimated by non-linear regression and the specific values are given in **Feil! Fant ikke referansekilden.**.
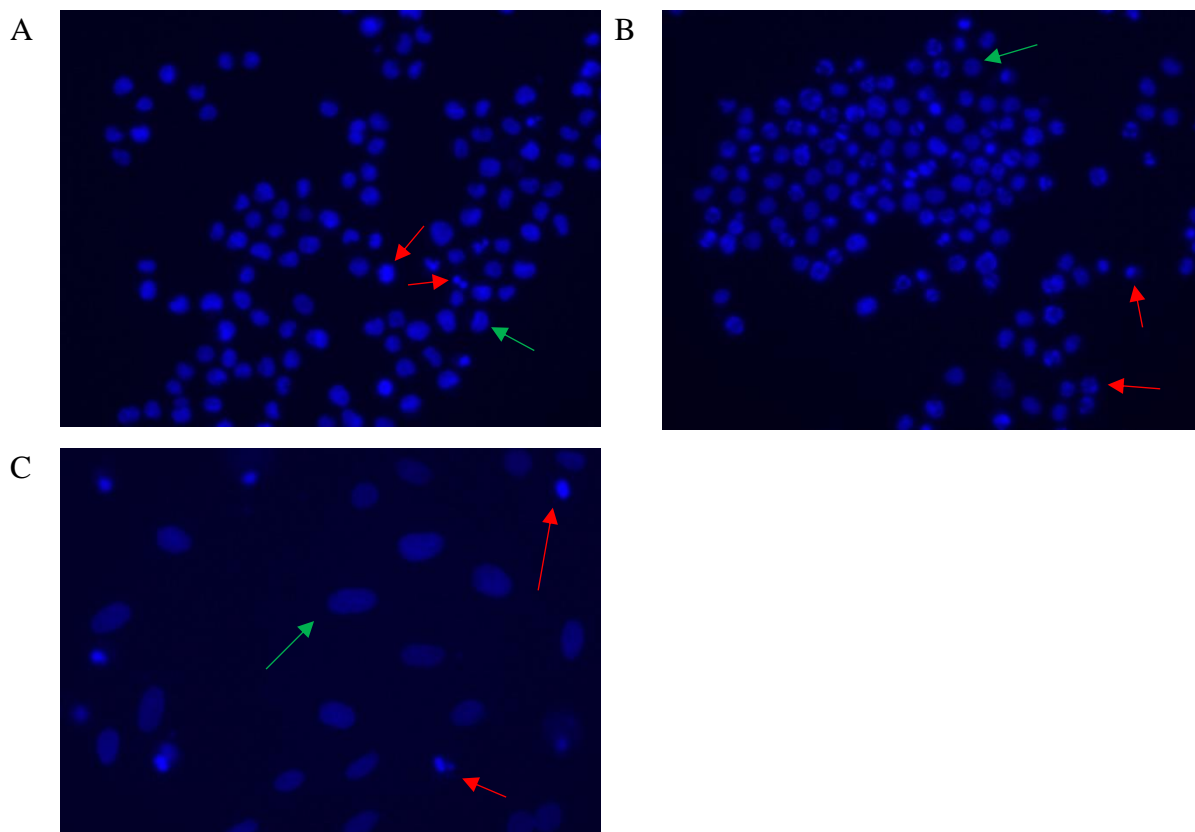
Figure 9: Fluorescence-microscope image of OCI-AML3 (A), MV4-11 (B) and H9C2 (C) cells. After the cells were treated with the ten compounds, the cell viability was determined using WST-1 before the cells were fixed in 2% buffered formaldehyde with the DNA-specific dye Hoechst 33342 in order to visualize the nuclear morphology. The green arrows show the normal nuclei, while the red arrows demonstrate apoptotic nuclei.

4.2 Testing for synergistic effects between phytochemicals and chemotherapeutic drugs

Next, we aimed to analyze effect of our natural compounds in combination with anticancer drugs. A synergistic test was performed with ten chosen test compounds in combination with selected chemotherapeutic drugs on MOLM-13 cells. The aim of this assay was to analyze the synergistic effect of the compounds in combination with anticancer drugs. The results are presented on Figure 11.

The chosen compounds were compounds **1**, **2**, **4**, **6**, **11**, **12**, **15**, **19**, **27** and **28**, and they were tested in combination with daunorubicin (DNR), cytarabine (AraC), emetine, venetoclax, cisplatin and bortezomib.

The coefficient of drug interaction (CDI) was estimated to distinguish whether the combination of drugs was synergistic, additive, or antagonistic (Figure 11). CDI value less than 0.7 represent

synergistic effect, between 0.7 and 1 indicate additive effect, while CDI over 1 indicate antagonistic effect (74).

Compounds **1** and **11** exhibited synergistic effect in combination with daunorubicin (Figure 11Figure 11A and 11E). Compound **6** also synergized in combination with DNR and venetoclax (Figure 11D), however combination data of venetoclax and compound **6** was only two, thus p-value of this combination were not determined. The other cytostatic drugs like emetine and cytarabine had additive effect with compound **1**, while the effect of cisplatin, bortezomib and venetoclax in combination with compound **1** was antagonistic (Figure 11A). As Figure 11D and Figure 11E demonstrate, emetine, cytarabine and ventoclax (only with compound **11**) had additive action in combination with compounds **6** and **11**, whereas the other two drugs (bortezomib and cisplatin) had weak antagonistic activity.

Compound **15** also synergized in combination with venetoclax (Figure 11G). Otherwise, it had an additive and antagonistic action in combination with other chemotherapeutic agents (Figure 11G). The six anticancer drugs combined with compounds **2**, **4** and **19** showed a mixture of an additive and weak antagonistic activity (Figure 11B, Figure 11C, Figure 11H), while compound **12** in combination with five chemotherapy drugs demonstrated additive CDI values, except for cytarabine which was weak antagonistic (Figure 11F). The combination of compound **27** and cytostatics had an antagonistic effect (Figure 11I).

The experiment that gave a result of 20% or less cell viability was not included on the further calculations. Very low viability values give very low predictability of the CDI, because small variations will influence the CDI greatly. For instances, compound **28** are excluded from this result, since it had high cytotoxicity in combination with all cytostatic drugs, except with emetine which had an additive effect. The results of compound **27** combined with cytarabine were also not considered, due to the low viability of cells. Combination of compound **27** and venetoclax only had one data with a cell viability over 20%, and therefore it is not included.
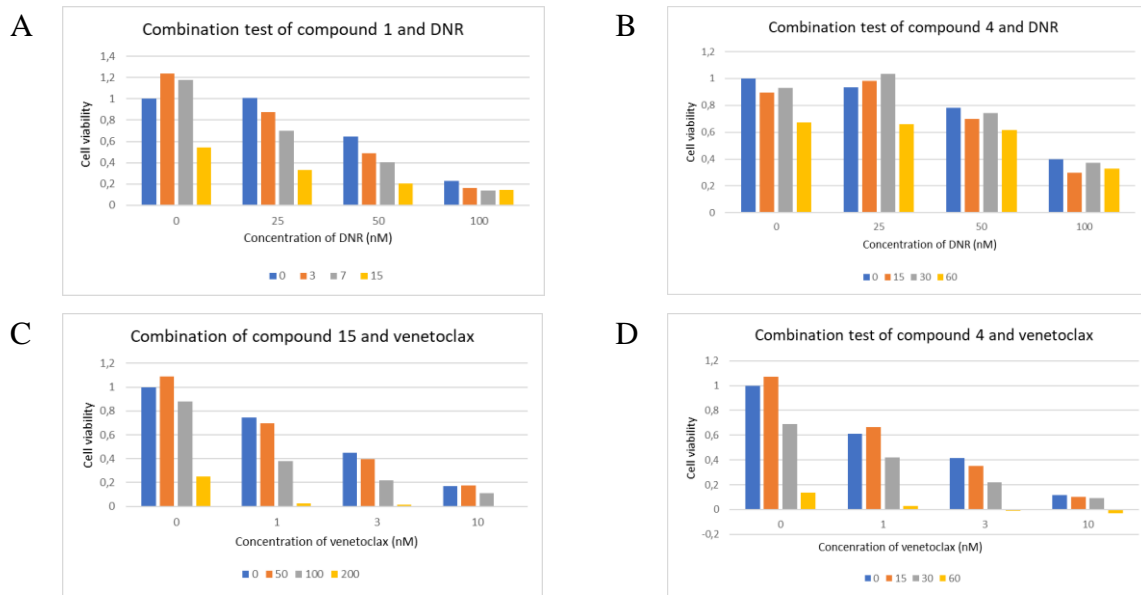
Figure 10: Bar chart examples from combination test of compounds **1** and **4** with daunorubicin (A and B) and compounds **4** and **15** with venetoclax (C and D), respectively. These examples show the result of MOLM-13 cell viability upon 24 hours of treatment. Both the compounds and cytostatics were tested in three different concentrations as indicated. The concentration of compounds **1**, **4** and **15** are in micromoles. The remaining bar charts are given in Appendix IV.
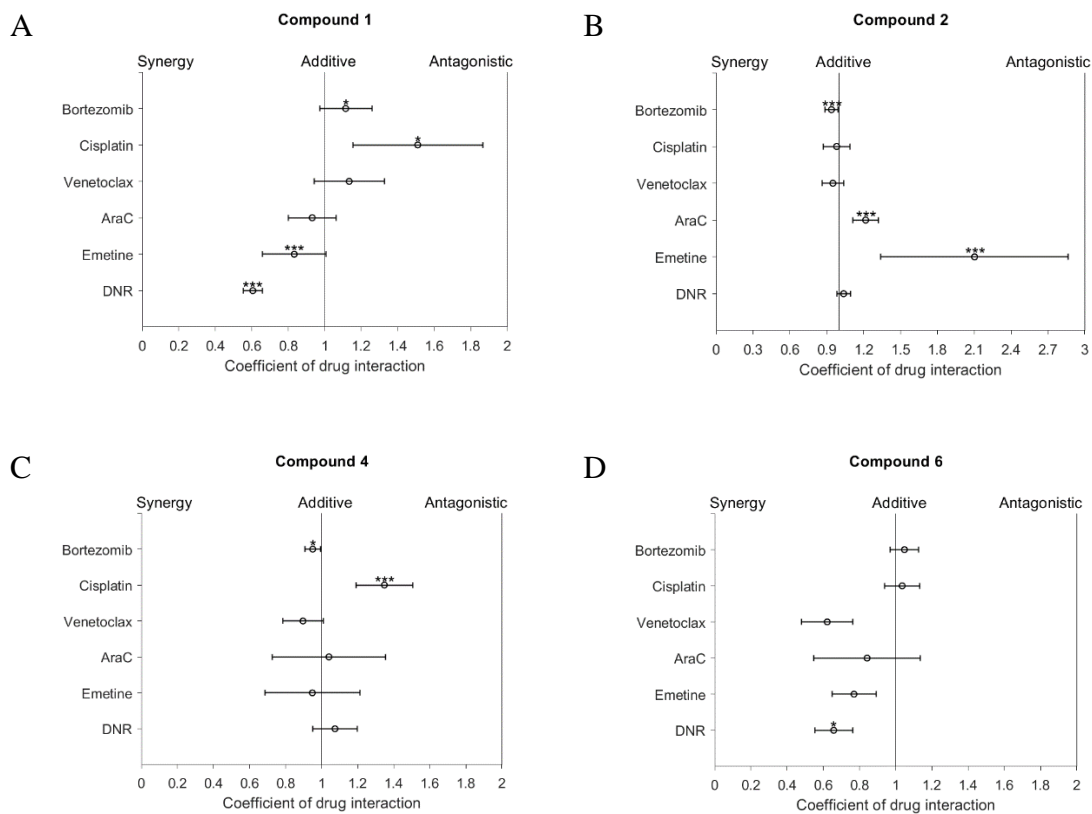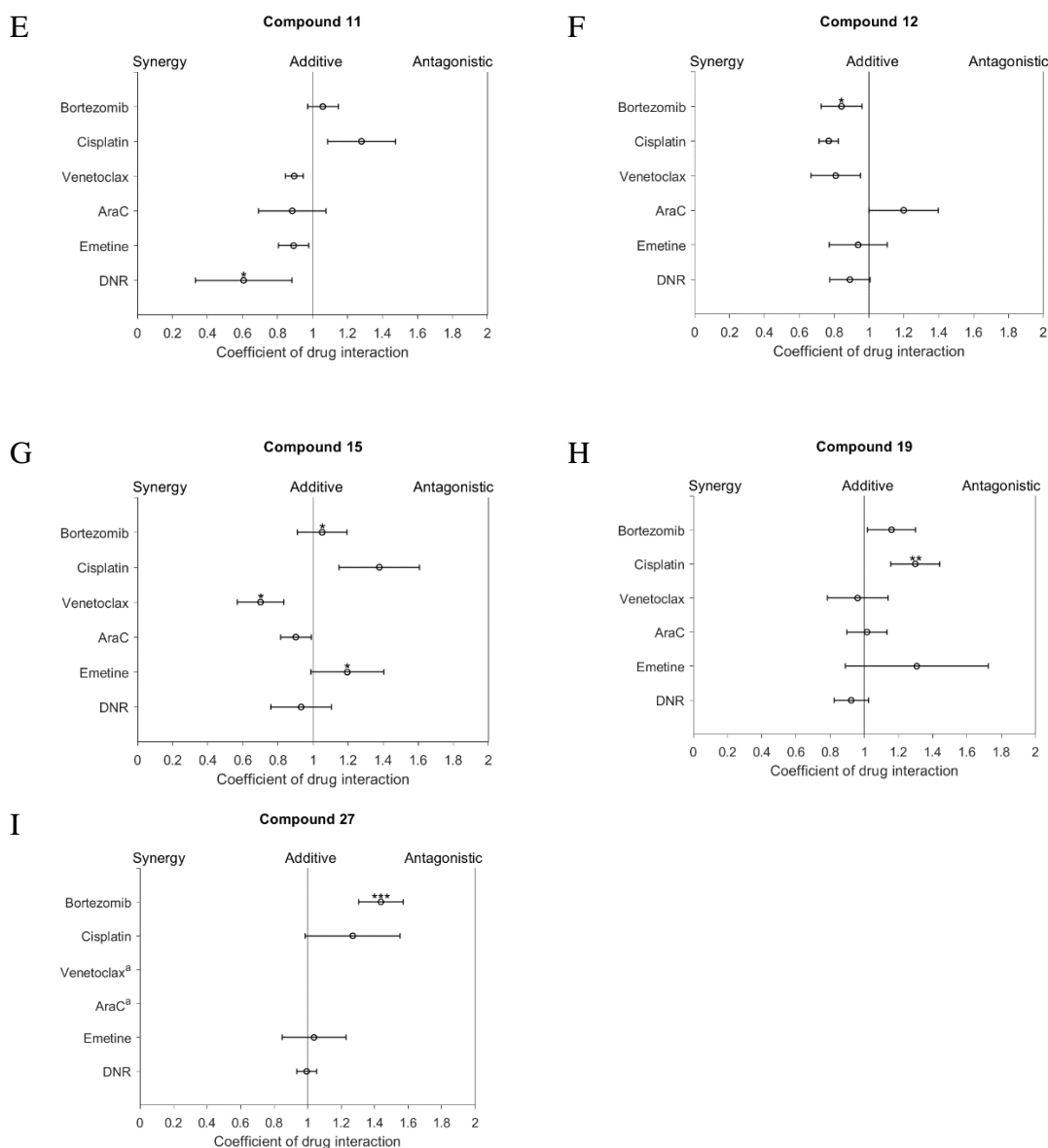
Figure 11: CDI values from combination test of six cytostatics and compounds **1** (A), **2** (B), **4** (C), **6** (D), **11** (E), **12** (F), **15** (G), **19** (H) and **27** (I). The result from compound **28** was excluded due to high apoptosis. This test was done on MOLM-13 cell line, and the results were used to determine the coefficient of drug interaction (CDI) using equation Eq (3). CDI values below 0.7 and above 1 indicates synergistic and antagonistic effect, respectively, while CDI values between 0.7 – 1 imply additive effect.

a = combination test with low viability where CDI could not be calculated

* indicates $p < 0.05$, ** indicates $p < 0.01$ and *** indicates $p < 0.005$

4.3 Kinetic experiment for time-course analysis

Three of the ten selected test compounds (**1**, **6** and **11**) were chosen to evaluate how fast these compounds induce apoptosis on MOLM-13 cells. This experiment was further used to decide the treatment time of the cells to analyze cell signaling events by (section 4.4 Investigation of

activation of apoptotic pathways by western blot analysis). The results from time series are presented in Figure 12.

The results were determined by examining the nuclear morphology of the treated cells (see Figure 6 for an example). All three compounds started to induce cell death already, after 1 hour, and after 12 hours, the apoptotic cell death was over 90% (Figure 12).
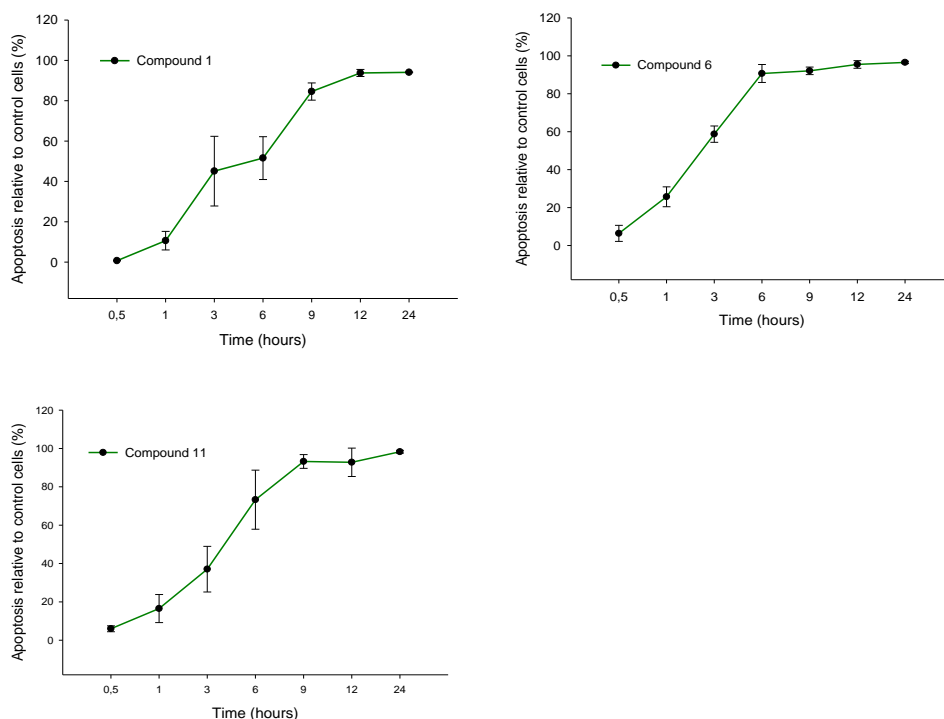

Figure 12: The results from time-kinetic assay on MOLM-13 cell line tested with compounds **1**, **6** and **11**, and this experiment was performed as described in section 3.3.5 Time kinetic experiment. The viability of the cells was evaluated under UV-microscope based on their nuclear morphology. The cell death was 11, 26 and 21 % after 1 hours on the cells treated with compounds **1**, **6** and **11**, respectively. While after 12 hours had passed, 90% of the cells were died.

4.4 Investigation of activation of apoptotic pathways by western blot analysis

In order to examine which molecular mechanisms that are involved in the observed induction of apoptosis, western blot analysis was performed. In the kinetic analysis, the compounds quickly started to induce cell death in MOLM-13 cells. After 2 hours, the percentage of apoptosis was 4% using 0.05 mM and 5.4% using 0.1 mM of compound **1**, 1% with 0.25mM and 3.5% with 0.5mM of compound **6**, 1% at 2 mM and 1.8% at 4mM compound **11**, and 1.5% using 0.5mM and 2 % using 4mM DMSO (0.06 and 0.26% DMSO). The percentage of DMSO in compound **1**, **6** and **11** was between 0.03-0.26%.

The standard curve from the Bradford assay was utilized to determine the concentration of proteins in the samples (Figure 13). The protein concentrations were further used to calculate the amount of the protein lysate loaded to electrophoresis gels on western blot analysis.

The first membrane demonstrated protein bands of PARP and phosphorylated STAT5 (Figure 14). While protein bands of caspase 9, 4E-BP1 and phosphorylated 4E-BP1 were observed on the second membrane as illustrated in Figure 16. Both membranes were stained with anti β-actin as loading control. Additionally, antibodies towards total protein STAT5, gamma-H2AX and caspase 7 were tested, however no bands were detected with these antibodies, presumable because they were too old, and degraded.

Figure 14 presents a band at around 116 kDa, which indicates full-length PARP. It was only the sample treated with 0.1mM of compound **1** that showed a clear protein band for cleaved PARP at 89 kDa (Figure 14). Relative to the intensity of β-actin, the intensity of the PARP is reduced compared to the control sample (Figure 14). Figure 14 also demonstrated a band of 90 kDa, which corresponds to phosphorylated STAT5. In comparison to untreated control cells, the cells treated with compounds **1**, **6**, **11** and DMSO, the amount of the phosphorylated STAT5 was decreased, especially at 0.1mM of compound **1** (lane 2) (Figure 15). However, MOLM-13 cells treated with 2mM of compound **11** appears to increase the level of phosphorylated STAT5 (Figure 15). Unfortunately, the antibody used against total STAT5 gave no band of 90 kDa and a comparison of phosphorylated to total protein could not be performed with these samples.

As illustrated in Figure 16, the western blot test revealed that the samples contained full-length procaspase 9, presented around 49 kDa. A band corresponding to caspase 9 was presented at around 37 kDa (Figure 16). After treatment of MOLM-13 cells with compounds **1**, **6**, **11** and DMSO, the amount of cleaved caspase 9 relative to procaspase 9 was increased, particularly in cells treated with 0.05 and 0.1 mM of compound **1**, 0.25mM of compound **6**, 2 and 4 mM compound **11**, and 0.5 and 4 mM of DMSO (Figure 17). Along with the increased level of procaspase 9 in cells treated with 0.5mM compound **6**, 2mM compound **11**, and 0.5 and 4 mM of DMSO, there is a reduction in the amount of procaspase on the remaining samples, but to a lesser degree (see Appendix V).

Protein band presented at around 15-20 kDa belongs to total protein 4E-BP1 and phosphorylated 4E-BP1 (Figure 16). As illustrated in Figure 18, the amount of phosphorylated 4E-BP1 relative to total 4E-BP1 is decreased in MOLM-13 treated with compound **1**, **6** and **11** however also by DMSO, but the reduction was most pronounced in the cells treated with 0.25mM of compound **6**, and 2 and 4 mM of compound **11** (Figure 18). The amount of the total 4E-BP1 protein was decreased in all samples, but the reduction was more noticeable in cells treated with both 0.05 and 0.1mM of compound **1**, 0.25mM and 0.5mM of compound **6**, and 4mM of compound **11** (Appendix V).
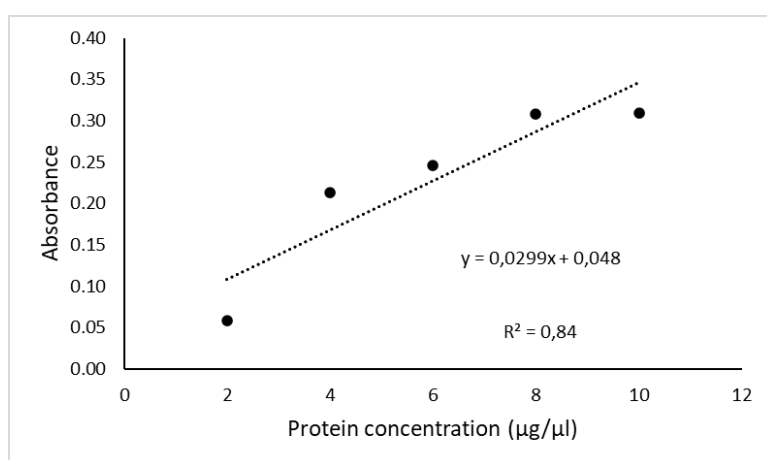

Figure 13: Bradford calibration curve of standard concentration of BSA protein and absorbance which is used to calculate the concentration of proteins in the cell extract.
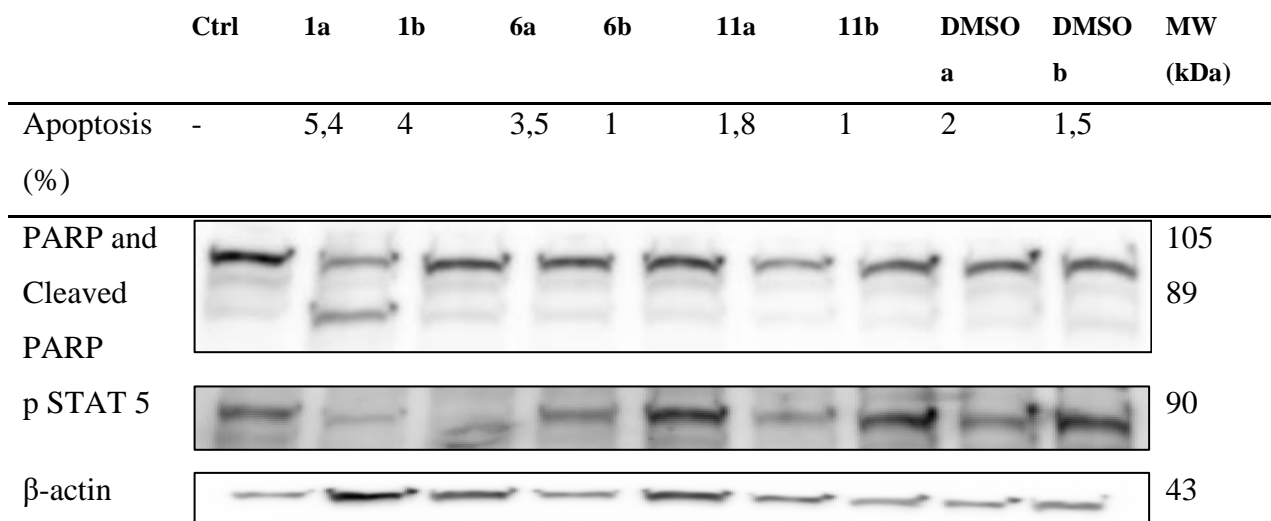
	Ctrl	1a	1b	6a	6b	11a	11b	DMSO a	DMSO b	MW (kDa)
Apoptosis (%)	-	5,4	4	3,5	1	1,8	1	2	1,5	
PARP and Cleaved PARP										105 89
p STAT 5										90
β-actin										43

Figure 14: Detection of PARP, phosphorylated STAT5 and β-actin on a PVDF membrane by western blot analysis. MOLM-13 cells were treated with compound **1**, **6**, **11** and DMSO at two different concentrations, as described in the main text, for 2 hours. The cells were lysed, and the proteins were separated on 10% gel, blotted over on a PVDF membrane, and stained with selected antibodies (see Table 2). Monoclonal β-actin antibody is used as loading control. The densitometric value of phosphorylated STAT5 were quantified by Image J (see Figure 15). Percent apoptosis is relative to untreated control cells.

a = highest concentration of each compound, b = lowest concentration. Ctrl = untreated control cells.
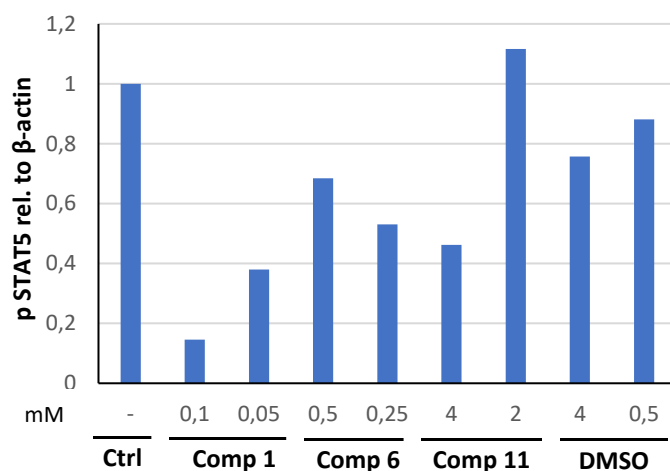

Figure 15: Quantification of phosphorylated STAT5 amount relative to β-actin in treated MOLM-13 cells relative to untreated control cells, using the gel analysis took in Image J. The amount of phosphorylated STAT5 was reduced relative to β-actin, particularly in the cells treated with 0.1mM of compound **1**. However, the cells treated with 2mM compound **11** demonstrated an increase in level of p STAT5.

Comp = compound

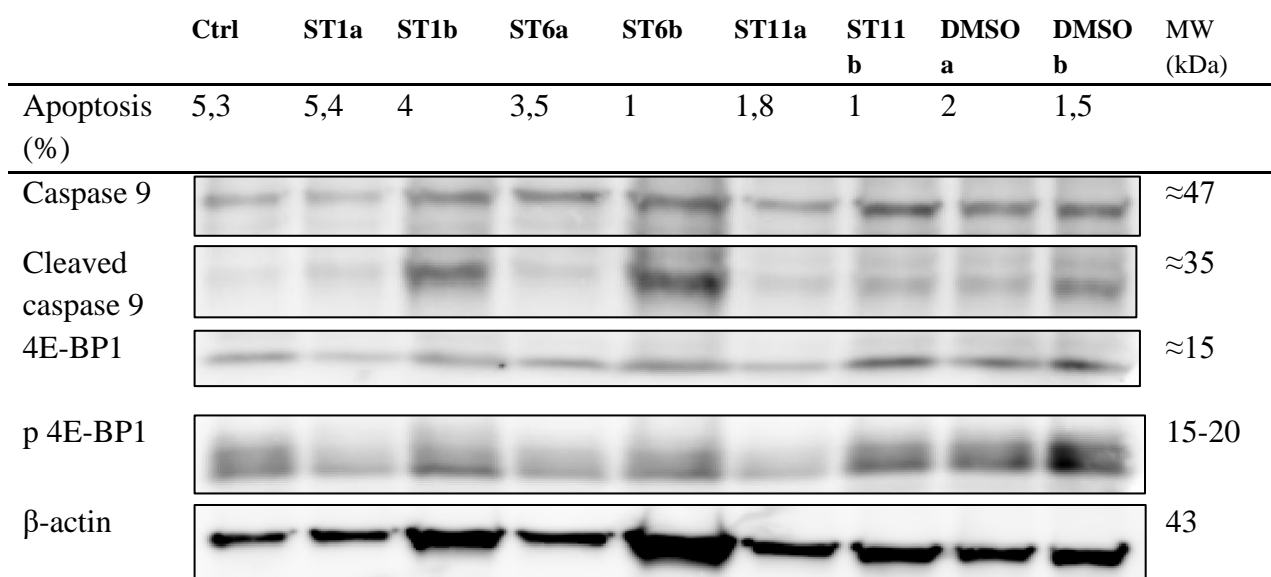|	Ctrl	ST1a	ST1b	ST6a	ST6b	ST11a	ST11 b	DMSO a	DMSO b	MW (kDa)
Apoptosis (%)	5,3	5,4	4	3,5	1	1,8	1	2	1,5	
Caspase 9										≈47
Cleaved caspase 9										≈35
4E-BP1										≈15
p 4E-BP1										15-20
β-actin										43

Figure 16: Western blot analysis of procaspase 9, cleaved caspase 9, 4E-BP1, phosphorylated 4E-BP1 and β-actin in MOLM-13 cells after treatment with two different concentrations compounds **1**, **6** and **11**, as described in the main text, for 2 hours. The cells were lysed and run on a 10% gel, blotted over on a PVDF membrane, and stained with selected antibodies (see Table 2). Monoclonal β-actin antibody is used as loading control. The densitometric values of procaspase 9, cleaved caspase 9, 4E-BP1 and phosphorylated 4E-BP1 were quantified by Image J (see Figure 17, Figure 18 and Appendix V). Percent apoptosis is relative to untreated control cells.

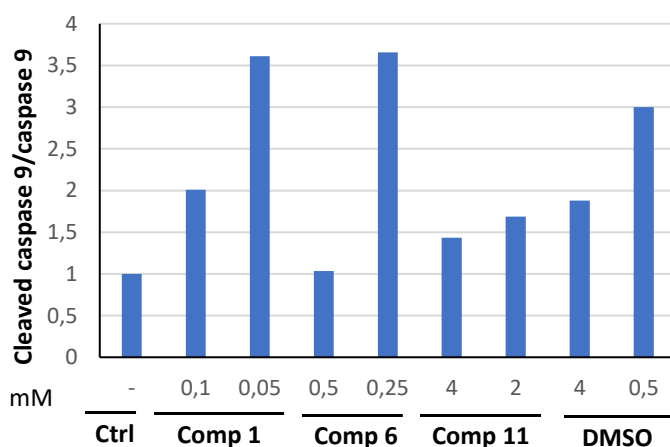a = highest concentration of each compound, b = lowest concentration. Ctrl = untreated control cells

Figure 17: The graph demonstrates the amount of cleaved caspase 9 relative to full-length caspase 9 using the Gel analysis took in Image J. MOLM-13 cells were treated with high and low concentration of compounds **1**, **6**, **11** and DMSO for 2 hours. 0.5 mM of compound **1**, 0.25mM of compound **6** and 0.5 mM of DMSO demonstrated an increased amount of cleaved caspase 9.
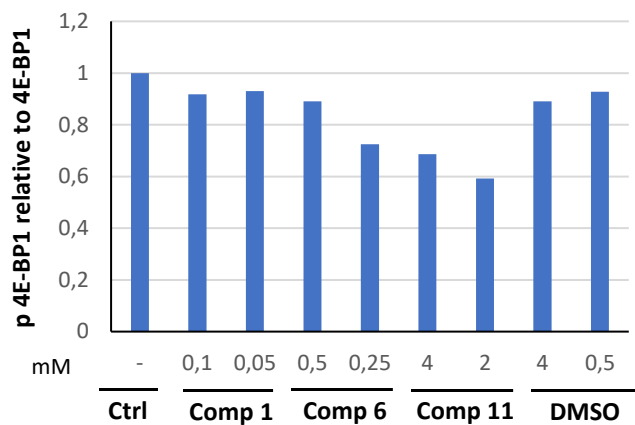
Comp = compound

Figure 18: The graph shows the amount of phosphorylated 4E-BP1 relative to 4E-BP1 in treated MOLM-13 cells relative to untreated control cells. The amounts were quantified using Image J. All samples show a slightly decrease in the level of phosphorylated 4E-BP1 relative to total protein, however the reduction is most pronounced on 0.25mM compound **6** and 2- and 4-mM compound **11**.

Comp = compound

5. Discussion

The present study aimed to explore a selection of phytochemicals as potential lead compounds or new cancer drugs which can be utilized in the treatment of AML. The natural compounds utilized in the thesis are either derived from plants or synthetic analogs. In order to observe their cytotoxicity, the compounds were examined as single agents in different leukemic cell lines and non-cancerous ones. Additionally, some were tested in combination with currently used anticancer drugs, and four compounds (**1**, **6**, **11**, and **15**) synergized with cytostatic drugs.

As described previously, all the natural compounds were dissolved in DMSO. DMSO is hydrophilic solvent, and it is utilized to dissolve both hydrophobic and hydrophilic compounds. Almost all the compounds have hydrophilic functional groups such as alcohol, ester, carboxylic acid, ketone, and amine (see Appendix I). This should make them easy to dissolve in DMSO. However, it was difficult to dissolve compounds **14** and **16**, and more DMSO than for the other compounds was needed. Compound **14** is a hydrophobic molecule with only one alcohol (OH) group, while compound **16** is a hydrophilic compound with four OH- and two ester groups. According to two studies, both compounds should be dissolved in DMSO (75, 76), but apparently, these compounds needed to be dissolved in concentration lower than 100mg/ml, the concentration which compounds **1**, **15**, **18**, **19** and **30** were dissolved to.

A screening test was performed on three leukemic cell lines (MOLM-13, MV4-11 and OCI-AML3) and two normal cell lines (NRK and H9C2) to examine the sensitivity of the natural compounds on these cells. The potency of relatively all compounds increased with time in all three leukemic cell lines (Appendix II and Appendix III). Drugs enter cells and accumulate by crossing the cell membrane via different mechanisms like passive diffusion, facilitated diffusion, active transport, and pinocytosis (77). The reduction of EC_{50} values over time for our test compounds may imply that the compounds need time to penetrate the cells and induce apoptosis. All the compounds, except compound **14**, have hydrophilic substituent, as mentioned above (Appendix I). These substituents can make it difficult for compounds to pass through the plasma membrane. Therefore, the compounds may only enter the cancer cells via active membrane transport, thus it takes time to concentrate the drug in the cells and the induction of antileukemic effect is delayed accordingly. A good example here is cytarabine, which enter AML cells via active transport (78). Another explanation could be the compounds interfere with cellular processes, such as signal transduction, gene expression, protein or nuclei acid synthesis, mitotic spindle formation and energy metabolism, which cause a delayed anticancer effect and

a slow induction of apoptotic cell death (79). This is seen for compounds like anti-metabolites such as cytarabine, which is given to patients as 7-day infusion in AML therapy (1). However, compound **12** had similar EC_{50} value towards MOLM-13 and MV4-11 cell lines at both 24- and 72-hours incubation. The molecular structure of this compound is large and hydrophilic, and entry into the leukemic cells may happen via pinocytosis or transport proteins. By contrast, the EC_{50} value for compound **12** was surprisingly low when examined on OCI-AML3 cells for 72 hours. However, the cell viability upon treatment with compound **12** was determined based on nuclear morphology due to unsatisfactory WST-1 result. The low EC_{50} values at 72 hours may be due to the use of a different method to measure cell death, but one cannot exclude the possibility that the compounds trigger a slow death pathway in the OCI-AML3 cells, which is suppressed in the other cell types.

Even though compounds **1**, **6** and **11** were most potent at 72 hours, Figure 12 illustrate that treatment of MOLM-13 cells with these compounds induced apoptosis very rapidly, where approximately 90 % apoptotic cell death was reached already after 12 hours. The concentration of a compound has the ability to affect the time of a cells' response (80). Therefore, the rapid cell death may be caused by the high concentration of these compounds. Lower concentrations showed decreased apoptosis after 2 hours (see section 4.4 Investigation of activation of apoptotic pathways by western blot analysis), and one can conclude that the rapid apoptotic cell death was concentration dependent.

From the screening of the 30 natural compounds on MOLM-13 and NRK cells, we wanted to identify the compounds which act selectively towards MOLM-13 cells. Except compounds **4**, **9**, **10**, **11**, **15**, **17**, **18**, **19** and **26** (Appendix II and Figure 4), the cytotoxicity of the remaining sixteen compounds were not selectively towards MOLM-13. As described previously, compounds **15** and **19** were chosen for further experiment, while the other compounds mentioned above were not selected for several reasons. Though compound **17** was very potent (Figure 4, Appendix II), which is a good criterion to be selected for testing, more compound could not be obtained by purification or synthesis because it was a human metabolite purified from biological samples. Compound **26** had a high EC_{50} value of 4.52mM, which is too high if the compound should have potential as a drug candidate (Figure 4, Appendix II). Ideally, the EC_{50} value of candidate compounds should be below 0.1mM.

Moreover, compounds **9** and **24** are identical, but had different stock concentration. These compounds showed small differences on EC_{50} values after 24 hours (88.9 µM comp **9** vs 153 µM comp **24**), while at 72 hours incubation the EC_{50} values was similar (see Appendix II). The difference of EC_{50} values at 24 hours may be due to inaccurate weighing of the compounds or impurities. Although there was a dose-dependent relationship, the toxicity of the compound toward NRK cells also increased at the same time (Appendix II).

When compounds **4** and **11** (at 24 hours), and compound **18** examined towards MOLM-13 cells, it was difficult to estimate exact EC_{50} value because of data variability, and it was not anticipated that these compounds had induced cytotoxicity when MOLM-13 cells were treated with a particular concentration. However, after 72 hours treatment, compounds **4** and **11** showed some cytotoxicity toward MOLM-13 cells with intermediate and low potency, respectively (Figure 5 and Appendix II). Moreover, compound **10** had high EC_{50} value of 10.57mM (Appendix II).

Although some compounds induced NRK cell death, it does not necessarily mean they are useless as anticancer compounds. If the EC_{50} value ratio between MOLM-13 and NRK cells of a compound is large, it might cause good anti-cancerous effects without causing large side effects. For instance, the ratio between MOLM-13 and NRK cytotoxicity of compounds 1, 6 and 28 was over nine, and increased with increasing exposure time (Appendix II). Based on the results, we assumed that these compounds were good candidates to perform further experiments on.

As described earlier, ten selected compounds were screened to examine the cytotoxicity of the compounds on two leukemic cells (OCI-AML3 and MV4-11) and one non-cancerous cardiomyocyte cell line (H9C2). Compounds **4**, **15** and **19** had selective antileukemic activity towards OCI-AML3 and MV4-11 cell lines, while the other remaining were toxic towards H9C2 cells to varying degrees (Appendix III,

Figure 8). The ratio of the EC_{50} values were not very large, as on MOLM-13 and NRK cells, except for compounds **1** and **28** with EC_{50} value ratio over 7. While EC_{50} values ratio between OCI-AML3 and H9C2 which was around 3 (Appendix III).

Even if our results have demonstrated some compounds with selective antileukemic activity, not all compounds were less potent on normal cells. As demonstrated in Figure 4 and Figure

7, compound **12** showed high cytotoxicity on AML cell lines, but was also toxic towards both the normal cells, NRK and H9C2. Even though compound **12** was active toward the leukemic cell lines, it did not act selectively towards leukemic cells because of its potential nephrotoxic and cardiotoxic activity, and because of this, compound **12** is not a good anticancer drug candidate.

Kidney is a target for drug toxicity and toxic injury because of high perfusion and filtration of the blood plasma at a high rate (81). Compound **6** has in previous studies been shown to have nephroprotective effect on kidney damage caused by cadmium, and it was not toxic against kidney cells at a concentration range of 3.1 - 100µM (81). In accordance, in our study compound **6** showed low potency and high EC_{50} value on NRK cells at 24- and 72-hour incubation. However, compound **6** have intermediate potency on cardiomyocyte H9C2 cells with small differences on EC_{50} value between OCI-AML3 and MV4-11 cells. Therefore, we can conclude that compound **6** has low potential nephrotoxicity, however it should be examined on several toxicity test before evaluating it as anti-cancer drug candidate.

OCI-AML3 had in general higher tolerance to the compounds compared with MV4-11 and MOLM-13 cells. This was particularly true, when the cells were treated with compounds fand **28** (Figure 4,Figure 7, Appendix II and Appendix III). This suggests that the compounds act on mechanisms which there is resistance towards in the OCI-AML3 cells. The OCI-AML3 cell line has unfavorable cytogenetic AML and is associated with a poor prognosis (61, 82). AML with adverse cytogenetic are challenging to treat and do not respond to the standard AML treatment. Thus, OCI-AML3 cell line could be resistant against compound **28** and a higher concentration is needed to induce cell death in these cells.

Based on the results from the three leukemic cells and two normal cells, compounds **1**, **4**, **15**, **19** and **28** could be possible candidate for treatment of AML.

As described in section 3.1 Natural compounds, compound **1** is a chalcone and belongs to the compound class of flavonoids. Several studies have been conducted on chalcones. In a recently published study, the cytotoxicity of 15 different synthetic and natural chalcones was examined on five leukemic cells. One of these compounds was effective in inhibiting directly FLT3 kinase on FLT3-dependent cells, as a result blocked FLT3 mediated survival signaling. This compound also induced mitotic arrest on FLT3-dependent cells and inhibited tubulin polymerization.

Therefore, this compound acted selective on FLT-3 tyrosine kinase and could have the ability to overcome FLT-3 resistance (83).

Compound **6** is a phenylpropanoid glycoside. Phenylpropanoid glycoside are a class of compounds with many different biological activities and has also antioxidant properties (84). Phenylpropanoid glycoside derivates conjugated silver nanoparticles have been examined on two cancer cells, CML and hepatocellular cancer lines. Chlorogenic acid and ferulic acids were the derivates which had anticancer effect towards CML cell line at concentration of around 1µM/ml. They also showed less toxic activity towards normal cell lines (85). Chlorogenic acid (compound **11**) and ferulic acid (compound **26**) were screened in this thesis (see Appendix I). Compound **6** also had good anticancer effect in breast cancer by inhibiting metalloproteinase 9 (MMP9) and MMP2 (86).

Compound **15** is an NSAID drug, and it has been performed some studies of NSAIDs in AML. The NSAIDs Diclofenac and Sulindac sulfide were studied on four different leukemic cells and primary cells from AML patients, and these drugs were shown to induce apoptosis in AML cells by increasing expression of AP-1 proteins. In addition, increased level of AP-1 proteins also promoted the differentiation of AML cells in primary patient cells, specially by Sulindac sulfide (87). Mefenamic acid (compound **15**) has also been studied in human liver cancer (88), and it have revealed to enhance anticancer drug sensitivity by inhibiting proteins involved in drug resistance (89).

A combination of two or more cytostatic drugs is quite common in cancer therapy. For instance, the standard induction therapy of AML has consisted of a combination of DNR and low dose cytarabine for more than 40 years. As described in section 4.2 Testing for synergistic effects between phytochemicals and chemotherapeutic drugs, compounds 1 and 11 synergized in combination with daunorubicin, compound 15 in combination with venetoclax, and compound 6 combined both DNR and venetoclax. This indicates that these compounds have different mechanism of action towards MOLM-13 cells than the chemotherapeutic drugs. A combination drug therapy with synergistical effect can enhance the effect of the anticancer drugs by acting on different pathways on cancer cells. In some cases, this can also prevent the development of resistance against anticancer drugs, leading to a more efficient therapy (90). Furthermore, the combined drugs may allow a reduction of the dose needed of each drug and as a result to minimize the risk of drug toxicity. In this case, a dose reduction of DNR is desirable, since it has a severe side effect, such as cardiomyopathy and bone marrow suppression. A combination

of each of the natural compounds and DNR can be a good drug candidate in the treatment of AML in the future.

The other remaining compounds showed either antagonistic or additive action when combined with cytostatic drugs. The antagonistic drug combinations could be due to blocking or altering the uptake or binding site of drugs on target proteins in cancer cells. This led to diminished effectiveness of the drugs. The additive effect could indicate that the compounds act on the same signal pathways or systems as the chemotherapeutic drugs. However, further research needs to be conducted to reveal the exact mechanism of action of these compounds.

During apoptosis, the morphology of the cells changes and the cell death is "characterized by cell shrinkage, chromatin condensation, loss of nuclear membrane integrity, plasma blebbing and apoptotic body formation" (80). Treatment of MOLM-13 cells with compounds **1, 6**, **11** and DMSO affected its nuclear morphology indicating apoptosis, thus possible explanatory mechanisms were explored by western blot analysis. PARP is an important protein in repairing DNA breaks, particularly single-stranded DNA break, and is activated by DNA breaks (91). During apoptosis, PARP is degraded into smaller fragment sizes by proteases (92). Therefore, the band at 116 kDa reveals full-length PARP that actively repair DNA single-strand break, and the 89 kDa band reveals one of the cleaved forms of PARP induced by apoptosis. Cleaved PARP loses the ability to respond to DNA break and contribute to cell death (91). The cells treated with a high concentration of compound **1** (lane 2) showed that PARP has started to be degraded by caspase 7 (93), while the other treatments did not have this effect.

Caspases are important proteolytic enzymes in programmed cell death (80). Caspase 7 is an effector caspase which is activated by caspase 9 after cleavage of procaspase 7 (94). It is responsible for the degradation of several substrates, including PARP, during apoptosis (93). Our result did not demonstrate that there is caspase 7 or procaspase 7 in the samples, even though there is a band for cleaved PARP at 89 kDa in lane 2 (Figure 14). The reason could be that the antibody solution was too old, and the antibody had degraded, and unfortunately neither procaspase 7 nor caspase 7 proteins could be detected in the samples. This is also probably the explanation for the lack of signal from the antibodies against ϒ-H2AX and STAT5. However, since the cells treated with compounds **1, 6, 11** and DMSO, at both high and low concentrations induced apoptotic cell death to some extent, and compound **1** also induced PARP cleavage, it was assumed that there was induction of apoptotic mechanism in cells treated with these

compounds. Still, the level of apoptosis in the samples was low (maximum level 5.4 in lane 2), and caspase cleavage could not yet be evident (Figure 14).

Figure 16 shows that, there is procaspase 9 in the samples, and induction of apoptosis causes procaspase to be cleaved into its activate form, caspase 9 (95). Cells treated with low concentration of compounds **1**, **6** and DMSO (lane 3, 5 and 9) detected cleaved caspase 9 at 37 kDa (Figure 16). Moreover, there is increased amount of cleaved caspase 9 relative to procaspase 9 in these samples (Figure 17). This, despite the low amount of apoptosis. One explanation for increased intensity of the band showing cleaved caspase could be the use of large amounts of protein samples which was confirmed by β-actin (Figure 16). In addition, it is noticed increased amount of procaspase 9 in cells treated with 0.5mM compound **6**, 2mM compound **11** and 0.5 and 4mM DMSO (Appendix V), which is not expected, especially on 0.5mM compound **6**, since the cell death is 3.5%, and it was considered that the apoptotic cell death were induced in the cells treated with this concentration. However, as shown in Figure 16, the size of the bands on lane 4, 7, 8 and 9 at 47 kDa is larger and denser than the untreated control cells (lane 1), and this can be the explanation for the increased level of procaspase 9 in cells treated with 0.5mM compound **6**, 2mM compound **11** and 0.5 and 4mM DMSO.

Treatment of cells with compounds **1**, **6**, **11** and DMSO resulted in detection of reduced level of phosphorylated 4E-BP1 relative to the total protein 4E-BP1 in all samples at 15-20 kDa with most pronounced reduction in the cell treated with 0.25mM of compound **6**, and 2 and 4 mM of compound **11** (Figure 16 and Figure 18). The reduced amount of phosphorylated 4E-BP1 in cells treated with 2mM compound **11** corresponds the with intensity of lane 6 which is lower when compared with untreated control cells. Phosphorylated 4E-BP1 is the inactive form of 4E-BP1 which is inhibited by active mTOR. This leads to elevated level of eukaryotic translation initiation factor 4E (elF4E), which promote protein synthesis, including synthesis of oncogenic proteins (96), which again results in increased survival of cancer cells. As expected by the induction of apoptosis, all the samples had a lower amount of phosphorylated 4E-BP1 than the total protein.

A protein band at 90 kDa indicates a detection of phosphorylated STAT5 at either tyrosine (Tyr) 694 and/or Tyr 699, which is the activated form of STAT5 (Figure 14) (97). As shown in Figure 15, the amount of phosphorylated STAT5 relative to β-actin was decreased in almost all compounds, with the most pronounced reduction in the cells treated by 0.1mM of compound **1**

(lane 2). While cells treated with 2mM compound **11** showed high level of phosphorylated STAT5 relative to β-actin. Unfortunately, the antibody against STAT5 did not work, and it is therefore not possible to compare the amount of phosphorylated STAT5 to total amount of STAT5. Moreover, as Figure 14 and Figure 15 illustrate, the low intensity on lane 2 and 3 relative to β-actin indicates a decreased amount of p STAT5 in cells treated with 0.1 and 0.05 mM concentration of compound **1**, respectively. This correlate with the apoptosis of the compound **1** (5.4 and 4%, respectively), and the induction of cell survival in MOLM-13 is diminished (98).

In this western blot analysis, it was difficult to conclude from the results, since the detection of important proteins, like caspase 7, phosphorylated ϒ-H2AX and total STAT5 are missing, and the quality of the results are not sufficient. It is necessary to repeat these experiments, preferably with fresh antibodies to obtain more certain results. Besides, the MOLM-13 cells should be treated with higher concentrations of the compounds or the exposure time should be longer in order to induce a somewhat higher percentage apoptosis. It is also important to beware that other types of cell death, independent from caspases, can occur, such as autophagy. It can be difficult to distinguish between the different cell death types by microscopy, and the molecular markers like caspase cleavage are therefore needed.

6.Conclusion

The aim of the thesis was to explore potential antileukemic drugs or lead compounds for the treatment of AML. We started the screening with 30 natural and synthetic compounds on MOLM-13 and NRK cell lines. Based on the cytotoxicity of the compounds on MOLM-13 and NRK cells, ten compounds were selected for further experiment in OCI-AML3, MV4-11 and H9C2 cells. Compounds **4**, **15** and **19** showed selectivity on leukemic cells, while compounds **1** and **28** had low EC_{50} value, except for the OCI-AML3 cells, and the ratio of EC_{50} value between the normal and AML cell lines was greater than seven.

The combination test with chemotherapeutic drugs demonstrated compound **1** and **11** synergized with DNR, compound **15** had synergy with venetoclax, while compound **6** showed synergistic effect in combination with both DNR and venetoclax. This implies that these four compounds could be possible candidate for treatment of AML. However, according to the criteria of EC_{50} definition, the potency of compound **11** is low (high EC_{50} value). In addition, compound **6** has intermediate potency on H9C2 cells, which needs further toxicity tests prior to verifying for potential anticancer effect. Therefore, the most promising candidates for AML therapy are compounds **1** and **15**.

6.1 Further investigation

These ten natural compounds should further be tested on other AML cell lines and non-cancerous cells, as well as on AML cells collected from patients. In addition, in this study, the synergistic test was only performed on MOLM-13 cells. A synergy test of the ten selected compounds should be performed on the other AML cells, including MV4-11 and OCI-AML3 in order to explore if other than compounds **1**, **6**, **11** and **15** have synergistic effect, or if these compounds synergize in combination with chemotherapeutic drugs on OCI-AML3 and MV4-11.

Further, to investigate which molecular mechanism that are involved in apoptotic cell death on OCI-AML3 and MV4-11 cell lines, western blotting should be done.
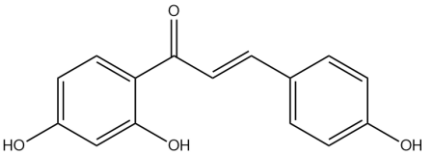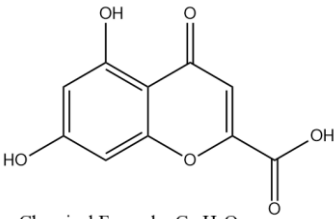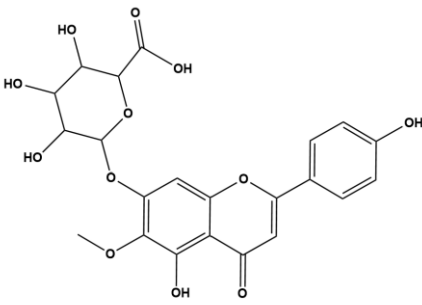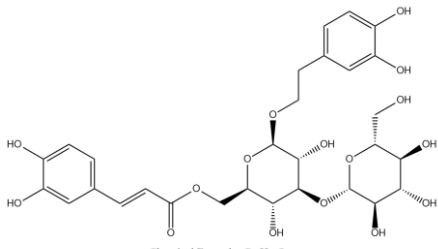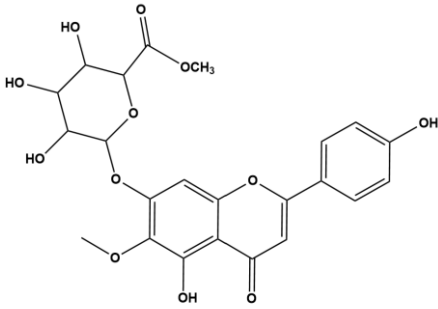
In this study, the mechanism of action of the compounds were not determined. And, it is important to know how the compounds act on the leukemic cells, therefore, this should be
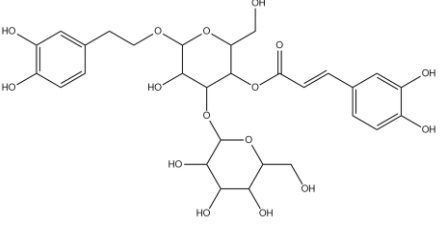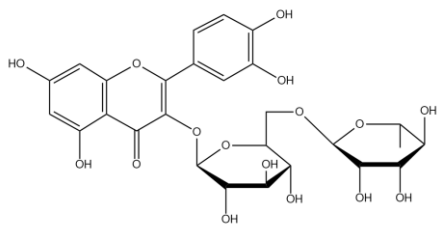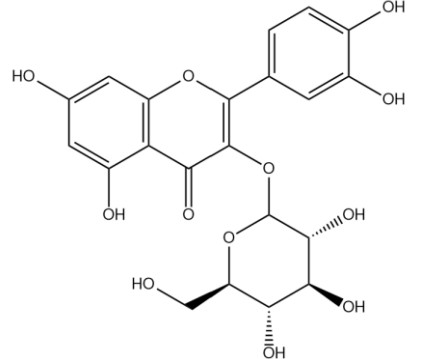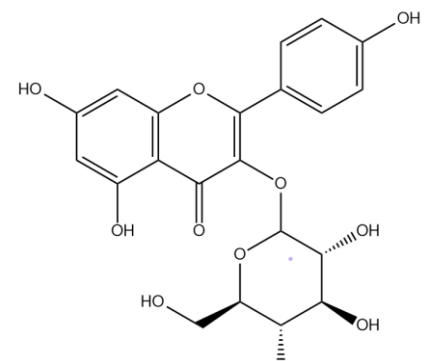
performed. In addition, the permeability and the uptake of the compound is also important to be determined.
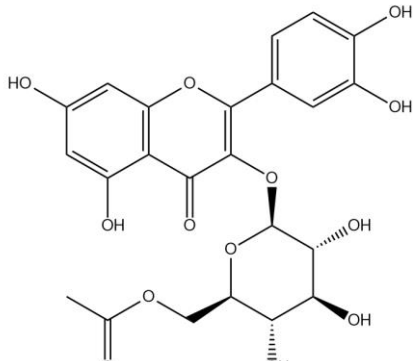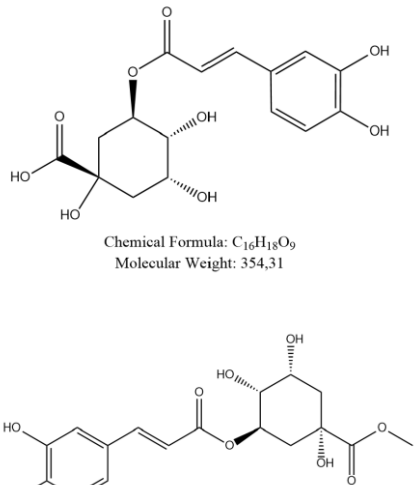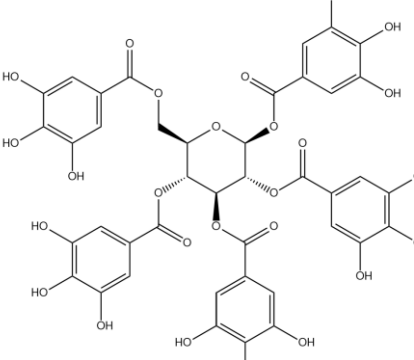
In *in vitro* studies, it is impossible to determine the pharmacokinetic of a drug, and it is important to understand how our body affects the drug when it is administrated. Therefore, pharmacokinetic studies of compound **1** and **15** should be determined, preferably in *in vivo* studies.
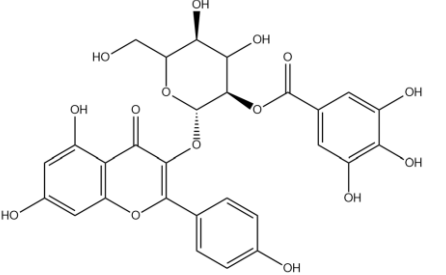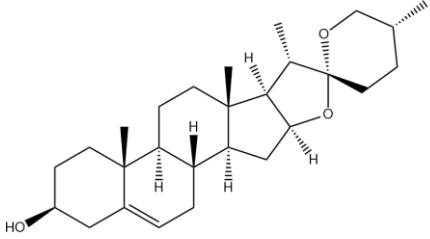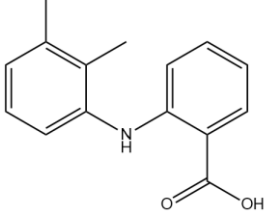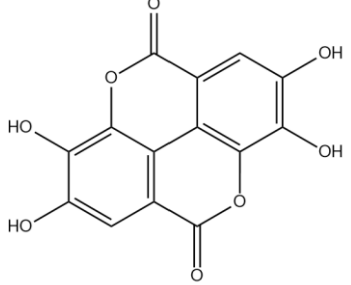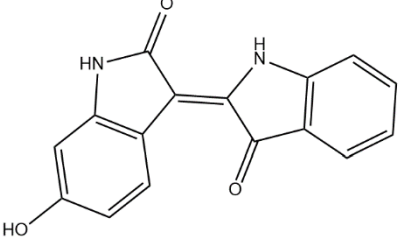
If these compounds have potential antileukemic effect, and the toxicity of the compound towards normal cells is determined, they can further be tested in vivo in an appropriate model the model for AML. There are several models available, the most popular being mouse models, but also other organisms, such as zebrafish can be used for this.
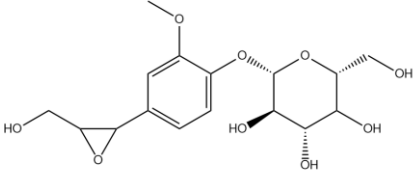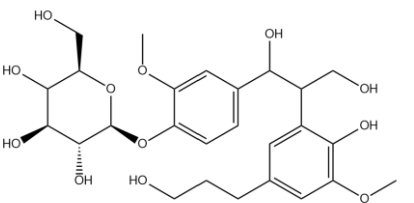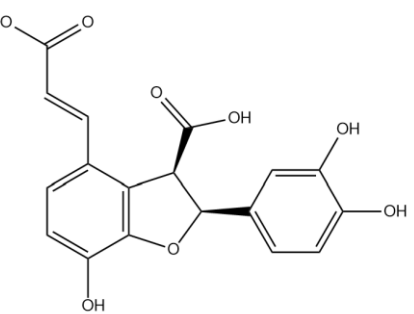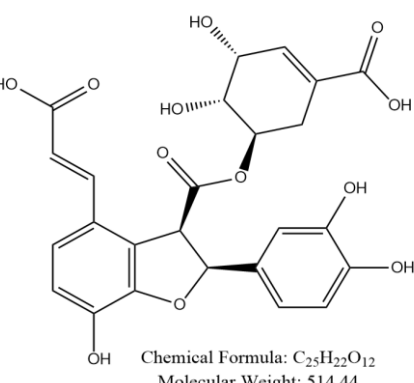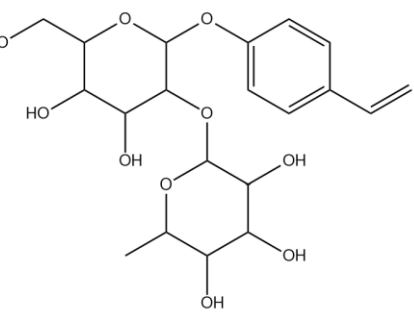
Appendix I
List of the compounds
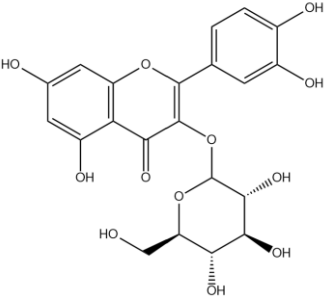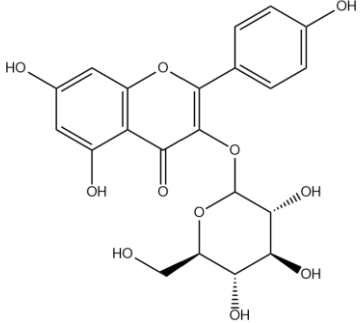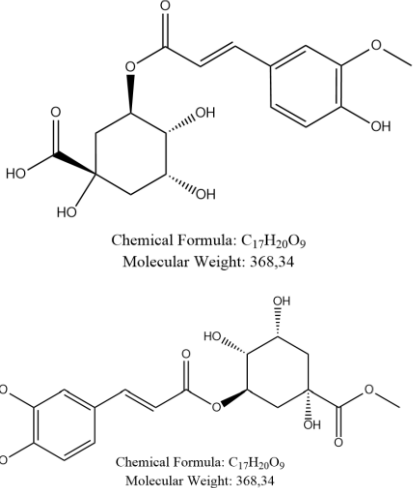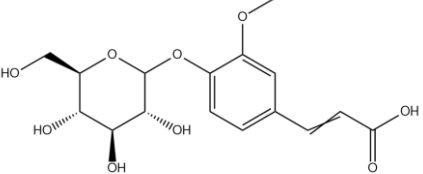
Nr	Name of compounds	Concentration of stock solution	Structure
1	2'-4,4'-trihydroxychalcone	100 mM	Chemical Formula: $C_{15}H_{12}O_4$ Molecular Weight: 256,26
2	Rumic acid	2.916 M	Chemical Formula: $C_{10}H_6O_6$ Molecular Weight: 222,15
3	Dinatin 7-glucuronide	11.9 mM	Chemical Formula: $C_{22}H_{20}O_{12}$ Molecular Weight: 476,39
4	Plantainoside D	62.4 mM	Chemical Formula: $C_{29}H_{36}O_{16}$ Molecular Weight: 640,59
5	Dinatin 7-methylglucuronide	15,9 mM	Chemical Formula: $C_{23}H_{22}O_{12}$ Molecular Weight: 490,42
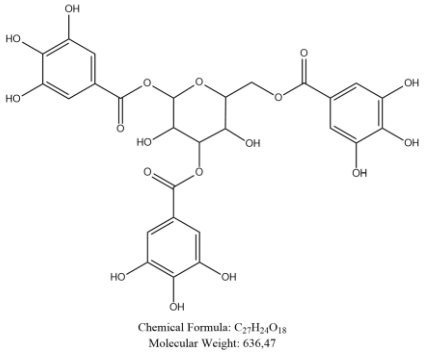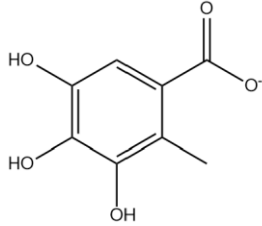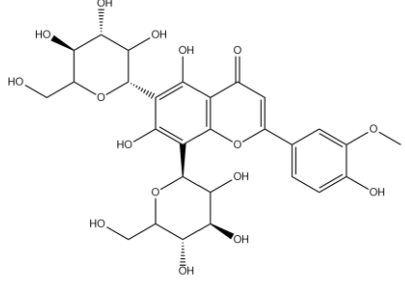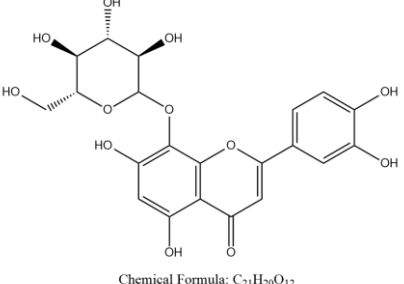
6	Plantamajoside	780 mM	
			Chemical Formula: $C_{29}H_{36}O_{16}$ Molecular Weight: 640,59
7	Quercetin 3-rutinoside (rutin)	174 mM	
			Chemical Formula: $C_{27}H_{30}O_{16}$ Molecular Weight: 610,52
8	Quercetin-3-glucoside	60,6 mM	
			Chemical Formula: $C_{21}H_{20}O_{12}$ Molecular Weight: 464,38
9	Kaempferol 3-glucoside	18,1 mM	
			Chemical Formula: $C_{21}H_{20}O_{11}$ Molecular Weight: 448,38

10	Quercetin 3-(6"-acetylglucoside) + quercetin 3-glucoside	1,057 M	Chemical Formula: $C_{23}H_{22}O_{13}$ Molecular Weight: 506,42
11	Chlorogenic acid and chlorogenic acid methyl ester (1:1)	1,520 M	Chemical Formula: $C_{16}H_{18}O_9$ Molecular Weight: 354,31 Chemical Formula: $C_{17}H_{20}O_9$ Molecular Weight: 368,34
12	Pentagalloylglucose	820 mM	Chemical Formula: $C_{41}H_{32}O_{26}$ Molecular Weight: 940,68

13	Kaempferol 3-(2''-galloylglucoside)	5,85 mM	Chemical Formula: $C_{28}H_{24}O_{15}$ Molecular Weight: 600,49
14	Diosgenin	5,425 mM	Chemical Formula: $C_{27}H_{42}O_3$ Molecular Weight: 414,63
15	Mefenamic acid	88,3 mM	Chemical Formula: $C_{15}H_{15}NO_2$ Molecular Weight: 241,29
16	Ellagic acid	9,525 mM	Chemical Formula: $C_{14}H_6O_8$ Molecular Weight: 302,19
17	RSRED	17,9 mM	Chemical Formula: $C_{16}H_{10}N_2O_3$ Molecular Weight: 278,27

18	WPS 9-11-7,8-Oxiran-coniferylalcohol 4-glucoside	278mM	Chemical Formula: $C_{16}H_{22}O_9$ Molecular Weight: 358,34
19	WPS 26-31 - Dihydrodehydroconiferylalcohol 4-glucoside	186 mM	Chemical Formula: $C_{26}H_{36}O_{12}$ Molecular Weight: 540,56
20	Blechnic acid	112 mM	Chemical Formula: $C_{18}H_{14}O_8$ Molecular Weight: 358,30
21	Brainic acid	342 mM	Chemical Formula: $C_{25}H_{22}O_{12}$ Molecular Weight: 514,44
22	Ptelatoside B	760 mM	Chemical Formula: $C_{20}H_{28}O_{10}$ Molecular Weight: 428,43

23	Quercetin-3-glucoside	269 mM	Chemical Formula: $C_{21}H_{20}O_{12}$ Molecular Weight: 464,38
24	Kaempferol 3-glucoside	275 mM	Chemical Formula: $C_{21}H_{20}O_{11}$ Molecular Weight: 448,38
25	Klorogensyrederivat (av ferulsyre) + metylester	240 mM	Chemical Formula: $C_{17}H_{20}O_9$ Molecular Weight: 368,34 Chemical Formula: $C_{17}H_{20}O_9$ Molecular Weight: 368,34
26	Ferulic acid 4-glucoside	452 mM	Chemical Formula: $C_{16}H_{20}O_9$ Molecular Weight: 356,33

27	Tannin	96,6 mM	
			Chemical Formula: $C_{27}H_{24}O_{18}$ Molecular Weight: 636,47
28	Methylgallate	303 mM	 Chemical Formula: $C_8H_7O_5^-$ Molecular Weight: 183,14
29	Chrysoeriol 6,8-di-C-glucoside	85,1 mM	 Chemical Formula: $C_{28}H_{32}O_{16}$ Molecular Weight: 624,55
30	Luteolin 8-C-glucoside	223mM	 Chemical Formula: $C_{21}H_{20}O_{12}$ Molecular Weight: 464,38

Appendix II

	EC$_{50}$ (uM) ($\pm$SEM) at 24 hours incubation		EC$_{50}$ (uM) ($\pm$SEM) at 72 hours incubation	
Compound	MOLM-13	NRK	MOLM-13	NRK
1	11.35 $\pm$ 31.82 12.59 $\pm$ 8.19 11.11 $\pm$ 15.12	126 $\pm$ 35.38 108.44 $\pm$ 12.58	7.16 $\pm$ 6.47 5.62 $\pm$ 5.11 5.28 $\pm$ 9.27	153.02 $\pm$ 8.21 103.54 $\pm$ 13.86
2	479.33 $\pm$ 4.45 1056.16 $\pm$ 10.73	12833.99 $\pm$ 16.35	630.06 $\pm$ 16.74 1342.19 $\pm$ 7.38	6434.61 $\pm$ 15.83
3	n.d.	n.d	n.d.	n.d.
4	35.17 $\pm$ 16.28	542.03 $\pm$ 7.63*	20.77 $\pm$ 8.61	120.52 $\pm$ 25.42
5	n.d.	n.d.	n.d.	n.d.
6	122.47 $\pm$ 14.55 108.64 $\pm$ 6.77	1000,58 $\pm$ 6.87	61.96 $\pm$ 5.87 72.54 $\pm$ 5.09	559.9 $\pm$ 12.07
7	451.08 $\pm$ 0,07[b]	n.d.	802.76 $\pm$ 0.12	n.d.
8	314.41 $\pm$ 0.15	n.d.	89.89 $\pm$ 0.15	366.29 $\pm$ 0.08
9	88.82 $\pm$ 0.1	n.d.	44.68 $\pm$ 0.18	n.d.
10	2490.46 $\pm$ 0.059[b]	n.d.	4953.78 $\pm$ 0.13	n.d.
11	1949.07 $\pm$ 8.69	13830.98 $\pm$ 9.23*	988.95 $\pm$ 10.72	5693.48 $\pm$ 8.08
12	14.35 $\pm$ 9.91	74.31 $\pm$ 4.64	13.36 $\pm$ 13.56	19.88 $\pm$ 5.06
13	n.d.	n.d.	n.d.	n.d.
14	n.d.	n.d.	27.78 $\pm$ 0.09	n.d.
15	142.75 $\pm$ 4.42	n.d.	98.50 $\pm$ 6.36	n.d.
16	n.d.	n.d.	n.d.	n.d.
17	14.86 $\pm$ 0.04	n.d.	6.42 $\pm$ 0.07[b]	
18	2522.46 $\pm$ 0.07	n.d.	2421.73 $\pm$ 0.23	n.d.
19	431.01 $\pm$ 7.35	n.d.	238.66 $\pm$ 23.59	n.d.
20	61.83 $\pm$ 0.10	447.36 $\pm$ 0.06	27.78 $\pm$ 0.12	174.89 $\pm$ 0.04

21	213.93 ± 0.15	1370.14 ± 0.07	63.64 ± 0.17	324.64 ± 0.03
22	332.99 ± 0.05	1879.57 ± 0.18	162.14 ± 0.05	938.83 ± 0.09
23	103.09 ± 0.14	1329.71 ± 0.05	52.43 ± 0.13	323.35 ± 0.7
24	153.05 ± 0.11	1618.99 ± 0.1	62.38 ± 0.11	666.04 ± 0.04
25	407.27 ± 0.06	2160.13 ± 0.06*	156.15 ± 0.07	630.88 ± 0.08
26	1511.43 ± 0.12	n.d.	359.22 ± 0.16	n.d.
27	36.81 ± 8.82	246.45 ± 7.72	10.2 ± 4.89	44.16 ± 14.47
28	58.01 ± 17.71	1687.39 ± 7.38	21.86 ± 20.41	400.39 ± 4.3
29	n.d.	n.d.	n.d.	n.d.
30	155.14 ± 0.1	n.d.	70.03 ± 0.1	926.45 ± 0.07

EC_{50} for MOLM-13 and NRK cell lines examined with 30 natural compounds for 24 and 72 hours. The cell viability was determined using WST-1 reagent before the cells were fixated in 2% fixative solution. The EC_{50} values of some compounds were calculated even though the compounds displayed less than 100 % cytotoxicity, and this represent compound 7, 10 and 18 on MOLM-13 for 24 hours experiment, and compounds 1 (for both 24- and 72-hours screening), 8 and 17 on NRK cells for 72-hours incubation.

n.d. indicate not determined. These compounds had cell viability ≥ 50% and this make difficult to estimate the right EC_{50} value.

* The compounds were not cytotoxic at that specific concentration, and cytotoxicity of the compounds was difficult to consider at higher concentration.

Appendix III

Comp	EC$_{50}$ (uM) ($\pm$SEM) at 24 hours incubation			EC$_{50}$ (uM) ($\pm$SEM) at 72 hours incubation		
	OCI-AML3	MV4-11	H9C2	OCI-AML3	MV4-11	H9C2
1	33.38 $\pm$ 9.74	9.73 $\pm$ 5.72	247.41 $\pm$ 24.45	11.55 $\pm$ 7.3	7.45 $\pm$ 5.37	162.68 $\pm$ 7.04
2	1956.51 $\pm$ 12.99	1001.21 $\pm$ 13.47	14938.64 $\pm$ 15.4	1950.21 $\pm$ 13.55	870.02 $\pm$ 10.93	3985.18 $\pm$ 11.98
4	215.86 $\pm$ 5.67	263.56 $\pm$ 5.99	430.11 $\pm$ 17.85	122.69 $\pm$ 7.88	126.55 $\pm$ 6.48	268.78 $\pm$ 12.48
6	256.32 $\pm$ 7.72	627.05 $\pm$ 7.55	337.53 $\pm$ 12.97	191.5 $\pm$ 7.86	252.93 $\pm$ 19.53	443.7 $\pm$ 17.33
11	1312.98 $\pm$ 8.52	855.05 $\pm$ 5.54	2637.62 $\pm$ 7.54	1269.58 $\pm$ 10.47	821.45 $\pm$ 9.68	2757.29 $\pm$ 7.87
12	72.83 $\pm$ 6.71	27.8 $\pm$ 12.32	59.98 $\pm$ 7.93	2.41 $\pm$ 12.22	25.55 $\pm$ 11.36	44.37 $\pm$ 17.33
15	307.16 $\pm$ 9.78	144.97 $\pm$ 6.86	n.d.	233.34 $\pm$ 4.97	94.98 $\pm$ 9.98	n.d.
19	997.45 $\pm$ 5.87	468.19 $\pm$ 5.78	n.d.	336.32 $\pm$ 13.52	242.04 $\pm$ 11.87	1603.35 $\pm$ 14.48
27	120.76 $\pm$ 22.96	121.24 $\pm$ 15.01	124.97 $\pm$ 19.24	50.0 $\pm$ 11.1	22.56 $\pm$ 9.5	231.64 $\pm$ 33.69
28	n.d.	69.55 $\pm$ 10.54	1152.6 $\pm$ 24.94	107.34 $\pm$ 7.31	38.0 $\pm$ 11.38	351.54 $\pm$ 23.61

EC$_{50}$ for OCI-AML3, MV4-11 and H9C2 cells incubated for 24 and 72 hours with 10 chosen compounds. The cell viability were determined using WST-1 reagent before the cells were fixated in 2% fixative solution. The EC$_{50}$ values of compounds 4 and 19 were calculated even though the compounds displayed no cytoxic acitivity on H9C2 cells.

n.d. indicate not determined. Those compounds had cell viability $\geq$ 50% and this make difficult to estimate the right EC$_{50}$ value. Comp = compound

Appendix IV
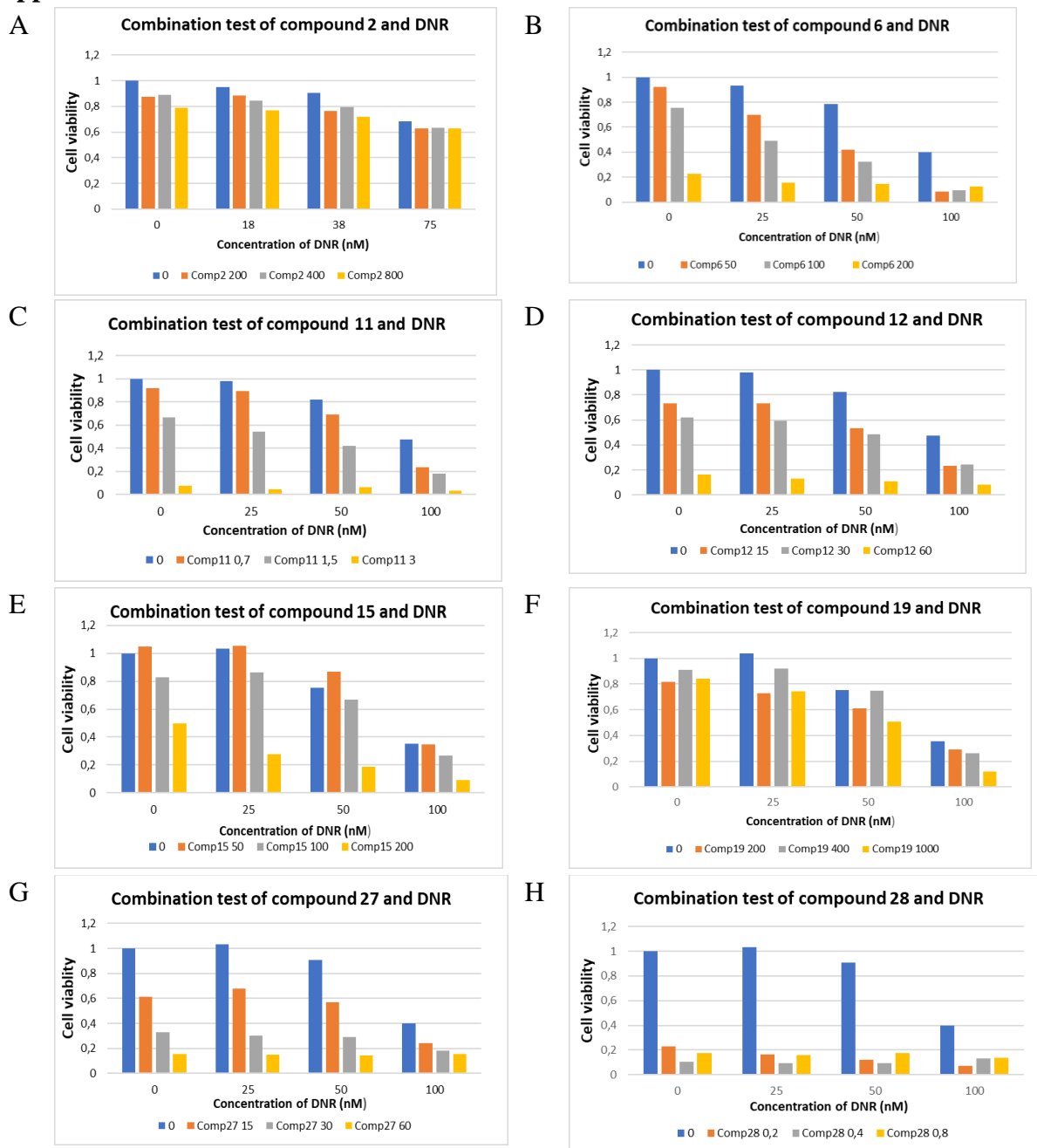
These bar charts were a result of synergy test between DNR and compounds 2 (A), 6 (B), 11 (C), 12 (D), 15 (E), 19 (F), 27 (G) and 28 (H). This test was performed with three different concentration of compounds and anticancer drug on MOLM-13 cells for 24 hours, before the metabolic activity of the cells were determined using WST-1 assay, and the data was used to determine the cell viability. The viability below 20% were not included in calculation of Coefficient of drug interaction (CDI). The concentration of compounds was in micromoles, except for compound 11 and 28 which were in millimoles.
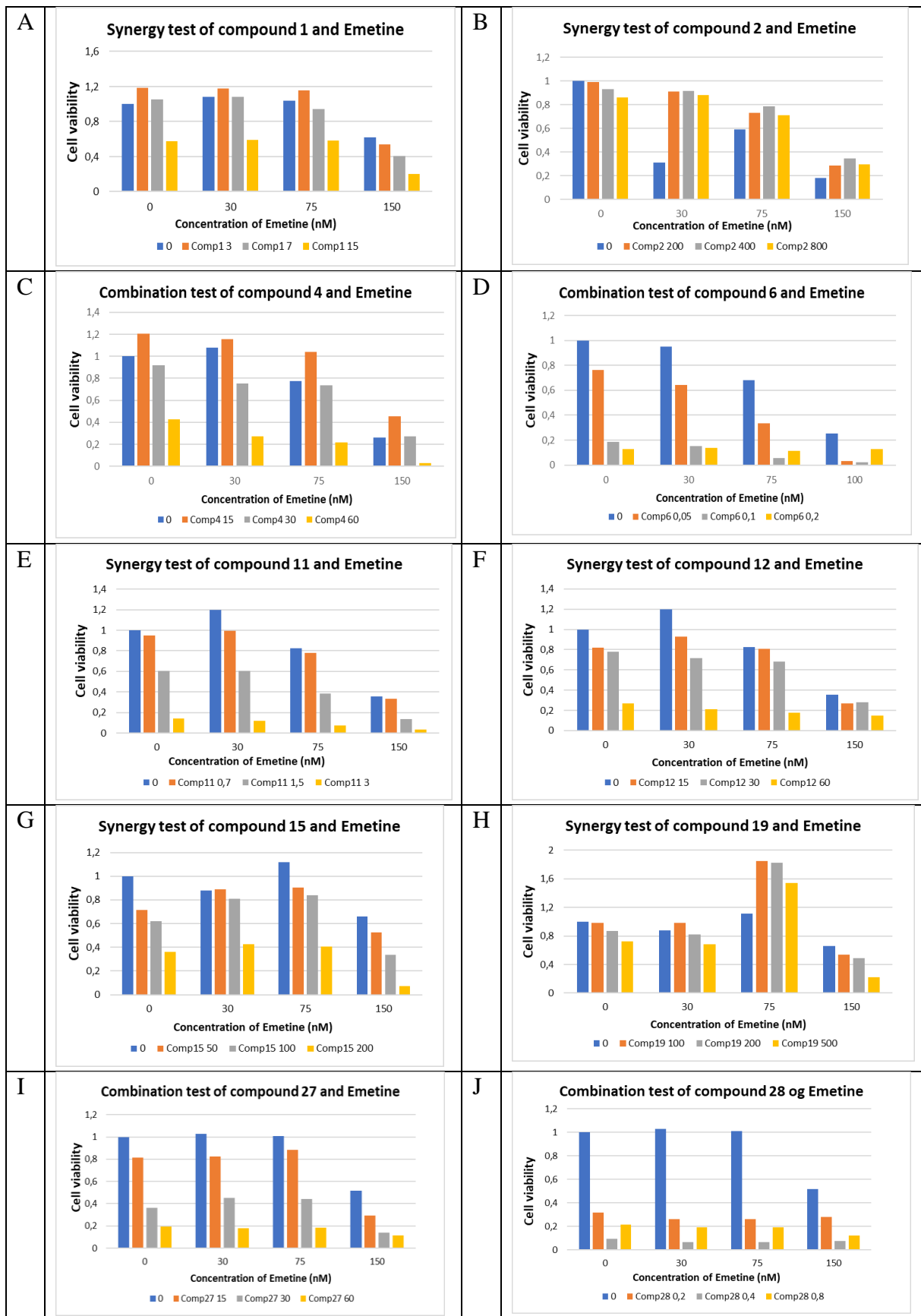
These bar charts were a result of synergy test of Emetine and compounds 1 (A), 2 (B), 4 (C), 6 (D), 11 (E), 12 (F), 15 (G), 19 (H), 27 (I) and 28 (J). This test was performed with three different concentration of compounds and

anticancer drug on MOLM-13 cells for 24 hours, before the metabolic activity of the cells were determined using WST-1 assay, and the data was used to determine the cell viability. The viability below 20% were not included in calculation of Coefficient of drug interaction (CDI). All combination of compound 28 and cytostatics had low cell viability as shown in other charts, except the combination with Emetine. The concentration of compounds was in micromoles, except for compound 11 and 28 which were in millimoles.
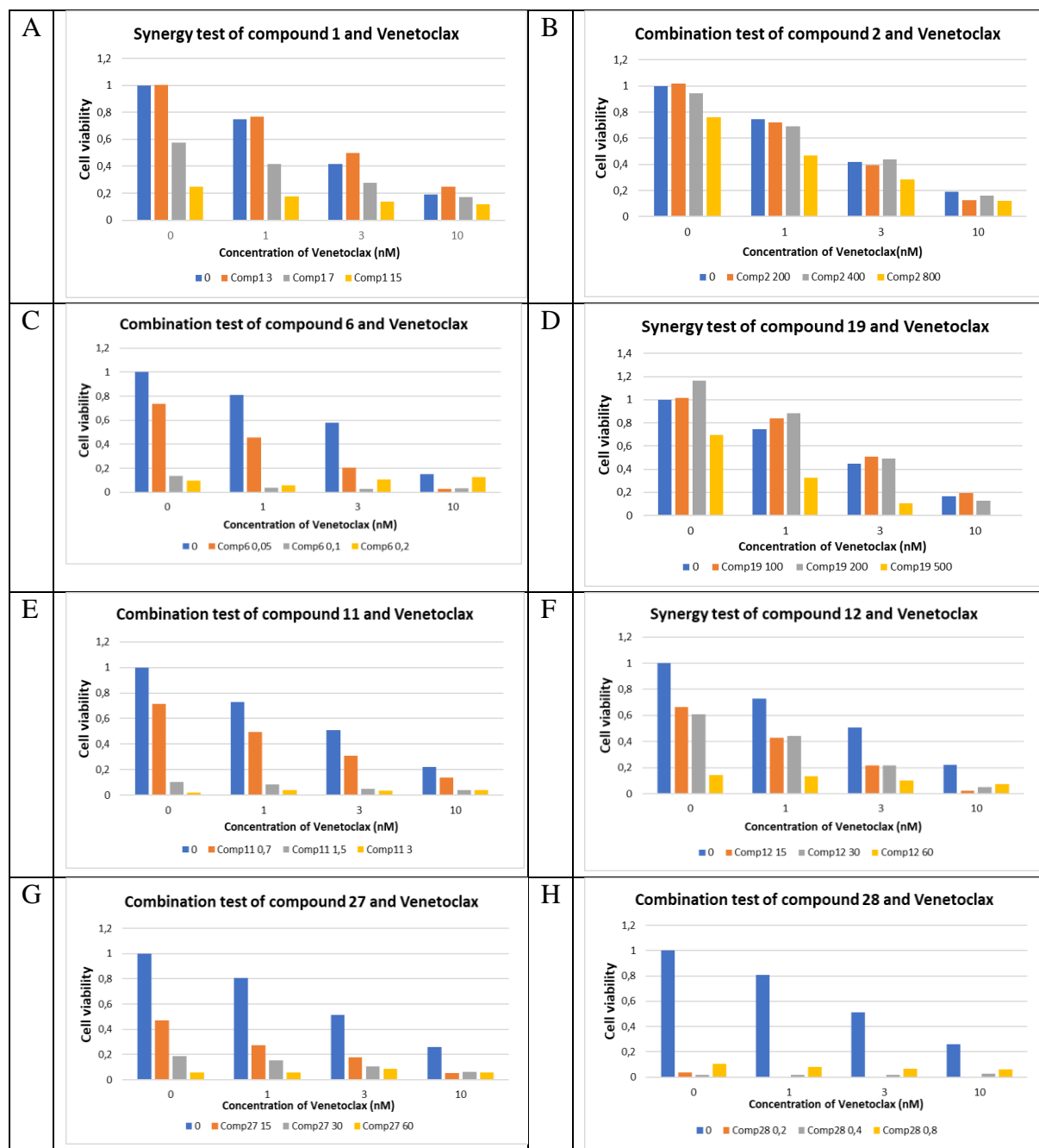

These bar charts were a result of synergy test of Venetoclax and compounds 1 (A), 2 (B), 6 (C), 11 (D), 12 (E), 19 (F), 27 (G) and 28 (H). This test was performed with three different concentration of compounds and anticancer drug on MOLM-13 cells for 24 hours, before the metabolic activity of the cells were determined using WST-1 assay, and the data was used to determine the cell viability. The viability below 20% were not included in calculation of Coefficient of drug interaction (CDI). The concentration of compounds was in micromoles, except for compound 11 and 28 which were in millimoles.
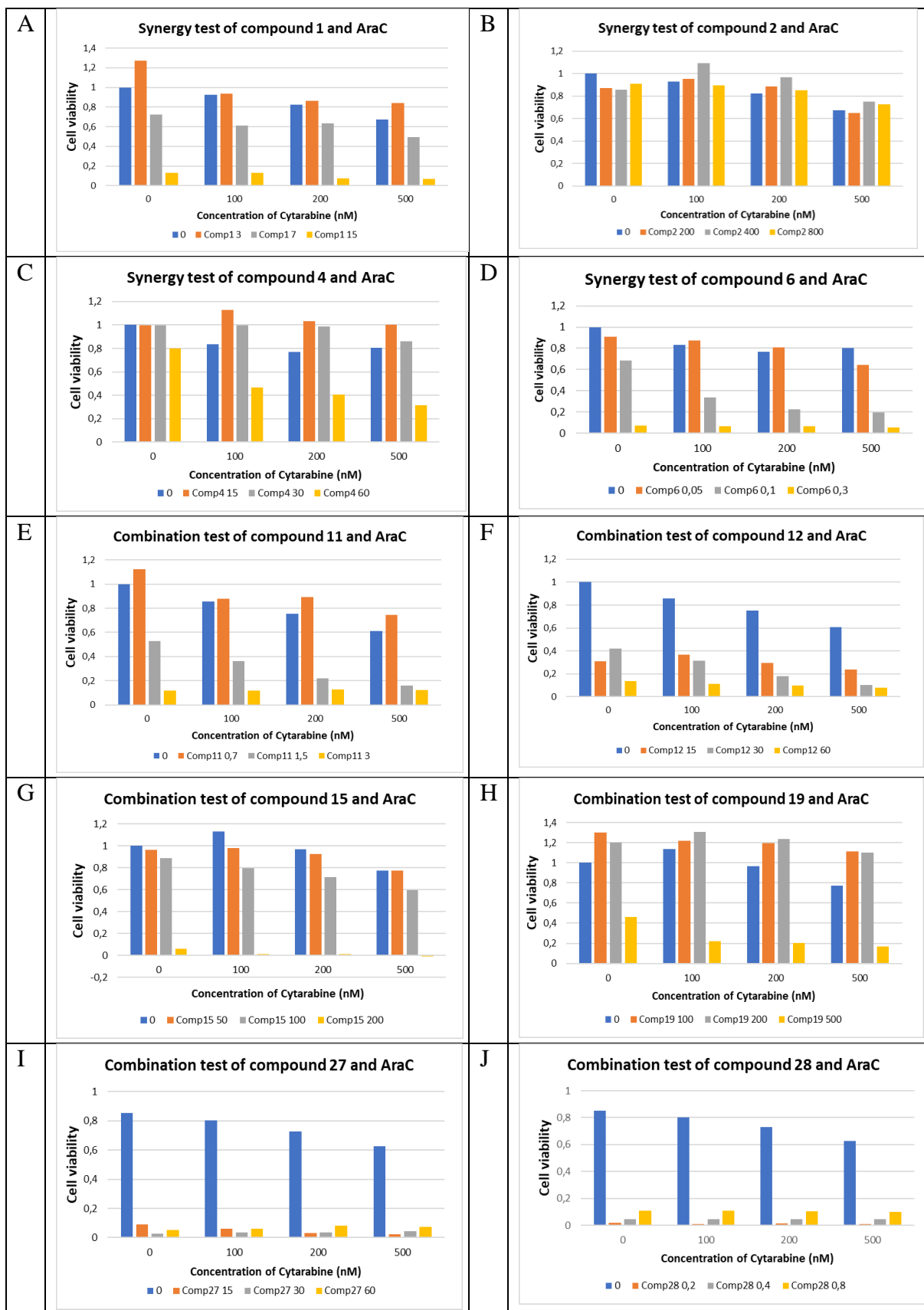
These bar charts were a result of synergy test of Cytarabine and compounds 1 (A), 2 (B), 4 (C), 6 (D), 11(E), 12 (F), 15 (G), 19 (H), 27 (I) and 28 (J). Combination test was performed as mentioned above and the cell viability was determined based on WST-1 results. The viability below 20% were not included in calculation of

Coefficient of drug interaction (CDI). The concentration of compounds was in micromoles, except for compound 11 and 28 which were in millimoles.

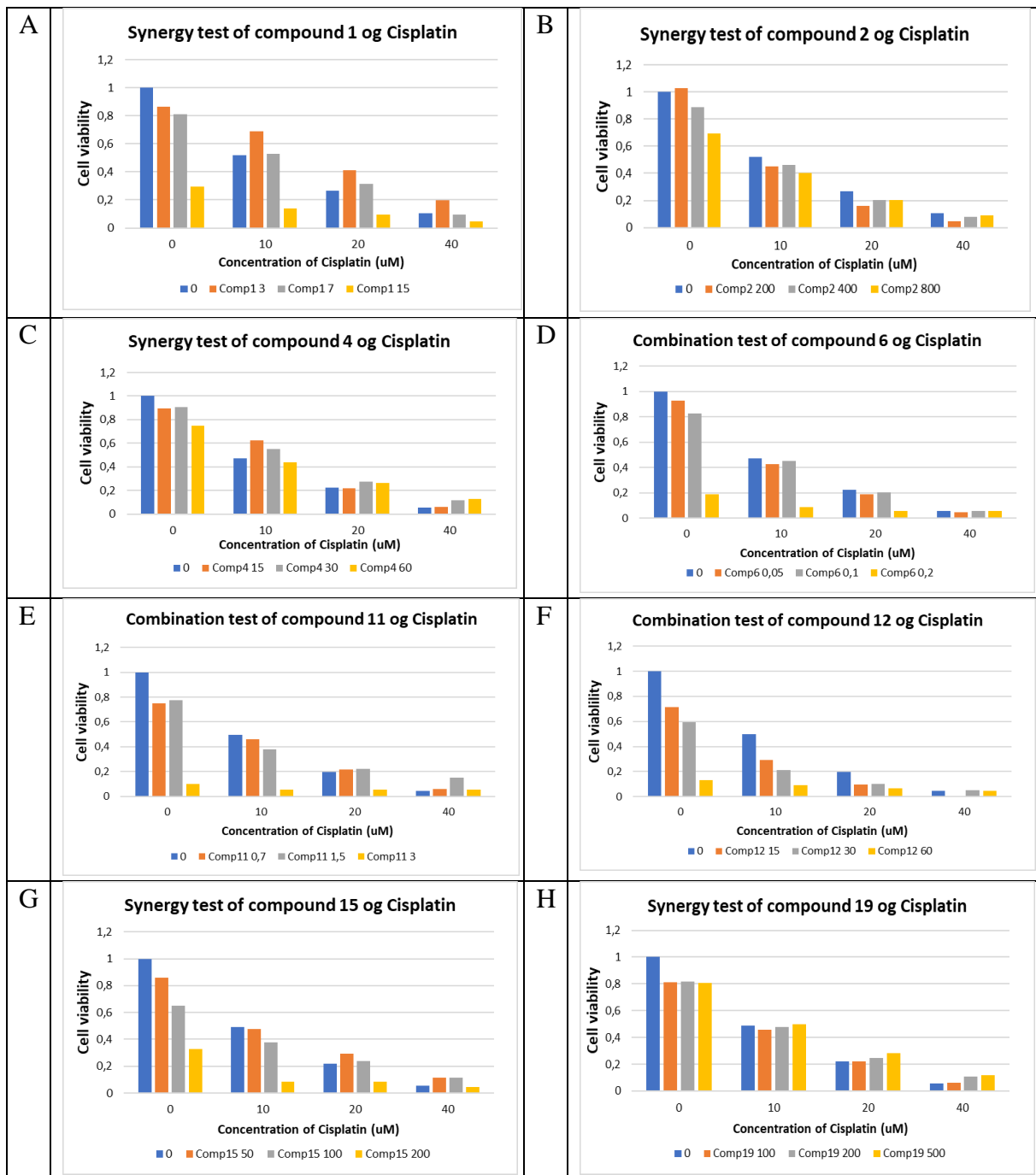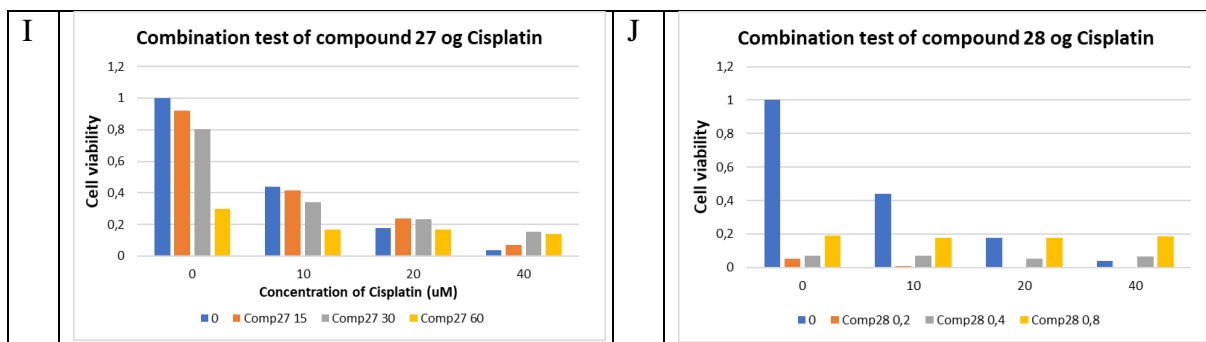These bar charts were a result of combination test of Cisplatin and compounds 1 (A), 2 (B), 4 (C), 6 (D), 11(E), 12 (F), 15 (G), 19 (H), 27 (I) and 28 (J). Combination test was performed as mentioned above and the cell viability was determined based on WST-1 results. The viability below 20% were not included in calculation of Coefficient of drug interaction (CDI).
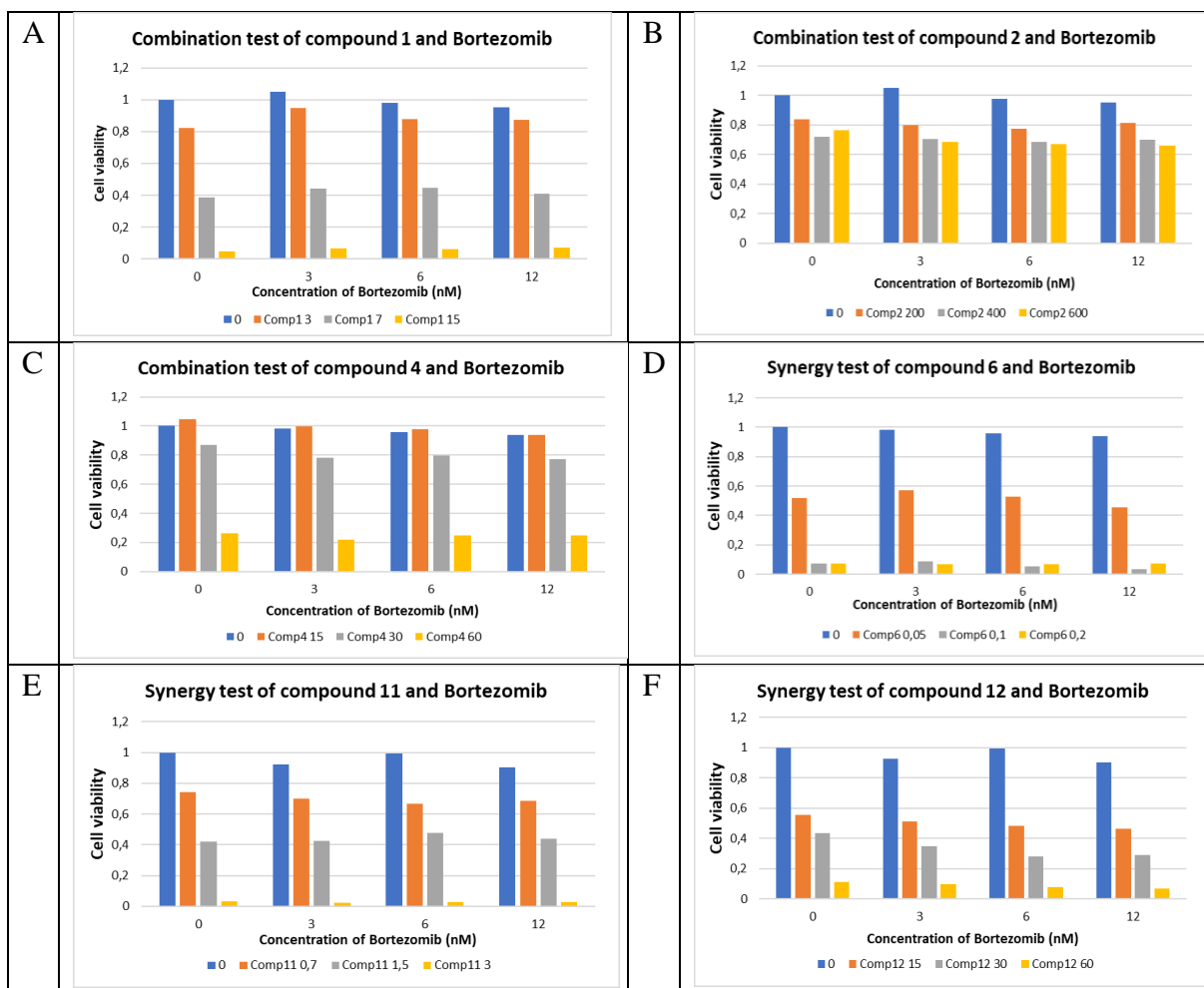
These bar charts were a result of combination test of Bortezomib and compounds 1 (A), 2 (B), 4 (C), 6 (D), 11(E), 12 (F), 15 (G), 19 (H), 27 (I) and 28 (J). Combination test was performed as mentioned above and the cell viability was determined based on WST-1 results. The viability below 20% were not included in calculation of Coefficient of drug interaction (CDI).
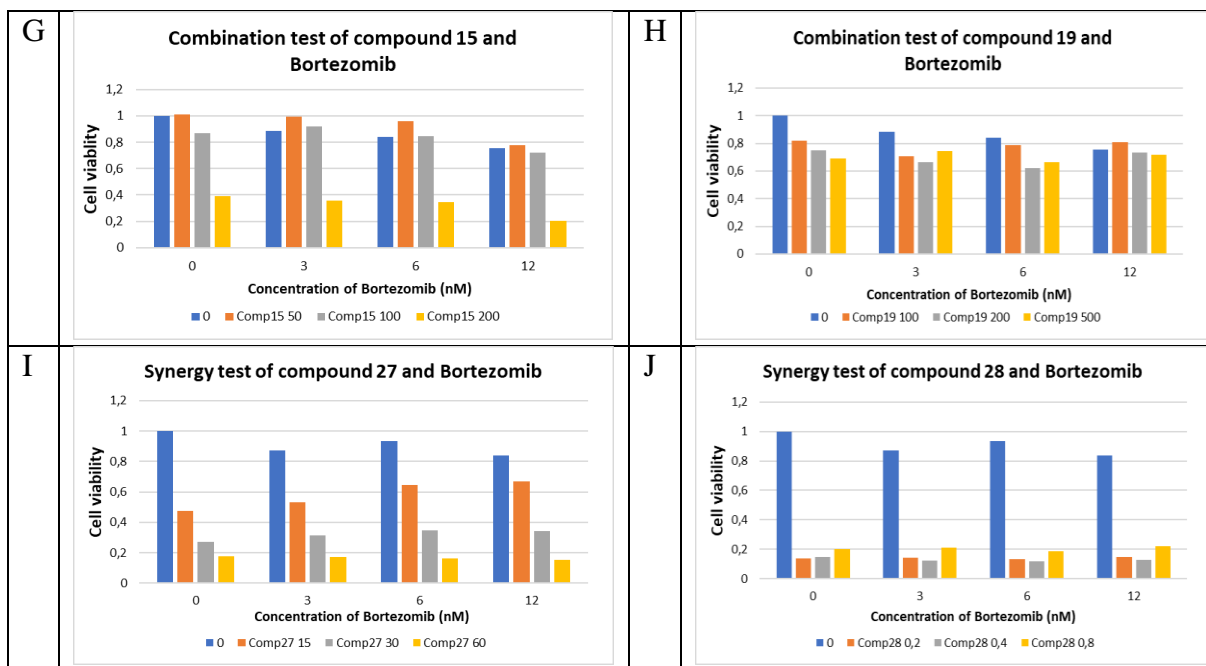
A

B

C
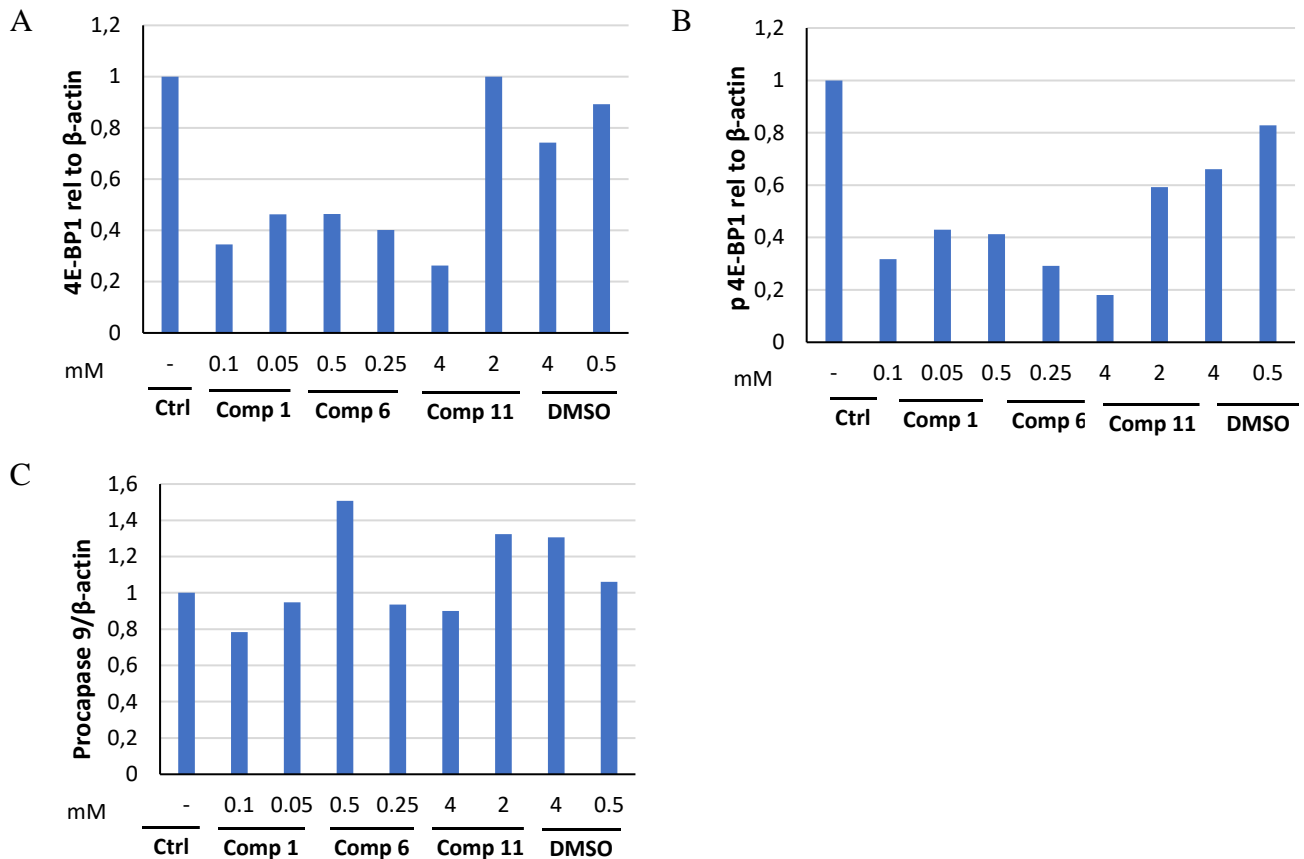
These graphs demonstrate the amount of 4E-BP1 (A), phosphorylated 4E-BP1 (B) and procaspase (C) relative to β-actin. The amount of these protein was quantified by Image>Analyze>Gels. MOLM-13 cells are treated with high and low concentration of compounds 1, 6, 11 and DMSO for 2 hours. Percentage apoptosis are given in Figure 14 and Figure 16. The amount of phosphorylated 4E-BP1 and 4E-BP1 relative to β-actin decreased when the cells treated with high and low concentration of compound 1 and 6, and high concentration of compound 11. While the amount of procaspase relative to β-actin slightly decreased when the cells were treated with 0.1 and 0.05 mM of compound 1, 0.25mM compound 6 and 4mM compound 11. However, treatment of MOLM-13 cells with 0.5 mM of compound 6, 2 mM of compound 11, 0.5 and 4mM of DMSO, showed an increased amount of procaspase 9.

Comp = compound

Appendix VI
Start concentration of compounds used in screening test toward the five cell lines

Compound	MOLM-13	NRK	OCI-AML3	MV4-11	H9C2
1	1 mM 0.25 mM 62.5 µM	1 mM 0.25 mM	0.25 mM	0.25 mM	0.5 mM
2	29.16 mM 3.6 mM	29.16 mM	10 mM	10 mM	30 mM
4	624 µM	624 µM	500 µM	500 µM	500 µM
6	7.8 mM 1 mM	7.8 mM	1 mM	1 mM	10 mM
11	15.2 mM	15.2 mM	20 mM	20 mM	20 mM
12	820 µM	820 µM	200 µM	200 µM	1 mM
15	883 µM	883 µM	1 mM	1 mM	1 mM
19	1.86 mM	1.86 mM	1.86 mM	1.86 mM	1.86 mM
27	966 µM	966 µM	483 µM	483 µM	966 µM
28	3.03 mM	3.03 mM	1 mM	1 mM	3.03 mM

References

1.   Cornell RF, Palmer J. Adult acute leukemia. Dis Mon. 2012;58(4):219-38.
2.   Juliusson G, Hough R. Leukemia. Prog Tumor Res. 2016;43:87-100.
3.   Lyengar V, Shimanovsky A. Leukemia. StatPearls. Treasure Island (FL): StatPearls Publishing

Copyright © 2021, StatPearls Publishing LLC.; 2021.
4.   Konieczny J, Arranz L. Updates on Old and Weary Haematopoiesis. International Journal of Molecular Sciences. 2018;19(9):2567.
5.   Evensen SA. Beinmargen Store medisinske leksikon på snl.no: sml; 2021 [Available from: https://sml.snl.no/beinmargen.
6.   Gleichmann N. What are Progenitor Cells? Exploring Neural, Myeloid and Hematopoietic Progenitor Cells technology networks2020 [January 25, 2021]. Available from: https://www.technologynetworks.com/cell-science/articles/what-are-progenitor-cells-exploring-neural-myeloid-and-hematopoietic-progenitor-cells-329519.
7.   Learning L. Production of the Formed Elements Lumen Learning [January 25, 2021]. Available from: https://courses.lumenlearning.com/cuny-kbcc-ap2/chapter/production-of-the-formed-elements/.
8.   Hiddemann W.
9.   Devine SM, Larson RA. Acute leukemia in adults: recent developments in diagnosis and treatment. CA Cancer J Clin. 1994;44(6):326-52.
10.   van't Veer MB. The diagnosis of acute leukemia with undifferentiated or minimally differentiated blasts. Ann Hematol. 1992;64(4):161-5.
11.   Roy P, Coleman MP. [Epidemiology of acute lymphoid leukemia]. Rev Epidemiol Sante Publique. 1992;40(5):323-34.
12.   Short NJ, Rytting ME, Cortes JE. Acute myeloid leukaemia. Lancet. 2018;392(10147):593-606.
13.   Grove CS, Vassiliou GS. Acute myeloid leukaemia: a paradigm for the clonal evolution of cancer? Dis Model Mech. 2014;7(8):941-51.
14.   De Kouchkovsky I, Abdul-Hay M. 'Acute myeloid leukemia: a comprehensive review and 2016 update'. Blood Cancer J. 2016;6(7):e441.
15.   Helsedirektoratet. Nasjonalt handlingsprogram med retningslinjer for diagnostikk, behandling og oppfølging av maligne blodsykdommer. Oslo: Helsedirektoratet; 2020. [updated May, 2020.January 30, 2021.]. Available from: https://www.helsedirektoratet.no/retningslinjer/maligne-blodsykdommer-handlingsprogram/Maligne%20blodsykdommer%20%E2%80%93%20Nasjonalt%20handlingsprogram%20med%20retningslinjer%20for%20diagnostikk,%20behandling%20og%20oppf%C3%B8lging.pdf/_/attachment/inline/0ec076b8-71ba-450e-83f3-76919e5ab024:3ed1339749fb85b1c91677079605e70baadab6f1/Maligne%20blodsykdommer%20%E2%80%93%20Nasjonalt%20handlingsprogram%20med%20retningslinjer%20for%20diagnostikk,%20behandling%20og%20oppf%C3%B8lging.pdf.
16.   Estey E, Döhner H. Acute myeloid leukaemia. Lancet. 2006;368(9550):1894-907.
17.   Wadleigh M, Dorfman DM, Skarin AT. 15 - Acute and Chronic Leukemias. In: Skarin AT, editor. Atlas of Diagnostic Oncology (Fourth Edition). Philadelphia: Mosby; 2010. p. 529-70.
18.   Appelbaum FR. 95 - Acute Leukemias in Adults. In: Niederhuber JE, Armitage JO, Kastan MB, Doroshow JH, Tepper JE, editors. Abeloff's Clinical Oncology (Sixth Edition). Philadelphia: Elsevier; 2020. p. 1783-97.e1.
19.   Hoffbrand AV, Moss PAH. Essential haematology. 6th ed. ed: Wiley Blackwell; 2011.
20.   Ross K, Gillespie-Twardy AL, Agha M, Raptis A, Hou JZ, Farah R, et al. Intensive chemotherapy in patients aged 70 years or older newly diagnosed with acute myeloid leukemia. Oncol Res. 2015;22(2):85-92.
21.   Cornelissen JJ, Blaise D. Hematopoietic stem cell transplantation for patients with AML in first complete remission. Blood. 2016;127(1):62-70.

22.   America. CTCo. Allogeneic stem cell transplant 2021 [February 12, 2021]. Available from: https://www.cancercenter.com/treatment-options/hematologic-oncology/allogeneic-stem-cell-transplant.

23.   Cancer Treatment Centers of America. Autologous stem cell transplant 2021 [February 12, 2021.]. Available from: https://www.cancercenter.com/treatment-options/hematologic-oncology/autologus-stem-cell-transplant.

24.   Takami A. Hematopoietic stem cell transplantation for acute myeloid leukemia. Int J Hematol. 2018;107(5):513-8.

25.   Koreth J, Schlenk R, Kopecky KJ, Honda S, Sierra J, Djulbegovic BJ, et al. Allogeneic stem cell transplantation for acute myeloid leukemia in first complete remission: systematic review and meta-analysis of prospective clinical trials. Jama. 2009;301(22):2349-61.

26.   Stelljes M, Krug U, Beelen DW, Braess J, Sauerland MC, Heinecke A, et al. Allogeneic transplantation versus chemotherapy as postremission therapy for acute myeloid leukemia: a prospective matched pairs analysis. J Clin Oncol. 2014;32(4):288-96.

27.   Levin-Epstein R, Oliai C, Schiller G. Allogeneic Hematopoietic Stem Cell Transplantation for Older Patients With Acute Myeloid Leukemia. Curr Treat Options Oncol. 2018;19(12):63.

28.   Amadori S, Del Principe MI, Venditti A. Advances in the treatment of elderly and frail patients with acute myeloid leukemia. Curr Opin Oncol. 2014;26(6):663-9.

29.   Döhner H, Estey E, Grimwade D, Amadori S, Appelbaum FR, Büchner T, et al. Diagnosis and management of AML in adults: 2017 ELN recommendations from an international expert panel. Blood. 2017;129(4):424-47.

30.   Krug U, Büchner T, Berdel WE, Müller-Tidow C. The treatment of elderly patients with acute myeloid leukemia. Dtsch Arztebl Int. 2011;108(51-52):863-70.

31.   Iqbal J, Abbasi BA, Mahmood T, Kanwal S, Ali B, Shah SA, et al. Plant-derived anticancer agents: A green anticancer approach. Asian Pacific Journal of Tropical Biomedicine. 2017;7(12):1129-50.

32.   håndboka. NL. Daunorubicin. [updated April 28, 2016.March 4, 2021.]. Available from: https://www.legemiddelhandboka.no/L2.1.4.3/Daunorubicin.

33.   Legemiddelhåndboka. N. Cytarabin. 2015. [updated May 25, 2017.March 4, 2021.]. Available from: https://www.legemiddelhandboka.no/L2.1.2.8/Cytarabin.

34.   Margarita G. Therapy-Related Acute Myeloid Leukemias. In: Gueorgui B, Margarita G, Gueorgui B, editors. Leukemia. Rijeka: IntechOpen; 2013.

35.   Feldman EJ. Novel Therapeutics for Therapy-Related Acute Myeloid Leukemia: 2014. Clin Lymphoma Myeloma Leuk. 2015;15 Suppl:S91-3.

36.   Kadia TM, Ravandi F, Cortes J, Kantarjian H. New drugs in acute myeloid leukemia. Ann Oncol. 2016;27(5):770-8.

37.   Winer ES, Stone RM. Novel therapy in Acute myeloid leukemia (AML): moving toward targeted approaches. Ther Adv Hematol. 2019;10:2040620719860645.

38.   Yu J, Jiang PYZ, Sun H, Zhang X, Jiang Z, Li Y, et al. Advances in targeted therapy for acute myeloid leukemia. Biomark Res. 2020;8:17.

39.   Zyad A, Leouifoudi I, Tilaoui M, AitMouse H, Khouchani M, Jaafari A, editors. Natural Products as Cytotoxic Agents in Chemotherapy against Cancer2018.

40.   da Rocha AB, Lopes RM, Schwartsmann G. Natural products in anticancer therapy. Curr Opin Pharmacol. 2001;1(4):364-9.

41.   Akshada Amit K. Natural Products in Drug Discovery. In: Rajendra Chandrashekar D, Shagufta P, Areej A-T, editors. Pharmacognosy. Rijeka: IntechOpen; 2019.

42.   Drug Discoverynull: InTechOpen; 2013.

43.   Desai AG, Qazi GN, Ganju RK, El-Tamer M, Singh J, Saxena AK, et al. Medicinal plants and cancer chemoprevention. Curr Drug Metab. 2008;9(7):581-91.

44.   Cragg GM, Pezzuto JM. Natural Products as a Vital Source for the Discovery of Cancer Chemotherapeutic and Chemopreventive Agents. Med Princ Pract. 2016;25 Suppl 2(Suppl 2):41-59.

45. Courdavault V, O'Connor SE, Oudin A, Besseau S, Papon N. Towards the Microbial Production of Plant-Derived Anticancer Drugs. Trends Cancer. 2020;6(6):444-8.

46. Moudi M, Go R, Yien CY, Nazre M. Vinca alkaloids. Int J Prev Med. 2013;4(11):1231-5.

47. Sinkule JA. Etoposide: a semisynthetic epipodophyllotoxin. Chemistry, pharmacology, pharmacokinetics, adverse effects and use as an antineoplastic agent. Pharmacotherapy. 1984;4(2):61-73.

48. Muriel Le R, Françoise G. 4 - From the Pacific Yew (Taxus brevifolia) to the English Yew (Taxus baccata): Steps Towards the Discovery of Docetaxel (Taxotere®). Elsevier Ltd; 2017. p. 151-212.

49. Weaver BA. How Taxol/paclitaxel kills cancer cells. Mol Biol Cell. 2014;25(18):2677-81.

50. Cragg GM, Newman DJ. Plants as a source of anti-cancer agents. J Ethnopharmacol. 2005;100(1-2):72-9.

51. Deep A, Marwaha RK, Marwaha MG, Jyoti, Nandal R, Sharma AK. Flavopiridol as cyclin dependent kinase (CDK) inhibitor: a review. New Journal of Chemistry. 2018;42(23):18500-7.

52. Ji HF, Li XJ, Zhang HY. Natural products and drug discovery. Can thousands of years of ancient medical knowledge lead us to new and powerful drug combinations in the fight against cancer and dementia? EMBO Rep. 2009;10(3):194-200.

53. Yakhni M, Briat A, El Guerrab A, Furtado L, Kwiatkowski F, Miot-Noirault E, et al. Homoharringtonine, an approved anti-leukemia drug, suppresses triple negative breast cancer growth through a rapid reduction of anti-apoptotic protein abundance. Am J Cancer Res. 2019;9(5):1043-60.

54. Uzor PF. Recent developments on potential new applications of emetine as anti-cancer agent. Excli j. 2016;15:323-8.

55. Cornet-Masana JM, Moreno-Martínez D, Lara-Castillo MC, Nomdedeu M, Etxabe A, Tesi N, et al. Emetine induces chemosensitivity and reduces clonogenicity of acute myeloid leukemia cells. Oncotarget. 2016;7(17).

56. K. C. D, Menon A, Rai LS. In-vitro Models in Anticancer Screening. In: Kumar S, Egbuna C, editors. Phytochemistry: An in-silico and in-vitro Update: Advances in Phytochemical Research. Singapore: Springer Singapore; 2019. p. 251-65.

57. Steinberg P. In Vitro–In Vivo Carcinogenicity. In: Reifferscheid G, Buchinger S, editors. In vitro Environmental Toxicology - Concepts, Application and Assessment. Cham: Springer International Publishing; 2017. p. 81-96.

58. Kitaeva KV, Rutland CS, Rizvanov AA, Solovyeva VV. Cell Culture Based in vitro Test Systems for Anticancer Drug Screening. Front Bioeng Biotechnol. 2020;8:322.

59. DSMZ. MOLM-13 ACC 554.: DSMZ-German Collection of Microorganisms and Cell Cultures GmbH.; [March 17, 2021.]. Available from: https://www.dsmz.de/collection/catalogue/details/culture/ACC-554.

60. ATCC. MV4-11 (ATCC® CRL-9591™). ATCC; [March 17, 2021]. Available from: https://www.lgcstandards-atcc.org/products/all/CRL-9591.aspx?geo_country=no#generalinformation.

61. DSMZ. OCI-AML3 ACC 582.: DSMZ-German Collection of Microorganisms and Cell Cultures GmbH.; [cited March 17, 2021. Available from: https://www.dsmz.de/collection/catalogue/details/culture/ACC-582.

62. ATCC. NRK (ATCC® CRL-6509™). ATCC.; [March 17, 2021]. Available from: https://www.lgcstandards-atcc.org/products/all/CRL-6509.aspx.

63. ATCC. H9c2(2-1) (ATCC® CRL-1446™). ATCC.; [March 17, 2021]. Available from: https://www.lgcstandards-atcc.org/products/all/CRL-1446.aspx#generalinformation.

64. Riss TL, Moravec RA, Niles AL, Duellman S, Benink HA, Worzella TJ, et al. Cell Viability Assays. In: Markossian S, Sittampalam GS, Grossman A, Brimacombe K, Arkin M, Auld D, et al., editors. Assay Guidance Manual. Bethesda (MD): Eli Lilly & Company and the National Center for Advancing Translational Sciences; 2004.

65.	SigmaAldrich. Protocol Guide: WST-1 Assay for Cell Proliferation and Viability.: SigmaAldrich.; [March 20, 2021]. Available from: https://www.sigmaaldrich.com/technical-documents/protocols/biology/roche/cell-proliferation-reagent-wst-1.html.

66.	Bucevičius J, Lukinavičius G, Gerasimaitė R. The Use of Hoechst Dyes for DNA Staining and Beyond. Chemosensors. 2018;6(2):18.

67.	Scientific. T. Hoechst 33342 Solution.: TermoFisher Scientific.; [March 20, 2021]. Available from: https://www.thermofisher.com/order/catalog/product/62249#/62249.

68.	Saraste A, Pulkki K. Morphologic and biochemical hallmarks of apoptosis. Cardiovasc Res. 2000;45(3):528-37.

69.	Ernst O, Zor T. Linearization of the bradford protein assay. J Vis Exp. 2010(38).

70.	He F. Bradford Protein Assay. Bio-protocol. 2011;1(6):e45.

71.	Bio-Rad. Bradford Assay.: Bio-Rad.; [April 5, 2021.]. Available from: https://www.bio-rad.com/featured/en/bradford-assay.html.

72.	Nouroozi RV, Noroozi MV, Ahmadizadeh M, editors. Determination of Protein Concentration Using Bradford Microplate Protein Quantification Assay2015.

73.	Mahmood T, Yang PC. Western blot: technique, theory, and trouble shooting. N Am J Med Sci. 2012;4(9):429-34.

74.	Bjørnstad R, Aesoy R, Bruserud Ø, Brenner AK, Giraud F, Dowling TH, et al. A Kinase Inhibitor with Anti-Pim Kinase Activity is a Potent and Selective Cytotoxic Agent Toward Acute Myeloid Leukemia. Mol Cancer Ther. 2019;18(3):567-78.

75.	Soh PN, Witkowski B, Olagnier D, Nicolau ML, Garcia-Alvarez MC, Berry A, et al. In vitro and in vivo properties of ellagic acid in malaria treatment. Antimicrob Agents Chemother. 2009;53(3):1100-6.

76.	Tohda C, Urano T, Umezaki M, Nemere I, Kuboyama T. Diosgenin is an exogenous activator of $1,25D_3$-MARRS/Pdia3/ERp57 and improves Alzheimer's disease pathologies in 5XFAD mice. Sci Rep. 2012;2:535.

77.	Le J. Drug Absorption.: MSD Manual Professional Version; October 2020. [Available from: https://www.msdmanuals.com/professional/clinical-pharmacology/pharmacokinetics/drug-absorption.

78.	Lamba JK. Genetic factors influencing cytarabine therapy. Pharmacogenomics. 2009;10(10):1657-74.

79.	Gülden M, Kähler D, Seibert H. Incipient cytotoxicity: A time-independent measure of cytotoxic potency in vitro. Toxicology. 2015;335:35-45.

80.	TERRI SUNDQUIST RM, ANDREW NILES, MARTHA O'BRIEN, TERRY RISS. TIMING YOUR APOPTOSIS ASSAYS.: PROMEGA CORPORATION.; 2006. [cited May 16, 2021. Available from: https://beta-static.fishersci.com/content/dam/fishersci/en_US/documents/programs/scientific/brochures-and-catalogs/publications/promega-timing-apoptosis-assay-publication.pdf.

81.	Jung HY, Seo DW, Hong CO, Kim JY, Yang SY, Lee KW. Nephroprotection of plantamajoside in rats treated with cadmium. Environ Toxicol Pharmacol. 2015;39(1):125-36.

82.	Kumar D, Mehta A, Panigrahi MK, Nath S, Saikia KK. DNMT3A (R882) mutation features and prognostic effect in acute myeloid leukemia in Coexistent with NPM1 and FLT3 mutations. Hematol Oncol Stem Cell Ther. 2018;11(2):82-9.

83.	Malik HS, Bilal A, Ullah R, Iqbal M, Khan S, Ahmed I, et al. Natural and Semisynthetic Chalcones as Dual FLT3 and Microtubule Polymerization Inhibitors. J Nat Prod. 2020;83(10):3111-21.

84.	López-Munguía A, Hernández-Romero Y, Pedraza-Chaverri J, Miranda-Molina A, Regla I, Martínez A, et al. Phenylpropanoid glycoside analogues: enzymatic synthesis, antioxidant activity and theoretical study of their free radical scavenger mechanism. PLoS One. 2011;6(6):e20115.

85.	Rajendran N, Subramaniam S, Raja MRC, Brindha P, Kar Mahapatra S, Sivasubramanian A. Plant phenyl-propanoids-conjugated silver nanoparticles from edible plant Suaeda maritima (L.) dumort. Inhibit proliferation of K562-human myeloid leukemia cells. Artif Cells Nanomed Biotechnol. 2017;45(7):1336-42.

86.   Cava C, Castiglioni I. Integration of Molecular Docking and In Vitro Studies: A Powerful Approach for Drug Discovery in Breast Cancer. Applied Sciences. 2020;10(19):6981.

87.   Singh R, Cadeddu RP, Fröbel J, Wilk CM, Bruns I, Zerbini LF, et al. The non-steroidal anti-inflammatory drugs Sulindac sulfide and Diclofenac induce apoptosis and differentiation in human acute myeloid leukemia cells through an AP-1 dependent pathway. Apoptosis. 2011;16(9):889-901.

88.   Woo DH, Han IS, Jung G. Mefenamic acid-induced apoptosis in human liver cancer cell-lines through caspase-3 pathway. Life Sci. 2004;75(20):2439-49.

89.   Shiiba M, Yamagami H, Yamamoto A, Minakawa Y, Okamoto A, Kasamatsu A, et al. Mefenamic acid enhances anticancer drug sensitivity via inhibition of aldo-keto reductase 1C enzyme activity. Oncol Rep. 2017;37(4):2025-32.

90.   Gale RP. Combination Cancer Therapy.: MSD Manual Consumer Version.; 2020. [May 16, 2021.]. Available from: https://www.msdmanuals.com/home/cancer/prevention-and-treatment-of-cancer/combination-cancer-therapy.

91.   Javle M, Curtin NJ. The role of PARP in DNA repair and its therapeutic exploitation. Br J Cancer. 2011;105(8):1114-22.

92.   Chaitanya GV, Steven AJ, Babu PP. PARP-1 cleavage fragments: signatures of cell-death proteases in neurodegeneration. Cell Commun Signal. 2010;8:31.

93.   Technology CS. Caspase-7 (D2Q3L) Rabbit mAb #12827: Cell Signaling Technology; [May 5, 2021]. Available from: https://www.cellsignal.com//products/primary-antibodies/caspase-7-d2q3l-rabbit-mab/12827.

94.   Puig B, Tortosa A, Ferrer I. Cleaved caspase-3, caspase-7 and poly (ADP-ribose) polymerase are complementarily but differentially expressed in human medulloblastomas. Neurosci Lett. 2001;306(1-2):85-8.

95.   Technology. CS. Caspase-9 (C9) Mouse mAb #9508: Cell Signaling Technology; [May 05, 2021]. Available from: https://www.cellsignal.com//products/primary-antibodies/caspase-9-c9-mouse-mab/9508.

96.   Zhang T, Guo J, Li H, Wang J. Meta-analysis of the prognostic value of p-4EBP1 in human malignancies. Oncotarget. 2018;9(2):2761-9.

97.   Technology. CS. Phospho-Stat5 (Tyr694) (C11C5) Rabbit mAb #9359: Cell Signaling Technology.; [May 06, 2021]. Available from: https://www.cellsignal.com//products/primary-antibodies/phospho-stat5-tyr694-c11c5-rabbit-mab/9359.

98.   Wingelhofer B, Maurer B, Heyes EC, Cumaraswamy AA, Berger-Becvar A, de Araujo ED, et al. Pharmacologic inhibition of STAT5 in acute myeloid leukemia. Leukemia. 2018;32(5):1135-46.